BMR JOURNAL
OF AUSTRALIAN GEOLOGY & GEOPHYSICS

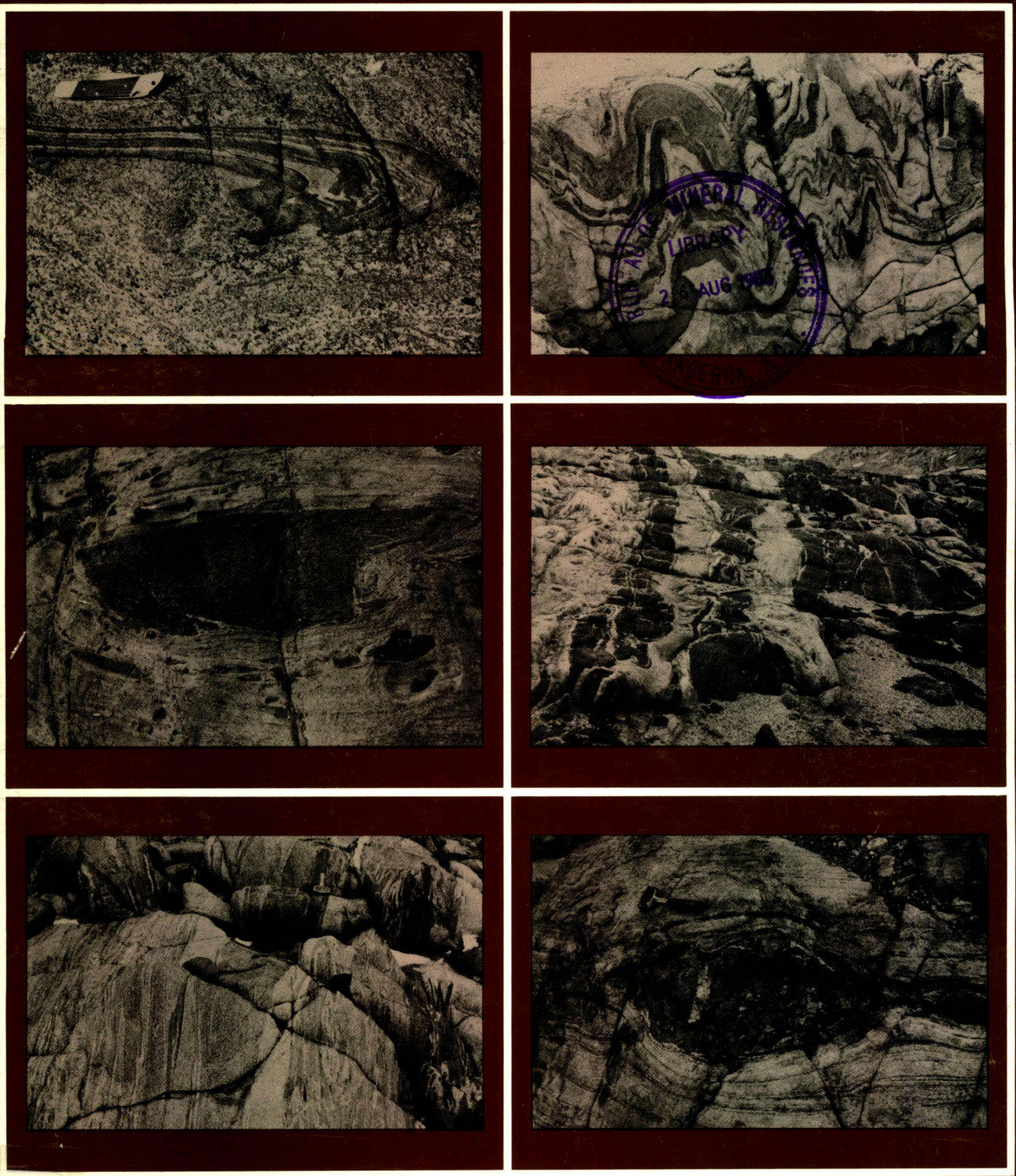

VOLUME 8 NUMBER 2 JUNE 1983

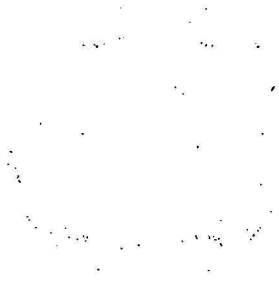

BMR JOURNAL
OF AUSTRALIAN GEOLOGY & GEOPHYSICS

VOLUME 8 NUMBER 2 JUNE 1983

CONTENTS

Front cover: Precambrian high-grade metamorphic rocks of the Vestfold Hills-Prydz Bay area, Princess Elizabeth Land, East Antarctica. The geology of these rocks is described in this issue in a paper by Sheraton & Collerson.

AUSTRALIAN GOVERNMENT PUBLISHING SERVICE CANBERRA 1983

The BMR Journal of Australian Geology & Geophysics is a quarterly journal of research and related activities. Contributions are from officers of the BMR, from BMR officers working in collaboration with others, or requested work sponsored by the BMR. In addition to articles the Journal may include shorter notes and discussion of papers published in it. Discussion of papers is invited from anyone.

Annual subscription to the Journal is $25 (Australian). Individual numbers, if available, cost $8.50. Subscriptions, etc., made payable to the Receiver of Public Moneys in Australian dollars should be sent to the Director, Bureau of Mineral Resources, Geology and Geophysics, P.O. Box 378, Canberra, A.C.T. 2601, Australia.

Other matters concerning the Journal should be sent to the Director, marked for the attention of the Editor, BMR Journal.

The text figures in this issue were drafted by P. Jorritsma, B. Pashley, M. Steele, & J. Gallagher

Cover design: Bernard Flannery

ISSN 0312-9608

Printed by Graphic Services Pty. Ltd. 516–518 Grand Junction Road, Northfield, S.A. 5085

BMR Journal of Australian Geology & Geophysics, 8, 99-108

CONTRASTING MARGINAL SEDIMENTS OF A SEASONALLY FLOODED SALINE LAKE — LAKE ELIZA, SOUTH AUSTRALIA: SIGNIFICANCE FOR OIL SHALE GENESIS

R.V. Burne & James Ferguson

Lake Eliza is a hypersaline coastal lake in southeast South Australia, a region of winter rainfall and summer drought. It is fed by groundwaters and has no connection with the sea. Salinity rises from < 100 ‰ in winter to > 360 ‰ in summer, with accompanying fall in lake level. The lake contains a biota of generally non-marine lineage. Two areas of the lake margin exposed in summer were studied. One, on the western shore, was protected from prevailing winds, the other, on the eastern shore was exposed to wave attack. The western shore is an area of fine carbonate sediments with high organic content. The eastern shore is an area of moderately sorted quartz–carbonate sand of lower organic content. The sediments of Lake Eliza are similar to some of those described from the Wilkins Peak Member of the Green River Formation, USA, and a comparison between the two systems suggests that the lamosite oil shales of the type found in the Green River Formation may not have been deposited on a fresh to brackish lake floor as has been supposed, but could have formed beneath cyanobacterial mats along a protected margin of a saline lake, in a setting equivalent to the western margin of Lake Eliza.

Introduction

Despite the widespread occurrence of saline lake deposits in the geological record, relatively few studies of present-day salt lakes and their sedimentary facies had been undertaken until recently.

Hardie & others (1978) have reviewed sedimentological knowledge of saline lakes and outlined the environments and facies of both ephemeral and perennial systems. However, they have pointed out there are still many gaps in our knowledge of saline lake basins and there is a need for further detailed studies of facies patterns within them. This is particularly true for the case of organic-rich facies of saline lakes, which give rise to many important petroleum source rocks (Kirkland & Evans, 1981) as well as some types of oil shales (Cane, 1976). Little is known of the environments of accumulation or preservation of this organic material.

In this paper we attempt to add to the understandingof saline lake facies by describing the sedimentology of two contrasting marginal areas of hypersaline Lake Eliza, which occupies an area of 14.6 km² southeast of Robe, South Australia (Fig. 1). This study is of interest because it describes facies variation in a seasonally flooded ephemeral lake basin, and, particularly, because it describes a potentially important environment of organic sedimentation that may be analogous to the depositional environment of some oil shales.

Regional setting

Unlike the arid desert setting conventionally associated with salt lakes, Lake Eliza lies in an area with an annual precipitation of 625 mm and characterised by a natural vegetation of *Melaleuca* forest with an understory of herbs (Brock, 1981). However, there is a marked summer drought, and annual evaporation greatly exceeds rainfall (Roe & others, 1980). Temperatures vary from below freezing in winter to over 40°C in summer with an annual average of 10–15°C (Bayly & Williams, 1966).

The lake is one of three large coastal lakes that occupy the interdune hollow between the Robe Range and the Woakwine Range (Fig. 2). These are the two most recent of a succession of linear coastal ridges that has accumulated in

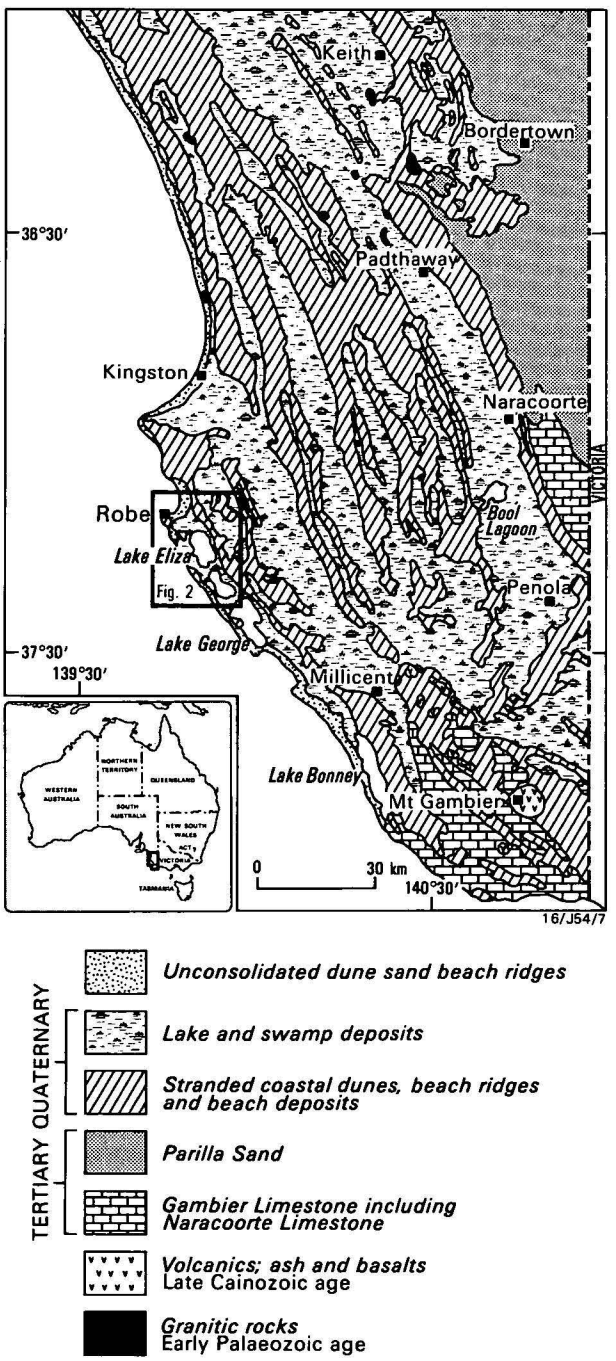

Figure 1. Regional setting and geology of southeast South Australia (modified from Cook & others, 1977).

Baas Becking Geobiological Laboratory, GPO Box 378, Canberra City, ACT 2601

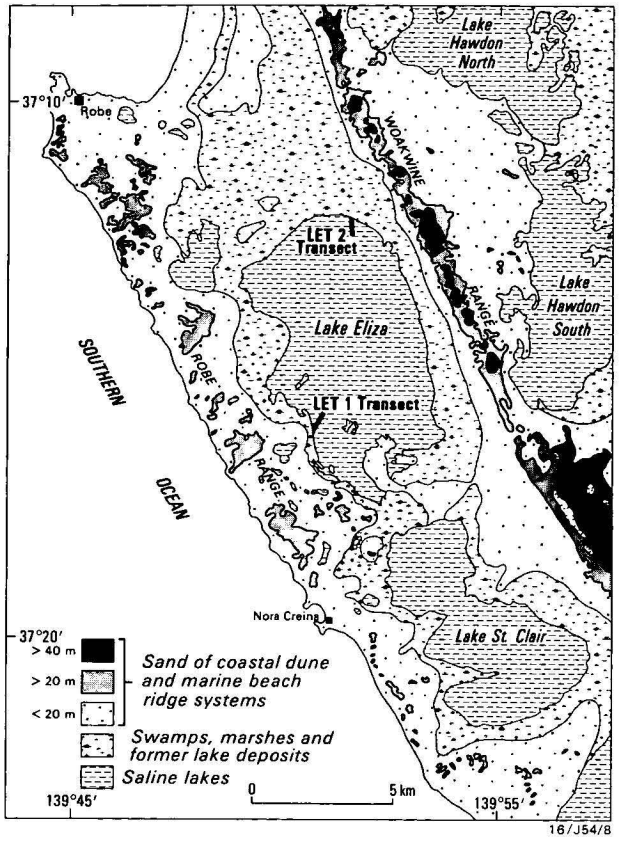

Figure 2. Morphological setting of Lake Eliza, showing location of study transects.

southeast South Australia over the last 690 000 years and has resulted in a 100-km progradation of the shoreline (Cook & others, 1977).

Lake Eliza has no direct connection with the sea, although the abundance of marine shells in older lake sediments is evidence of the existance of normal marine conditions in former times.

Hydrology

Lake Eliza lies below mean sea level and therefore acts as a local 'sink' for groundwater. The groundwater flows from the surrounding dunes as well as from the underlying regional carbonate aquifer systems, in which flow is generally directed westwards toward the coast (von der Borch & others, 1975). Studies of neighbouring Lake St Clair (Fig. 2) (Harris, 1969) have shown the presence of a marked interface between saline and fresh groundwater along the eastern margin of the lake. The situation along the western, seaward margin is less clear. There is an input of fresh water from the Robe Range aquifer, but it is uncertain whether there is also an input from subsurface invasion of seawater.

The proximity of Lake Eliza to the ocean and the evidence of a former marine connection suggest that the salts in the lake are of marine origin (Bayly & Williams, 1966), although the geochemical evidence is equivocal and does not discount the possibility that the salinity could be due either partly or wholly to the evaporative concentration of continental groundwaters.

Biota

The fauna of the lake has been briefly described by Bayly (1970), who found that it consists mainly of organisms of non-marine origin and fresh-water lineage, including insects, amphipods, calanoid and cyclopiod copepods, ostracods, and rotifers. In addition, there are some copepods of marine or brackish water descent, and the gastropod, *Coxiella*, which may be descended from a terrestrial or semi-terrestrial ancestor. Detailed faunal studies have yet to be undertaken.

The flora has been described by Brock (1981), and consists of the angiosperms, *Lepilaena cylindrocarpa*, *Ruppia megacarpa*, and *Ruppia tuberosa*, the charophyte, *Lamprothamunium papulosum*, species of the green alga, *Cladophora*, and cyanobacteria, which form extensive mats around the lake margin. There have been no detailed studies of the cyanobacteria.

Marginal environments and the location of study transects

The eastern border of the lake is formed by the steep escarpment of the Woakwine Range, which rises to an elevation of 57 m. At the foot of this slope an 800-m wide plain falls gently to the lake. The plain is the site of numerous springs, formed by discharging Woakwine groundwater, and has been extensively drained for agriculture.

The western and southwestern margin of the lake is delineated by the less steep leeward slope of the Robe Range. This area has a complex topography of dune lobes and local hollows, which contain groundwater outcrops in the form of lakes of varying permanence and salinity (Bayly & Williams, 1966, Bayly, 1970). The lake margin consists of salt marshes, inundated by high winter lake levels (Brock, 1981).

The northwestern margin of the lake is bordered by a plain composed of raised beach ridges, presumably formed at higher stands of lake level. The southeastern margin of the lake is an area of rocky outcrop, and erosion of these rocks, lithified aeolian dunes, has formed a rocky platform at the lake edge.

The prevailing winds are southwesterlies blowing from the Southern Ocean. The southwestern lake margin, in the lee of the coastal dunes, is, therefore, protected from the wind and not exposed to wave attack. The northeastern shore is exposed to the full force of the prevailing winds, to attack by waves generated across the maximum fetch of the lake, and to inundation resulting from wind set-up.

In summer, low lake levels leave a 400–100-m wide exposed margin around the lake. At this, time there is little or no surface discharge into the lake, and its waters are highly saline. The mixing zone between groundwaters flowing towards the lake and concentrated lake brines occurs in the sediments beneath this marginal flat.

Two transects were delineated for study of sediments, groundwaters, and their interactions. One crossed the finer-grained protected margin at the southwestern corner of the lake, and the other crossed the sandier exposed marginal flat at the northeastern extremity (Figs. 2, 3, 4). The following observations were made along these transects in 1981.

Protected transect LET 1 (Fig. 3)

Topography and surface features.

The western margin of the lake is flanked by a salt marsh about 100 m in width with an association of halophytes and underlying cyanobacterial mats (Brock, 1981) (Fig. 5). This

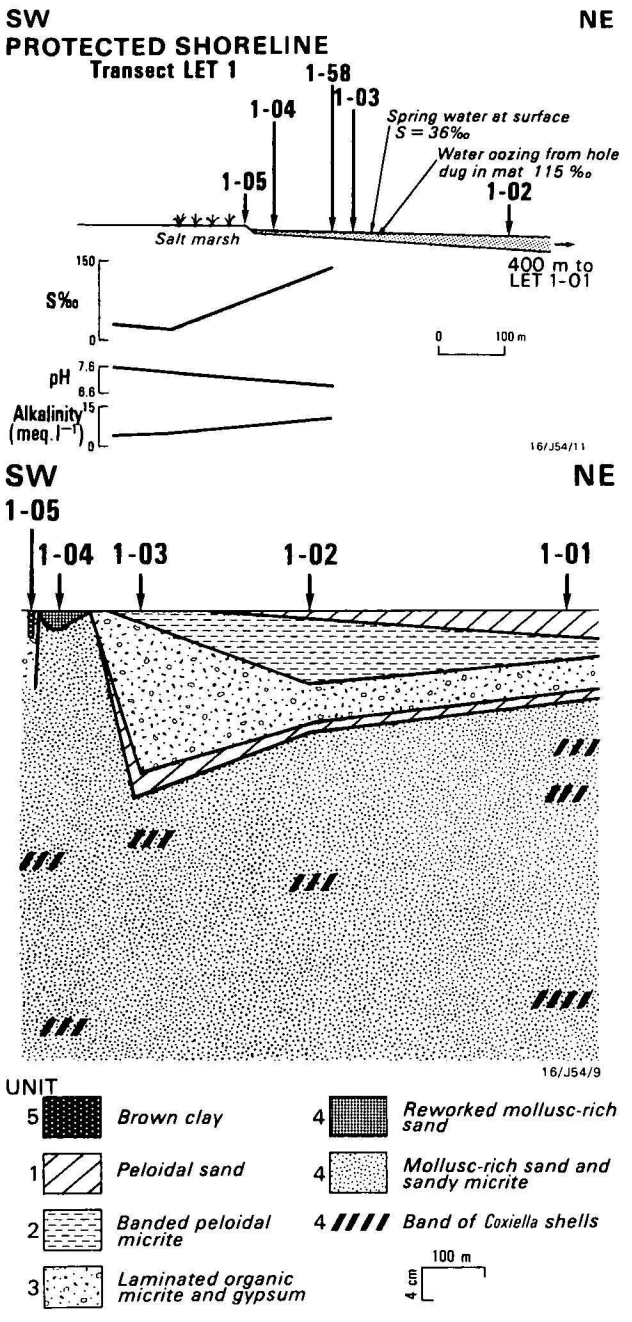

Figure 3. (A) Topographic and salinity variation along protected transect LET 1. (B) Sedimentological facies variation along transect LET 1.

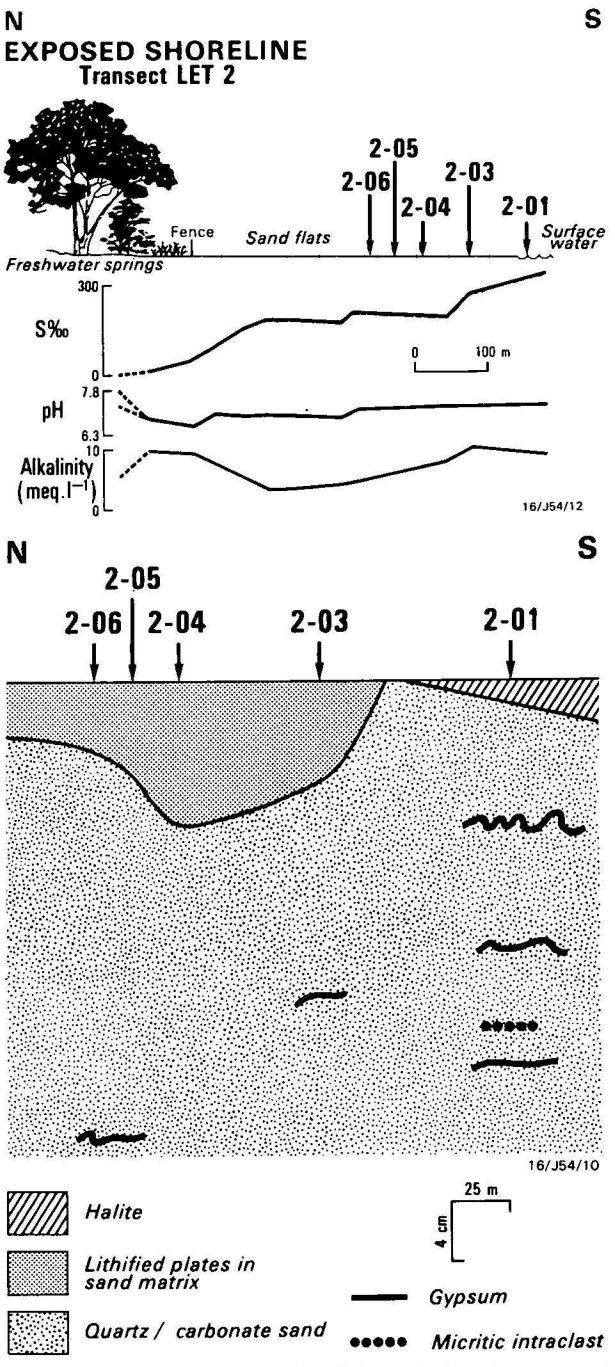

Figure 4. (A) Topographic and salinity variation along exposed transect LET 2. (B) Sedimentological facies variation along transect LET 2.

is covered by 10 cm or more of water during the wet winter season. The salt marsh passes into a shell-covered low-angle ramp, which marks the margin of the lake basin proper. This is about 120 m wide and covered by mollusc shells, including large, bored oyster shells (Fig. 6). The sediment surface is sandy and bears a pattern of polygonal cracks, 2 cm wide and filled with sandy sediment. This zone passes into a plain of grey-yellow fine-grained carbonate capped by a dry gypsiferous crust. At the lake margin this forms a firm surface, but towards the lake it gradually becomes softer. After about 240 m, crenulate cyanobacterial mat appears on the moist surface, and 5-m scale networks of polygonal fissures are clearly defined (Fig. 7). Surface water occurs in isolated springs, which are surrounded by well-developed cyanobacterial mat (Fig. 8). About 400 m further toward the centre of the lake, remains of aquatic angiosperms, such as *Ruppia*, occur, first localised along polygonal fissures, and then ubiquitously. The surface is encrusted in halite, and this is underlain by a pink microbial layer.

Groundwater and hydrochemistry.

Groundwater salinity is low (20‰) beneath the landward margin of the salt marsh (Fig. 3A). The fine-grained organic-rich sediments of the marginal plain (Fig. 9) have low permeabilities and act as an aquiclude, confining the groundwater of the underlying coarser-grained sediments. The confined water breaks through the surface sediments at some places, forming isolated springs, which have relatively low salinity (e.g. 36 ‰). They deposit small amounts of red ferric oxides on the sediment surface, as traces of Fe^{2+} in the waters are oxidised. In contrast, the interstitial water from

Figure 5. Marginal salt marsh (LET 1-5), showing extensive halophyte colonisation.
Land snail shells are stranded in upper parts of plants. Lake basin at upper left. Robe Range in distance.

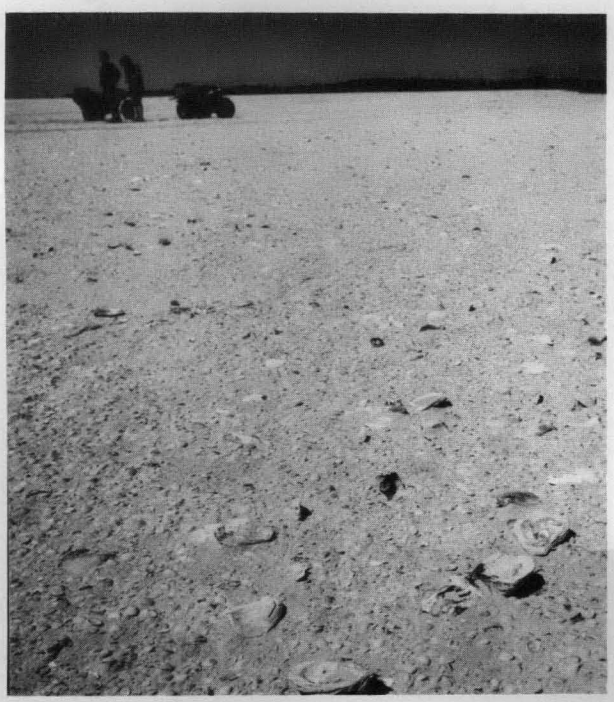

Figure 6. Shell lag on surface of sandyramp at margin of lake basin (LET 1-4).
Salt marsh at right. Note large oyster shells.

Figure 7. Gypsum and halite encrusted surface (LET 1-3).
Dark areas are cyanobacterial mat. Note irregular pattern of filled polygonal fissures. Robe Range in distance.

Figure 8. Groundwater spring (LET 1-2) with crenulate (dark) and smooth (light) cyanobacterial mat and rare halophytes colonising the surrounding sediments.

Figure 9. Organic-rich, reducing, laminated sediments composed of organically bound micrite and interlaminated gypsum, forming beneath surface cyanobacterial mat and evaporite crust (LET 1-3).

the fine-grained sediments has much higher salinity (e.g. 142‰) and smells strongly of H_2S. Both the high salinity and the strong establishment of bacterial sulphate reduction are favoured by the fact that only a slow rate of of groundwater movement is possible through the fine-grained sediment.

Sediments.

Five sediment units are recognised: peloidal sand; interbedded micrite and peloidal sand; finely laminated organic-rich micrites with interlaminated gypsum; mollusc-rich skeletal sands and biomicrites; and brown clay. These sediments are all rather fine-grained (6–25% clay), with a carbonate content of 72–96 per cent and organic carbon values of 2.3–6 per cent by weight.

Unit 1: peloidal sand (Figs. 10, 11)

Description. This unit forms the surface sediments at the northeastern end of the transect, especially where the surface has been colonised by *Ruppia* and other plants. Vertical roots penetrate the top 1 cm or so of the sediment, and relict root structures occur throughout the unit, often as gypsum-filled moulds. 2 mm of halite encrusts the surface. The sediment consists of ovoid to subangular aragonite peloids, 0.3 mm diameter, composed of micrite clots together with skeletal grains, mainly ostracods and forams, and 4 × 1 mm angular intraclasts of clotted micrite, which are either dispersed through the unit or arranged in indistinct layers. The unit is 2–4 cm thick, and grey-yellow to yellow-grey. Organic carbon content is about 3 per cent by weight.

Interpretation. The sediments are formed in the more frequently inundated areas of the lake. They reflect the deposition of carbonate from the lake waters in areas occupied by angiosperm fields and an associated biota of ostracods and other organisms. The origin of the peloids is not clear, although they may be the result of aragonite precipitated from lake waters and then reworked to form

Figure 10. Impregnated box core from exposed *Ruppia* bed at lake end of LET 1 (LET 1-1).
Cracks original, but accentuated by drying. 2-mm halite crust overlies 3 cm of peloidal sand (unit 1) — note root structures at top and intraclasts at the base; 3–6 cm (unit 2) — note indistinct laminations and mudcracks; 6–8 cm, interlaminated gypsum and finely laminated micrite (unit 3); 8–95 cm, peloidal sand (unit 1); 9.5 cm to base of core, mudcracked mollusc-rich sandy micrite (unit 4).

Figure 11. Impregnated box core from locality LET 1-02, an area of scattered *Ruppia* growth.
2 mm of halite crust overlies 1.5 cm of unit 1, peloidal sand; 1.5–9 cm, weakly banded alternations of peloidal micritic and peloidal sand (unit 2) with desiccation and intraclasts at the base; 9–13 cm, finely laminated organic-rich micrite and discoidal gypsum (units); 13–14 cm, peloidal sand (unit 1); and 14–17 cm, shell-rich sandy micrite (unit 4).

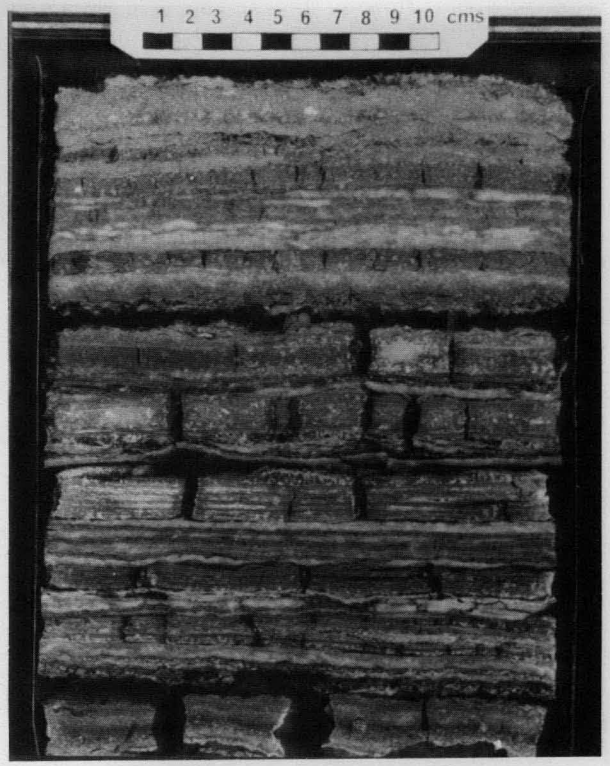

Figure 12. Impregnated box core from area of scattered cyanobacterial mat growth (LET 1-03).
1–2 cm, weakly banded alternating peloidal micrite and peloidal sand layers with micrite intraclasts (unit 2); 2–19 cm, finely laminated organic-rich micrite with gypsum layers (unit 3); and 19–1 cm, peloidal micrite (unit 1).

Figure 13. Impregnated box core from shelly ramp at margin of lake basin (LET 1-04).
Mollusc-rich micritic sand at base (unit 4), extensive desiccation cracks. Overlain by a shell-lag deposit, note bored oyster and a later shelly sand deposit. Note younger layers partially filling desiccation cracks in the basal unit.

faecal pellets from anostracan crustaceans (brine-shrimp), ostracods, or gastropods. Evaporation produces a thin halite crust, but desiccation does not progress far enough to produce extensive mud cracking.

Unit 2: interbedded micrite and peloidal sand (Figs. 10, 11, 12)

Description. Unit 2 is composed of 1-cm couplets, grading from dark greenish-grey peloidal micrite into grey-yellow peloidal sand, identical with that of the previous unit. Mud cracks, 0.5 cm wide and 3–7 cm deep, penetrate the unit. The cracks may be empty, rimmed with gypsum or halite, or partly filled by peloidal sand from an overlying unit. Halite and gypsum occur along bedding surfaces. Locally, layers of 8 × 2 mm angular micrite intraclasts have developed. Organic carbon values are about 3 per cent by weight. The unit is 3–5 cm thick and occurs only around the margin of the area of dense *Ruppia* colonisation.

Interpretation. This unit forms in an environment intermediate between that of units 1 and 3. Frequent exposure reduces biological activity, and aragonitic micrite is deposited without reworking. Peloidal sands form during periods of more extensive inundation. The more frequent exposure and desiccation results in the extensive development of mud cracks.

Unit 3: finely laminated organic rich micrites with interbedded gypsum (Figs. 9, 12)

Description. This unit, 4–18-cm thick, underlies the lake margin in the zone of maximum cyanobacterial colonisation. It consists of 1-mm scale, finely laminated, light olive-green, peloidal micrite. The laminae are characterised by anastomosing, thin, horizontal organic films, probably of cyanobacterial origin. Layers of gypsum, either as 2-mm discs or as milky layers, are interbedded with this organic-rich sediment in layers 1 mm to 2 cm thick. Thin layers of peloidal sand and partings of halite also occur. The unit is penetrated by open cracks, 1.5–4 cm deep and 0.1–1 cm wide. Organic carbon values range between 3 and 4 per cent by weight.

Interpretation. Unit 3 is considered to represent an accumulation of fine- grained carbonate bound by cyanobacterial mat growing in an intermittently exposed marginal setting. High-salinity interstitial water precipitates gypsum, and vertical cracks result either from upward seepage of groundwater or desiccation.

Unit 4: mollusc-rich skeletal sands and skeletal micrites (Figs. 10, 11, 13)

Description. This unit underlies the other units in the central part of the lake, and occurs at the surface along the shelly ramp at the margin of the lake basin. Its base has not been penetrated in the shallow 60-cm cores. It is characterised by an association of gastropods and bivalves, including marine forms, such as oysters, which do not live in the lake today. Some of the shells are extensively bored. At other horizons, there are concentrations of shells of the lake-dwelling gastropods *Coxiella*. These shells occur either in a very poorly sorted, light olive-grey micritic sediment or as poorly sorted skeletal sand. This unit is extensively disrupted by a system of open cracks, some partly filled by overlying sands derived apparently from winnowing of the more muddy sediment.

Interpretation. Unit 4 formed under more permanent water conditions of varying salinity, and the extensive cracking is due to later exposure and desiccation. The margins of the lake are flooded too rarely to allow cyanobacterial colonisation, and can be inundated only when the lake is full of relatively fresh water. Consequently, the present sediment surface at the lake margin is composed of a mollusc sand winnowed from this unit and without significant chemical contribution from lake waters. This sand fills old desiccation cracks.

Unit 5: brown clay

Description. Unit 5 forms an oxidised brown earth with root remains in the halophyte and cyanobacterial salt marsh around the margin of the lake. It is composed of micritic carbonate and organic debris.

Interpretation. The unit represents the oxidised deposits of organic material and carbonate trapped by cyanobacterial mat in the salt marsh and subjected to frequent drying and oxidation. It is essentially a salt marsh soil.

Relations between the units.

A summary of the relations between the units observed in the cores (Figs. 10–13) is shown in Figure 3. At the lake centre, a sequence of units, from base to top, of 4, 1, 3, 2, 1 is observed and reflects initially falling lake levels, followed by increasingly wet conditions. The presence of sediments of unit 3 beneath the salt marsh implies former high lake levels.

Exposed transect LET 2 (Fig. 4)

Topography and surface features.

Freshwater marshes occur between the lake margin and the foot of the Woakwine Ranges. These marshes have dense growths of Mallee (*Eucalyptus*) and Ti Trees (*Melaleuca*) around a network of freshwater springs. The area has recently been artificially drained. The trees give way to a belt of grasses and reeds, and then a salt marsh which extends to the margin of the lake.

The margin of the lake is a 250-m wide zone of quartz and carbonate sand with abundant lithified plates of similar sand scattered over the surface or piled in 10–50-cm high mounds and ridges (Fig. 14). The lithified plates are flat and irregular, and are generally 2–3 cm across, although they may be as much as 10 cm across (Fig. 15). Crenulate cyanobacterial mats are developed irregularly in this zone (Fig. 14).

There follows an 80-m wide zone in which the sandy sediments form low, 20-cm high, shoreward-migrating megaripples (Fig. 14). Lithified plates are scattered over the surface and also occur in the top few centimetres of the sediment. Windrows of ostracods and dried *Ruppia* fragments occur locally, marking a seasonal shore of a fuller lake containing fresher water. The megaripple zone passes lakeward into a zone of sandy sediment with straight-crested ripples, 0.5–1 cm high with a 10-cm wavelength (Fig. 16). The ripple crests are oriented parallel to the shore-line. The surface is indurated, possibly by gypsum or carbonate cementation, and tepee structures have developed locally.

Between this zone and the area of surface lake water, the sediment surface is covered by a thin crust of gypsum and halite, which coats the ripple morphology. Foam forms abundantly along the margin of surface lake water. The water has a brownish-pink coloration and mounds of 1-cm size halite cubes are accumulating along the edge of the water (Fig. 17).

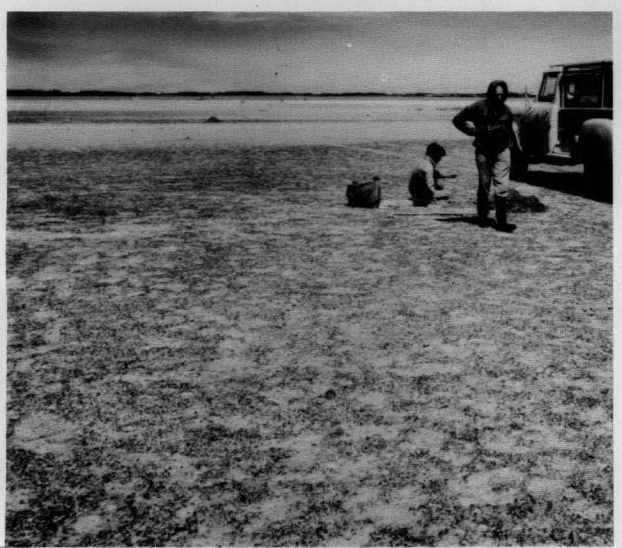

Figure 14. View along exposed transect from LET 2-06.
Hard sand surface with a covering of crenulate cyanobacterial mat and chips of lithified sand. Lighter coloured megaripples in background. Lake and Robe Range in distance.

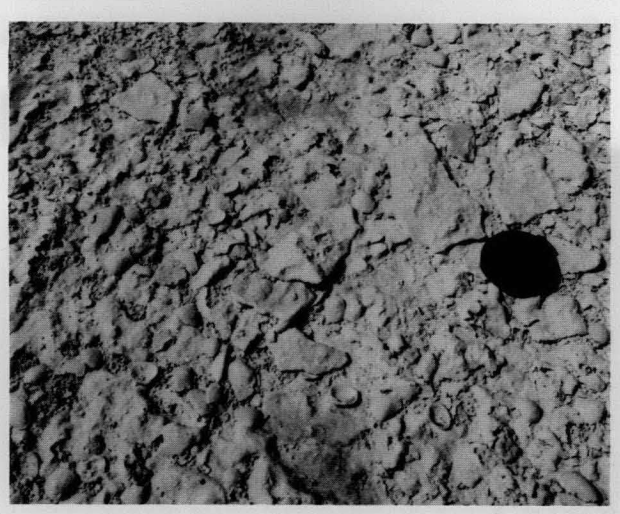

Figure 15. LET 2-05 surface ,showing scattered flat plates of lithified sand.

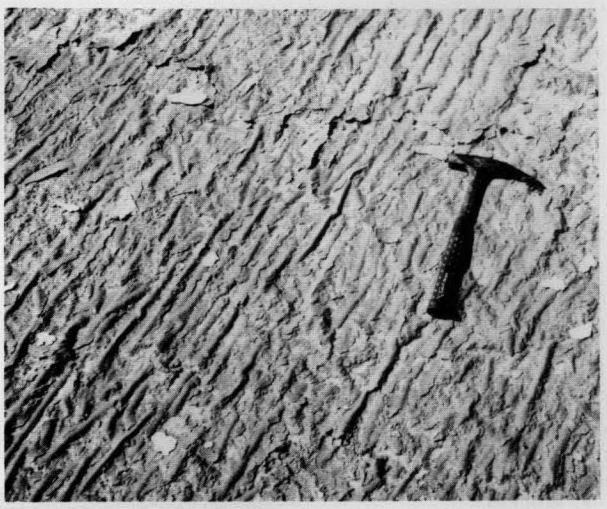

Figure 16. Straight crested ripples now lithified, at LET 2-02.

Figure 17. Lake margin at LET 2-01.
Halite crust overgrowing rippled surface, and forming polygonal tepee structures. Note mound of halite cubes above hammer, and foam on surface of lake waters.

Groundwater and hydrochemistry.

The freshwater springs are fed from aquifers in the Woakwine Range and have very low salinity (typically < 1). They are calcium bicarbonate waters containing traces of NaCl. When sampling was undertaken in February 1981, groundwater salinity at the margin of the swamp was about 12‰. The groundwaters beneath the 500-m wide sandy flat exposed around the lake showed a zone of mixing between spring and lake waters, and salinity gradually increased from 12‰ to the 360‰ found in the surface water.

Alkalinity was highest at the landward end of the transect, and first decreased lakewards, and then increased again. Solution conditions in the groundwater favoured the precipitation of carbonate as aragonite, because mMg/mCa ratios range upwards from 5.5, a figure close to the seawater value. As the salinity increases towards the lake centre, the solubility of gypsum and then halite is exceeded.

Sediments

Description. Sampling was restricted to the sandy plain, and no samples were taken from the swamp or marsh environments. The sandy plain is underlain by a moderately sorted (90% sand) quartz–carbonate (63–82% carbonate) sand with scattered disarticulated bivalves. The subangular to sub-rounded quartz grains are coated by 30-μm wide rims of micrite. Organic carbon contents are 0.5–3 per cent by weight.

At the lake margin the sands are overlain by a 1–3-cm unit of crystalline halite, with cubes up to 1 cm. Fragments of *Ruppia* are present in the halite crust. The sands here are

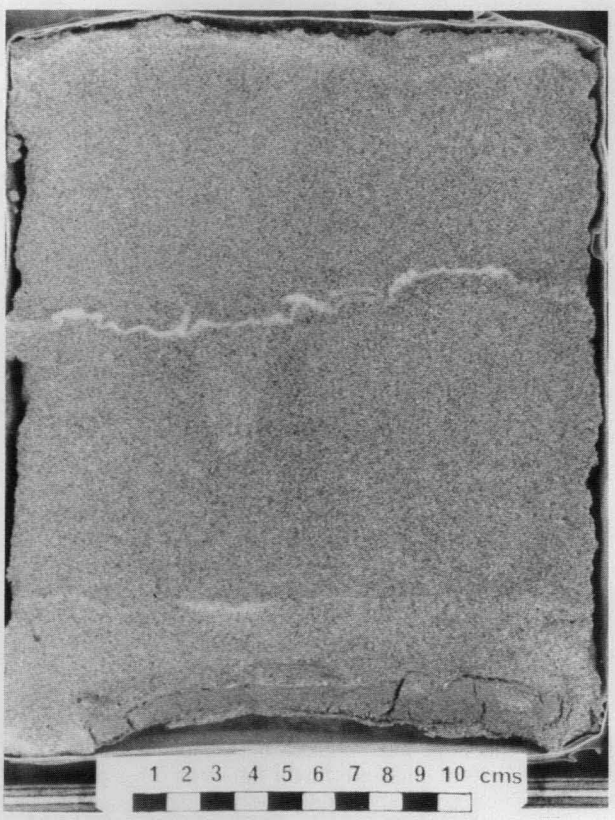

Figure 18. Slice through impregnated box core from exposed lake margin at LET 2- 01.
Note structureless quartz–carbonate sand, enterolithic vein of gypsum, and large micritic intraclast at base.

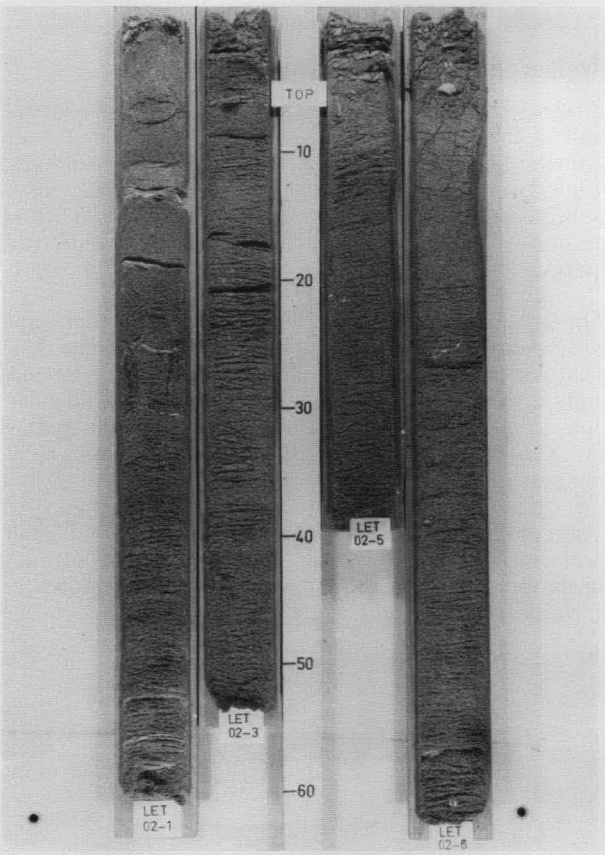

Figure 19. Laquer peels of cores through exposed lake margin at localities (left to right) LET 02-1, 02-3, 02-5, and 02-6.
Note generally cross-laminated sand. Top of LET 2-01 structureless, but with gypsum vein, tops of LET 2-05 and 2-06 structureless with small lithified chips.

Figure 20. Laquer peel of box core from LET 2-04, showing selective lithification of laminations in upper part of cross laminated quartz-carbonate sands.

Figure 21. Slice through impregnated slab of same box core as Fig. 20, showing cross-sections of lithified laminations.

either faintly laminated, or have a homogeneous texture reminiscent of a fine sponge. Partings of gypsum occur, including one well-developed 2-mm wide enterolithic vein, 7.5 cm beneath the surface (Fig. 18). 5 cm × 1.5 cm intraclasts of sandy clay occur within the sands.

Shorewards, beneath the zone of well-developed surface ripples, the sands have a well-developed structure of unidirectional shoreward-facing cross- laminations with co-sets up to 2 cm high (Fig. 19). Gypsum partings are still present, and lithified 3 cm × 2 cm flat plates of carbonate-cemented sand occur in the top 3 cm at the landward margin of the zone and in the area of surface megaripples.

In the lakeward margin of the zone of extensive surface-lithified chips, the cross-laminated sands are overlain by an 11-cm layer in which laminations have been selectively lithified to form plates averaging 3 cm × 1 cm (Figs. 20, 21). Some plates are overlain by a thin rim of gypsum. Shoreward of this zone 'in situ' plates give way to a surface 3-cm layer of 'edgewise conglomerate', consisting of redeposited lithified plates, 2 cm × 2 mm and larger, set in a sandy matrix. This overlies cross-laminated sands (Fig. 19).

Origin of sediments. The sediments of the eastern lake margin reflect the diagenetic effects of the groundwater regime superimposed on a sandy facies produced under relatively high-energy conditions.

The quartz sands are, presumably, derived from aeolian input to the lake and reworking of Woakwine Range sediments. The carbonate grains consist both of organisms, such as gastropods and forams, currently living in the lake and molluscs and forams reworked from older sediments. The sediments have been deposited under the influence of waves or currents generated by the prevailing onshore winds.

The diagenetic effects observed in the sediments are consistent with the chemistry of the pore waters. Thus, halite precipitation is occurring in the area of surface water where halite saturation levels are exceeded, gypsum is formed within the sediments at the margin of this zone, and carbonate is forming both within the lake itself, where it forms aragonite coatings on sand grains, and beneath the sand flat, where it selectively cements laminations within the sediments. Erosion of this area of near-surface lithification provides a source for the chips of lithified sand that scatter the surface of the shoreward margin of the plain. The scattered surface cyanobacterial mats are subject to erosion and leave no detectable sedimentary structures.

Discussion

Lake Eliza provides an example of saline lake deposition intermediate between that of playa lakes and permanently filled lakes. The most important feature of this example is the complexity of the marginal facies, resulting from frequent alternation of inundation and exposure, which produce sediments in some ways analogous to intertidal facies of normal marine environments. The 'bulls-eye' zonation of facies, typical of many salt lake basins, is modified by the influence of prevailing winds, which results in the formation of contrasting shore lines of, on the one hand, sandy higher-energy sediments, and, on the other, fine-grained low-energy sediments.

The marginal facies of Lake Eliza are in many ways comparable to the sedimentary facies described from the Wilkins Peak Member of the Green River Formation by Eugster & Hardie (1975). The geological setting of Lake Eliza is quite different from that of the lake in which the Wilkins Peak Member was deposited, and the waters of the Green River Lake system were highly alkaline and deposited trona, whereas Lake Eliza is a Ca-sulphate-chloride lake in a hydrochemical setting unsuitable for trona precipitation. The parallels between the two systems are otherwise reasonably close. The trona–halite facies of the Wilkins Peak Member compares with the halite sediments of Lake Eliza, the lime–sandstone facies equates closely with the quartz–carbonate sands of the western margin of Lake Eliza, and the peloidal mudstone facies compares with the peloidal sediments of Lake Eliza. The flat-pebble conglomerate facies of the Green River Formation has no direct parallel, but the presence of coated grains and their overall structure compare with the edge-wise conglomerates of lithified sand plates found on the eastern shore of Lake Eliza. The laminated oil shales of the Wilkins Peak Member have some similarities with the organic- rich laminated sediments forming beneath the cyanobacterial mats on the western margin of Lake Eliza.

This last point is of interest, since it suggests the possibility that the oil-shale facies of the Green River Formation, which contains desiccation cracks and evaporite pseudomorphs, did not necessarily form on the floor of a fresh to brackish lake, as suggested by Eugster & Hardie (1975), but could have been deposited along a cyanobacterial mat covered, protected margin of a saline lake, such as that found on the western shore of Lake Eliza.

The oil-shale facies of the Wilkins Peak Member contains fish bones, algae, fungi, and insect fossils, as well as burrows and shortite casts. However, the nature of the material that contributed the organic matter to the oil-shales is obscure. It is composed largely of disorganised and unrecognisable organic matter (Cane, 1975). Bradley (1970) considered it predominantly of blue-green algal (cyanobacterial) origin, and that the only other significant organic component was

pollen, derived from land plants around the lake. The oil shales were described by Eugster & Hardie (1975, p.333) as having formed on 'a very shallow fresh to brackish lake bottom covered by thick flocculent gelatinous algal-fungal ooze. Occasionally mud cracked'. It is significant that *Botryococcus*, an important algal source for oil shales of fresh-water origin, has not been recognised in the Green River Formation (Bradley, 1970).

The petrological descriptions of the Green River oil shales presented by Eugster & Hardie (1975) and Hutton & others, (1981) suggest that they have formed, not from flocculated material, but as a cohesive, prostrate, laminated deposit. According to Bauld (1981a), this is definitive of a benthic microbial mat. Such mats commonly consist of a dominant microbial species associated with minor species, and accumulate in environments where grazing pressure is limited by some permanent or transient extreme. Because of this, most well-developed mats develop in marginal, intermittently exposed areas of marine intertidal zones or, as at Lake Eliza, along lake margins. They do occur in permanently submerged settings, but only in rather unusual areas such as in stratified lakes, hot springs, and Antarctic saline lakes (Bauld, 1981b).

Bauld (1981a) has suggested that the best location for preserving organic matter of cyanobacterial mats is an environment where anoxic conditions are rapidly reached, and where further microbial decay is halted either by desiccation or high pore-water salinity (in the region of halite saturation). These conditions are most likely to be met in or around a saline lake, especially one of seasonally fluctuating salinity or level or both. Such an environment is found in the area of cyanobacterial mat colonisation on the sheltered western shore of Lake Eliza. Here, relatively impermeable conditions prevent free groundwater movement, and organic material is preserved (Fig. 9). We suggest that this facies, which is characteristic of a protected saline lake margin, is the precursor of at least some types of what Hutton & others (1980) have termed lamosite oil shale.

Acknowledgements

We thank D.B. Fitzsimmons, L. Pain, and M. Tratt for technical assistance. The Baas Becking Laboratory is supported by the Bureau of Mineral Resources, the Commonwealth Scientific and Industrial Research Organisation, and the Australian Mineral Industries Research Association Ltd.

References

Bauld, J., 1981a — Geobiological role of cyanobacterial mats in sedimentary environments: production and preservation of organic matter. *BMR Journal of Australian Geology & Geophysics*, 6, 307–317.

Bauld, J., 1981b — Occurrence of benthic microbial mats in saline lakes. *Hydrobiologia*, 81, 87–111.

Bayly, I.A.E., 1970 — Further studies on some saline lakes of southeast Australia. *Australian Journal of Marine and Freshwater Research*, 21, 117–129.

Bayly, I.A.E., & Williams, W.D., 1966 — Chemical and biological studies on some saline lakes of southeast Australia. *Australian Journal of Marine and Freshwater Research*, 17, 177–228.

Bradley, W.H., 1970 — Green River Oil Shale — concept of origin extended. *Geological Society of America Bulletin*, 81, 985–1000.

Brock, M.A., 1981 — The ecology of salt lake halophytes: the synecology of saline ecosystems and the autecology of the genus *Ruppia* L. in the southeast of South Australia. *Ph.D. thesis, University of Adelaide*.

Cane, R.F., 1976 — The origin and formation of oil shale. *In* Yen, T.S., & Chillingarian G.V. (editors). Oil shale. *Elsevier, Amsterdam*, 28–59.

Cook, P.J., Colwell, J.B., Firman, J.B., Lindsay, J.M., Schwebel, D.A., & von der Borch, C.C., 1977 — The late Cainozoic sequence of southeast South Australia and Pleistocene sea-level changes. *BMR Journal of Australian Geology & Geophysics*, 2, 81–88.

Eugster, H.P., & Hardie, L.A., 1975 — Sedimentation in an ancient playa-lake complex: the Wilkins Peak Member of the Green River Formation of Wyoming. *Geological Society of America Bulletin*, 86, 319–334.

Hardie, L.A., Smoot, J.P., & Eugster, H.P., 1978 — Saline lakes and their deposits: a sedimentological approach. *In* Matter, A., & Tucker, M.E., (editors). Modern and ancient lake sediments. *International Association of Sedimentologists, Special Publication*, 2, 7–41.

Harris, B.M., 1969 — Southeast water resources hydrology progress report No. 4, test area 1. Results of geological investigations. *South Australian Department of Mines and Energy, Unpublished Report* 75/96.

Hutton, A.C., Kanstler, A.J., Cook, A.C., & McKirdy, D.M., 1980 — Organic matter in shales. *The APEA Journal*, 20, 44–59.

Kirkland, D.W., & Evans, R., 1981 — Source-rock potential of evaporitic environment. *American Association of Petroleum Geologists Bulletin*, 65, 181–190.

Roe, G.P., Nitschke, J.E., Nosworthy, S.H., & Spehr, L.R., 1980 — Environmental impact study on the effect of drainage in the southeast of South Australia. *South Eastern Drainage Board, Adelaide, South Australia*.

von der Borch, C.C., Lock, D.E., & Schwebel, D.A., 1975 — Groundwater formation of dolomite in the Coorong region of South Australia. *Geology*, 3, 283–85.

BMR Journal of Australian Geology & Geophysics, 8, 109-117

GEOCHEMICAL DISCRIMINATION OF ACID VOLCANIC UNITS IN THE MOUNT ISA REGION, QUEENSLAND

I.H. Wilson[1].

A systematic examination of multivariate geochemical data for two predominantly felsic volcanic units from the Proterozoic of the Mount Isa region, the Leichhardt Metamorphics (1865 Ma) and the Argylla Formation (1777 Ma), has established practical criteria to distinguish these units. The criteria are applied to volcanics from the Ewen Block, Wonga Belt, and Bottletree Formation, which have been difficult to correlate using lithologic and structural criteria. Histograms provide limited discrimination, because of the large range of most elements. Variation diagrams using SiO_2 as the independent variable allow clear distinction of the two formations to be made from their relative abundances of Ti, Al, Fe, K, Ce, Cr, Nb, Pb, Sr, Th, Y, and Zr at any particular SiO content. An examination of ratios of elements with similar chemical properties effectively distinguishes the two formations. The similarity co efficient and discriminant analysis allow classification of the two formations and are of use in assigning analyses of unknown specimens. All techniques indicate that the Ewen Block volcanics are probably Leichhardt Metamorphics and that the Wonga Belt and Bottletree Formation specimens more closely resemble the Argylla Formation. The higher CaO, Sr, and Pb, and lower K_2O distinguish the Bottletree Formation from the Argylla Formation and support its status as a separate formation.

Introduction

This paper examines the usefulness of chemical analyses in solving stratigraphic problems in a sequence of predominantly felsic volcanics in the Mount Isa Inlier (Fig. 1). The Inlier contains approximately thirty formally named volcanic units (Plumb & Derrick, 1975; Plumb & others, 1980), ranging in age from Early Proterozoic to Carpentarian, according to U-Pb zircon determinations (Page, 1978). Two of the most extensive felsic volcanic units were called the Leichhardt Metamorphics and Argylla Formation by Carter & others (1961). Recent mapping has shown that some of the earlier correlations are wrong or dubious. In particular, the sequence of volcanics in the Ewen Block previously mapped as Argylla Formation has been tentatively mapped as Leichhardt Metamorphics (Derrick, 1978; Derrick & Wilson, in press; Wilson & Grimes, in press). Also, the validity of applying the name Argylla Formation to rocks in the Wonga Belt and west of the Leichhardt Metamorphics (Bottletree Formation) has recently been challenged (Blake, 1980).

Carter & others (1961) distinguished the Leichhardt Metamorphics from the Argylla Formation volcanics on the basis of the higher 'overall grade of metamorphism' and the grey colour of the former unit. Their use of field criteria to identify lithostratigraphic units is commendable, as the International Stratigraphic Guide requires that 'only major lithologic features readily recognizable in the field should serve as the basis for lithologic units' (Hedberg, 1976, p. 31). Unfortunately, the criteria of Carter & others are inadequate, as both formations are now known to have widely ranging and overlapping metamorphic grades and varied colours in shades of grey, pink, and brown. The discontinuous outcrop and structural complexity in the Mount Isa Inlier, coupled with the probability that in a volcanic region similar rock types would have been repeatedly extruded, make correlation difficult (Blake, 1980).

A geochemical sampling program was commenced in 1972 with one of its aims being the recognition of chemical differences between the Leichhardt Metamorphics and the Argylla Formation (Wilson, 1978). The sampling and analytical program was continued up to 1980, greatly increasing the amount of geochemical data. Over 200 specimens of felsic volcanics have been analysed for as many as 55 major and trace elements.

The main aim of this paper is to use the geochemical data and statistical techniques to define the chemical characteristics of the Leichhardt Metamorphics and the Argylla Formation, and to compare specimens from three sequences, the Ewen Block, Wonga Belt, and Bottletree Formation, that may or may not belong to either of these formations. The three graphical and two numerical techniques evaluated in this study are: (i) percentage frequency histograms, (ii) variation diagrams, (iii) element ratios, (iv) similarity coefficients, and (v) discriminant analysis.

Acknowledgements

The Bureau of Mineral Resources is acknowledged for providing most of the analytical results as a part of their contribution to the joint BMR/GSQ 1:100 000 mapping project. Special thanks are due to Dr G.M. Derrick (formerly of BMR) who was involved in the field work, and selection and submission of specimens for analysis. Dr L.A.I. Wyborn (BMR) also assisted with specimen submission and data presentation. Technical and computing assistance were provided by Mr S. Badgley (University of Queensland), and Mr P.R. Murphy (GSQ). Fruitful discussions have been held over the many years this project has spanned with Drs G.M. Derrick (Tenneco), R.W. Page, L.A.I. Wyborn, D.H. Blake (BMR), A. Ewart (U. of Qld), C.G. Murray (GSQ) and Messrs R.M. Hill and R.J. Bultitude (formerly BMR). This paper is published with the permission of the Director-General, Department of Mines, Queensland.

Analytical procedures

Specimens for analysis were selected from more than 1000 felsic volcanic rocks thin-sectioned during the mapping of the Mount Isa Inlier by the BMR and GSQ. Specimens that showed evidence of alteration such as patchy coloration, veining, and extreme schistosity were not analysed. As metamorphism throughout the sampled area is in the high greenschist or lower amphibolite facies (Derrick & others, 1977), some element mobility is to be expected (Burwash & Kupricka, 1969; Jolly & Smith, 1972; Condie & others, 1977), but, because each formation shows chemical coherence for specimens collected from widely spaced areas and covering a wide range of metamorphic conditions, alteration is considered to be insignificant or to have affected each formation in a uniform manner. This assumption is further justified by the preservation of recognisable 'igneous' trends in the geochemical data and limited variance. Except for some of the alkalis and alkaline earths, the elemental variations caused by alteration are believed to be less than the analytical errors, listed in Table 1.

[1] Geological Survey of Queensland, GPO Box 194, Brisbane, Queensland 40001

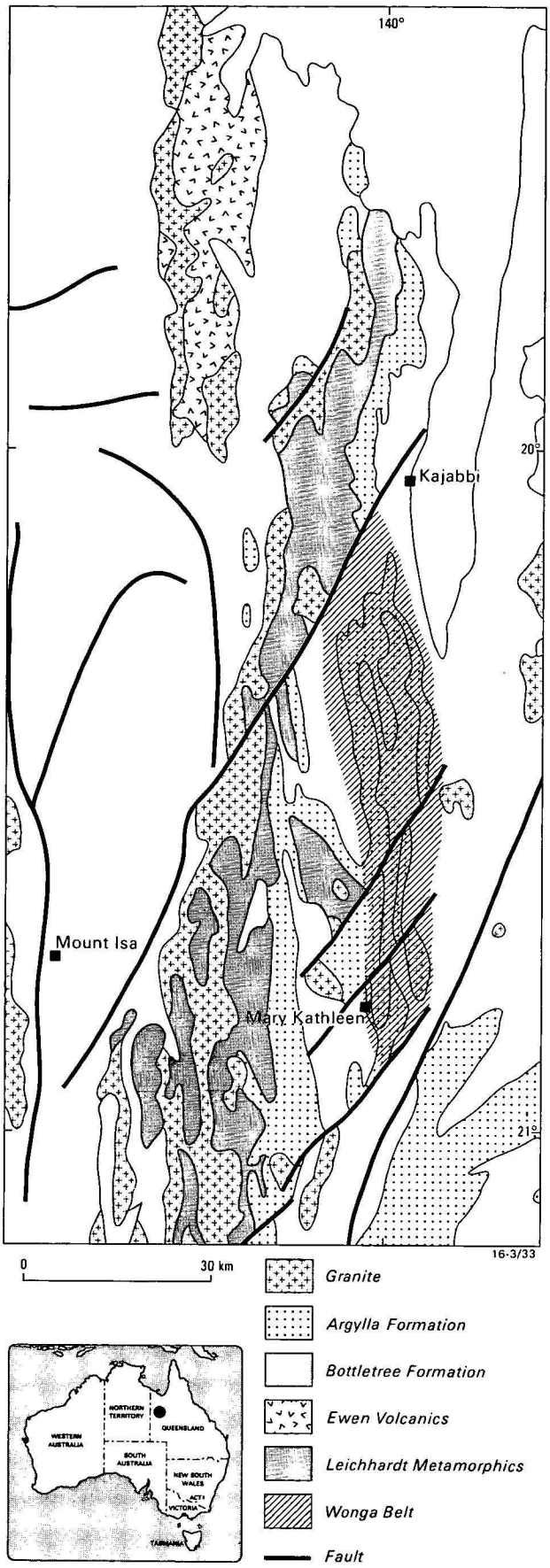

Figure 1. Locality map showing the older felsic volcanics and granites of the Mount Isa Inlier.

Table 1. Analytical methods and expected relative errors

Elements	*Method*	*Analyst*	*Relative error (%) at 68% Confidence Level*	
			Expected	*Calculated*
Si, Ti, Al, Fe, Mn, Ca, K, P	XRF*	AMDEL	3 or better	0.6–6.7
Mg, Na	AA*	"	3	4.3–6.3
Fe^{++}, H_2O^+, H_2O^-, CO_2, SO_3	Classic	"	5	2.2–40.5
As, Ba, Ce, La, Nb, Pb, Rb, Sc, Sn, Sr, Th, U, Y, Zr	XRF	"	5 or better	0.8–32.0
Ag, Au, Bi, Cd, Co, Cr, Cu, Mn, Mo, Ni, Pb, V, Zn	AA	"	5	4.3–35.6
Ba, Ce, La, Nb, Pb, Rb, Sn, Sr, Th, U, V, Y, Zr	XRF	BMR	5–10	1.5–14.0
Ba, Ce, Co, Cr, Cu, Nb, Nd, Ni, Pb, Rb, Sr, Th, Ti, U, V, Y, Zn, Zr	XRF	IHW	5	0.9–9.6
Ba, Bi, Hf, Mo, Nb, Pb, Sc, Sn, Th, Tl, U, W, Y, Zr and 14 REE	SSMS	IHW	3–5	0.0–22.5
B	Colorimetric	QGA	5	11.8
F	Selective ion-electrode	QGA	5	7.1

* Some of the more recent analyses by ICP.
AMDEL — Australian Mineral Development Laboratories; BMR — Bureau of Mineral Resources; IHW — I.H. Wilson; QGA — Queensland Government Analyst.

For discriminant analysis, training sets of 14 specimens were established from each formation, using the same SiO_2 class interval ($69\% < SiO_2 < 72\%$). This interval was chosen because: (i) it covers the modal class of each formation, (ii) it is wide enough to provide statistically significant sample size, and (iii) it is narrow enough to prevent variance within each formation swamping variance between the formations. To minimise the effects of SiO_2 variation within the chosen class interval, the distribution of samples within each set was made as close as possible by selecting pairs of analyses with essentially similar SiO_2 content.

Some analyses of As, Cr, Ni, and Sn were below the limit of detection of the methods used and, to remove bias by excluding these low values, values were interpolated from plots of cumulative percent probability versus log concentration, i.e. assuming a log-normal distribution of these elements (cf. Lepeltier, 1969). In the few cases where only total iron was reported, these values have been recalculated as FeO and Fe_2O_3, assuming the ratio $Fe_2O_3/FeO = 0.15$, as suggested by Green & others (1974).

The statistical analyses were performed by the SPSS processor on the Queensland Government Computer Centre Univac 1108 and by programs written by the author on the Queensland Mines Department GA minicomputer. Some diagrams for this paper were originally plotted at the Bureau of Mineral Resources, Canberra, using an HP 9825 desk-top computer and programs written by M. Owen.

Percentage frequency histograms

Wilson (1978) used percentage frequency histograms to show differences between the Leichhardt Metamorphics and Argylla Formation, especially for TiO_2, Al_2O_3, Fe_2O_3, CaO, K_2O, Nb, Sr, Th, Y and Zr. The examples shown in

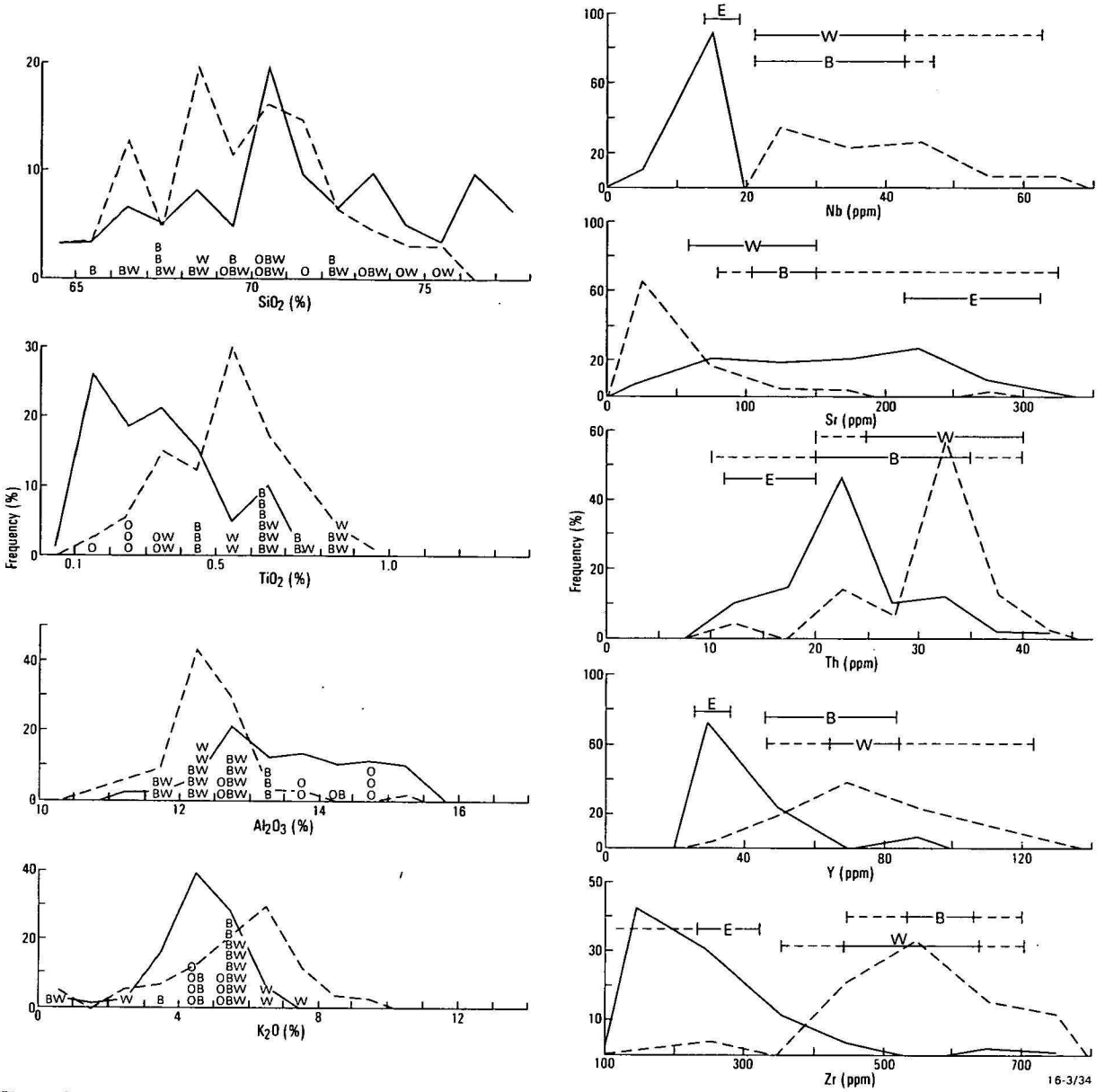

Figure 2. Percentage frequency histograms for Leichhardt Metamorphics (solid line) and Argylla Formation (dashed) compared to range of values from Ewen Block (E), Bottletree Formation (B) and Wonga Belt (W).
The solid part of the ranges represents the more frequent classes.

Figure 2 are based on all currently available data for these two formations. Compared to the Leichhardt Metamorphics, the Argylla Formation tends to be richer in TiO_2, K_2O, Nb, Th, Y, and Zr; and poorer in Al_2O_3 and Sr, and to a lesser extent SiO_2. This diagram indicates that unambiguous discrimination can be made using Nb, and less reliable discrimination is provided by Zr, Y, Th, Sr, Al_2O_3, and TiO_2. Most of the other elements analysed have considerably more overlap or have been analysed in few specimens and are of little use as discriminants.

Figure 2 also shows the distribution of specimens from the Ewen Block, the Bottletree Formation, and the Wonga Belt. For the major elements, each determination is shown, but for the trace elements, the total range and more frequent classes (solid line) are shown. There is good evidence that the specimens from the Ewen Block are related to the Leichhardt Metamorphics and that the Wonga Belt and Bottletree Formation specimens are similar to the Argylla Formation. It should be noted that the Bottletree Formation tends to overlap the Leichhardt Metamorphics distribution for Sr (and also CaO) and tends to have values between the peaks of the Leichhardt Metamorphics and the Argylla Formation distributions for some elements. On this basis, there are grounds for retaining the Bottletree Formation as a distinct unit, but none to doubt the correlation of the Ewen Block rocks with the Leichhardt Metamorphics or the Wonga Belt rocks with the Argylla Formation.

Variation diagrams

Variation diagrams enable graphical comparison of two or more sets of chemical data. Plots of oxides against SiO_2 (Harker, 1909) have been used widely. The main disadvantage of these plots is the effect of the constant sum of major oxides to approximately 100 percent. This introduces an apparent negative correlation component into these plots and can introduce positive correlations between other element pairs (Chayes, 1964; Cox & others, 1979).

A distinction between the Leichhardt Metamorphics and Argylla Formation can be seen in plots of TiO_2, Al_2O_3,

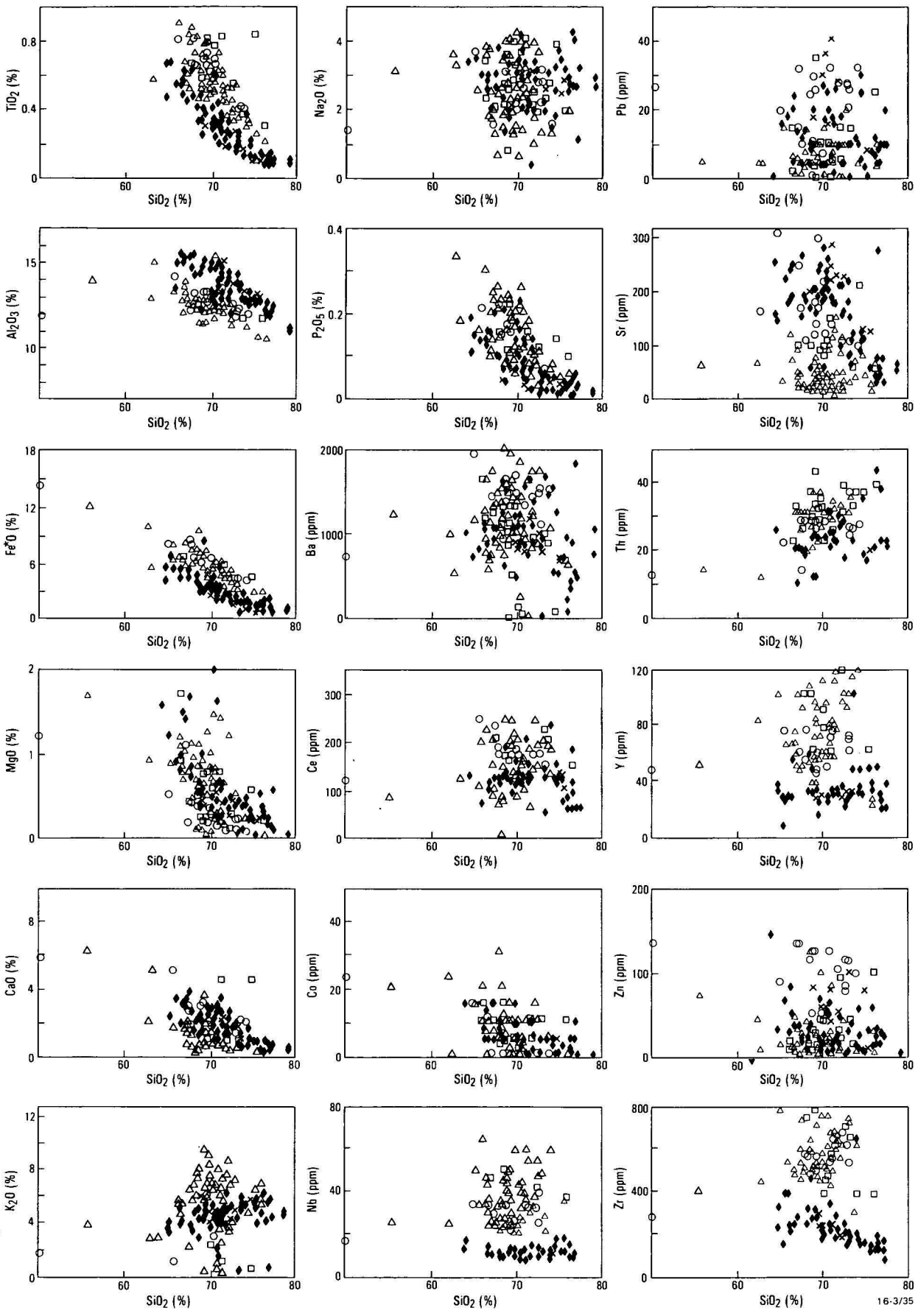

Figure 3. SiO_2 variation diagrams for felsic volcanic units.
Leichhardt Metamorphics (diamonds), Argylla Formation (triangles), Ewen Block (crosses), Bottletree Formation (circles), and Wonga Belt (squares).

Fe*O, K_2O, Ce, Nb, Pb, Sr, Th, Y, and Zr versus SiO_2 (Fig. 3). The examples show that some overlap is generally present, preventing classification of an individual unknown analysis, but allowing a more confident classification of a suite of unknown analyses than that provided by histograms. Several specimens from the Ewen Block, Bottletree Formation and Wonga Belt are also plotted in Figure 3. The Ewen Block specimens consistently plot within the fields defined by the analyses of Leichhardt Metamorphics and are generally clearly separated from the fields defined for the Argylla Formation. The specimens from the Wonga Belt mostly plot within the fields of the Argylla Formation, although some anomalous behaviour is observed. The specimens from the Bottletree Formation are also closely associated with the Argylla Formation, but generally contain more CaO, Pb, and Sr, and less K_2O than most specimens from the Argylla Formation. These compositional deviations of the Bottletree Formation specimens are consistent with a higher plagioclase/potash feldspar ratio, but could also be due to the removal of less Ca and related elements during alteration.

Element ratios

It has been stressed above that most elements show a strong correlation with SiO_2, either because of natural processes or (partly) because of the effect of closure of the system (Chayes, 1964: Cox & others, 1979). The effects of these correlations on the range of dependent element abundance can be restricted by choosing groups of analyses from a narrow range of SiO_2 values. Alternative numerical and graphical techniques to overcome this problem use the ratios of element abundances rather than individual element abundances. The ratio of two chemically related elements will in general vary considerably less than the abundance of each individual element during normal geological processes.

Where large amounts of data are involved, it is common to display ratio data in two element graphs, as used by Shaw (1968), Pearce & Cann (1973), and Floyd & Winchester (1975). Many other examples of the use of these plots occur in the geological literature. Distinction between the Leichhardt Metamorphics and the Argylla Formation can be achieved relatively easily with plots involving the most diagnostic elements such as Nb, Y, Sr, Ti, and Zr (Fig. 4).

An extension of this technique is the comparison of three elements in a triangular diagram. This approach was employed by Jack & Carmichael (1968) to 'fingerprint' felsic volcanic rocks using plots of Sr:Zr:Rb, Ba:Ti:Mn and Y:Nb:Pb. Pearce & Cann (1973) also used this approach to establish a classification scheme for mafic volcanic rocks. Some examples using Mount Isa data in plots of Sr:Zr:Rb, Ti:Mnx3:Ba, Y:Nb:Pb and Y:Nb:Zr/10 are presented in Figure 5. The specimens from the Ewen Block generally have ratios very similar to those of the Leichhardt Metamorphics, and the Bottletree Formation and Wonga Belt specimens generally have similar ratios to each other and the Argylla Formation. Ratios involving CaO, Pb, and Sr are exceptions to this generalisation for the Bottletree Formation.

Similarity coefficients

The similarity coefficient $d_{(A,B)}$ was introduced by Borchardt & others (1972) to allow easy geochemical identification of individual felsic tuff layers. The coefficient is defined: $d_{(A,B)}$

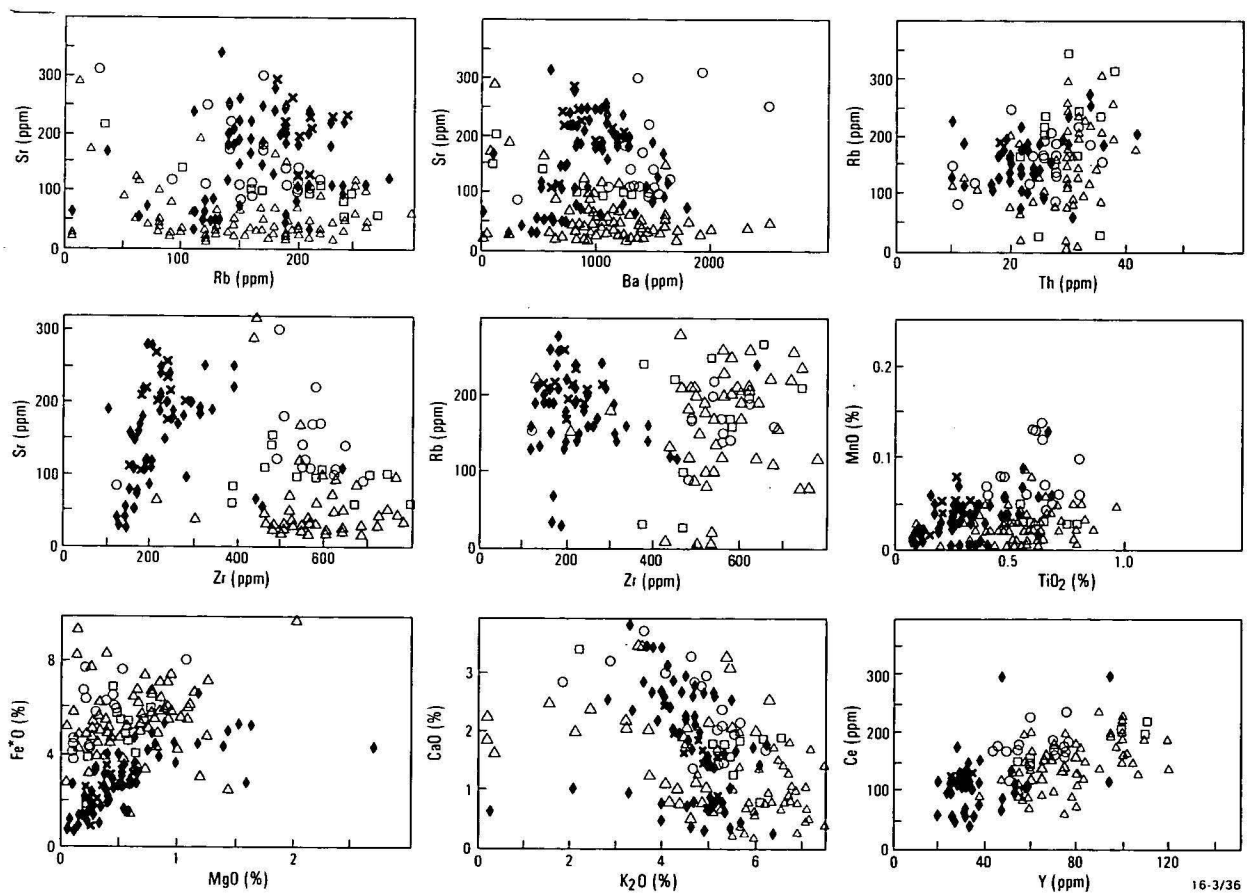

Figure 4. Two-element variation diagrams for felsic volcanic units.
(Symbols as Figure 3).

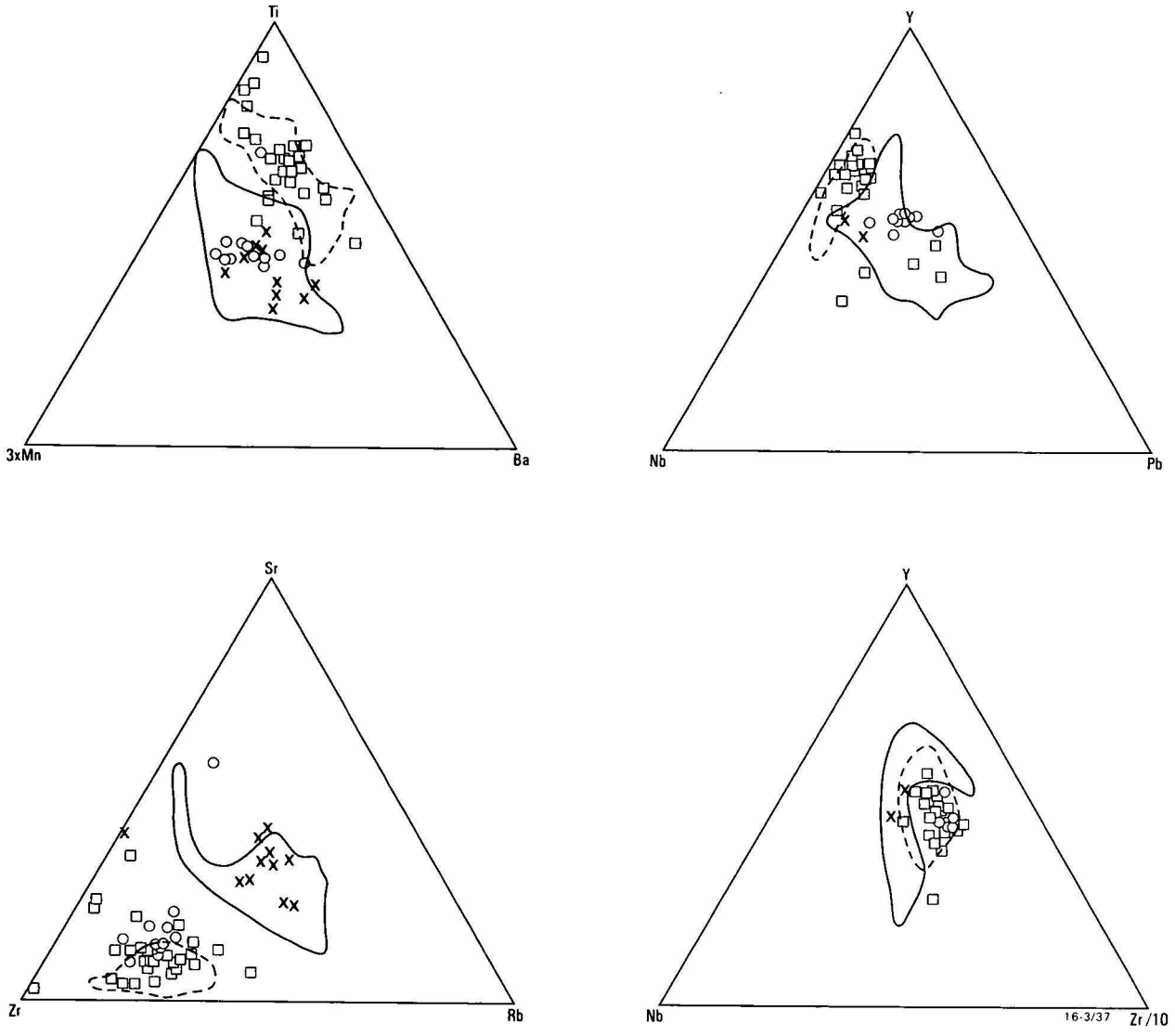

Figure 5. Triangular variation diagrams for felsic volcanic units.
Leichhardt Metamorphics field (solid) and Argylla Formation field (dashed), other symbols as Figure 3.

Table 2. Table of analytical error and weighting coefficient used in similarity coefficients

Element	*r*	*G*	*Element*	*r*	*G*	*Element*	*r*	*G*
SiO_2	.006	.952	K_2O	.067	.468	Rb	.025	.800
TiO_2	.024	.808	P_2O_5	.057	.548	Sn	.350	0
Al_2O_3	.015	.880	Ba	.030	.760	Sr	.025	.880
FeOt	.040	.680	Ce	.040	.680	Th	.200	0
MnO	.018	.856	Co	.100	.200	V	.050	.600
MgO	.043	.656	Nb	.100	.200	Y	.075	.400
CaO	.035	.720	Ni	.090	.280	Zn	.075	.400
Na_2O	.063	.500	Pb	.132	0	Zr	.015	.880

$= {}_{i=1}\Sigma^{l} R_i G_i / {}_{i=1}\Sigma^{l} G_i$, where R_i is the ratio of the i th element content (X_{iA} and X_{iB}) of two rocks A and B such that $R_i \leq 1$, and G_i is a weighting coefficient that decreases the influence on $d_{(A,B)}$ of ratios of elements that have poor analytical precision. For exactly similar analyses $d_{(A,B)} = 1$, but, in practice, closely related igneous rocks have $d_{(A,B)} > 0.8$. The derivation of G_i used here differs from that of the G_i used by Borchardt & others (1972) in that (i) analytic error is calculated on the sum of the relative errors, rather than the square root of the sum of the squares of the individual relative errors, (ii) a set of analytic errors is established, using replicate analyses of several Mount Isa volcanics, rather than calculating errors, which depend on the analytical precision of both A and B individually; and (iii) the maximum tolerable analytical error is set at 0.25. The formula used here for calculating G_i is $G_i = 1\text{-}2r/c$ unless $(1\text{-}2r/c)$ is negative, then $G_i = O$, where r = relative analytical error calculated from replicate pairs using a 68 per cent confidence level, and c = tolerable analytical error.

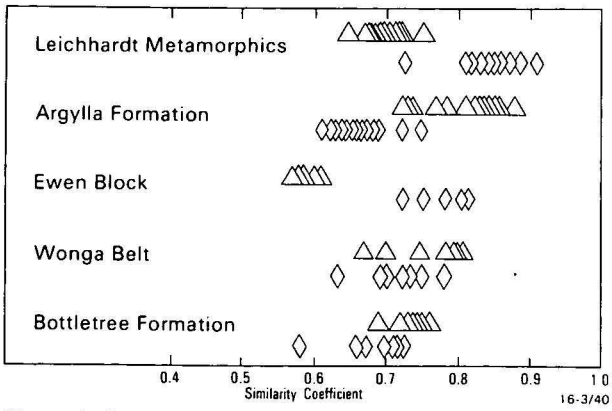

Figure 6. Some representative values of the similarity coefficient compared to the Leichhardt Metamorphics (diamonds) and the Argylla Formation (triangles).

Table 2 contains values of r and G_i for the Mount Isa felsic volcanic suite. Some examples of the range of $d_{(A, B)}$ values are given in Figure 6. It is evident that, compared with their respective means, individual analyses from a formation typically have similarity coefficients of greater than 0.80, whereas analyses from other formations rarely have similarity coefficients greater than 0.75.

The volcanics from the Ewen Block have much higher values of $d_{(A, B)}$ compared with the mean Leichhardt Metamorphics than compared with the mean Argylla Formation. The opposite is true for the volcanics from the Wonga Belt and the Bottletree Formation, although the difference is less marked.

Discriminant analysis

The object of this analysis is to find a linear combination of the variables (element abundances) that maximises the differences between sets of data. This linear combination is called a discriminant function and has the form $Di = d_{i1}Z_1 + d_{i2}Z_2 + \ldots\ldots + d_{ip}Z_p$, where Di = score on the i th discriminant function; d_{in} = weighting coefficient in the i th discriminant function for the n th discriminating variable (element); Z_n = standardised value of the n th discriminating variable (all variables are assumed to be normally distributed); and p = number of discriminating variables.

This function was calculated by computer, using the SPSS processor (Nie & others, 1975), following the method of Cooley & Lohnes (1971). The variables were selected in a stepwise fashion according to their ability to increase the value of Rao's V, which is a measure of the distance between the centroids of the two distributions in n-dimensional space. The selection criteria were the default values set by SPSS, i.e. tolerance = 0.001, partial F-to-enter = 1, and partial F-to-remove = 1.

A limit of 20 variables (elements) was imposed by the computer program used. Elements were selected to give maximum separation between the discriminant scores for the Leichhardt Metamorphics and Argylla Formation. This was accomplished by including elements whose means in the training sets from the two formations were determined to have the most significant differences by t-tests (Johnson & Leone, 1964). Although the variable is assumed to be normally distributed in the t-test, this assumption can be violated if the samples are of near equal size and the underlying populations have similar shape (Boneau, 1960). These requirements have generally been met in the training sets. The results of the t-tests for elements that were analysed in sufficient specimens are shown in Table 3. Uranium was excluded because of poor precision in some sets of data.

Because only two sets of data are being examined, only one discriminant function can be obtained, using a particular set of discriminating variables. This function is $D_1 = 1.92422 + 0.01763\ As - 0.00014\ Ba - 0.00838\ Ce + 0.01643\ Cu + 0.05205\ Nb - 0.00773\ Sr - 0.04672\ Th + 0.01067\ Y + 0.00269\ Zn$. Figure 7 displays histograms of the scores on this function for the Leichhardt Metamorphics, Argylla Formation, Ewen Block volcanics, Bottletree Formation, and Wonga Belt rocks. The success of the discrimination of the

Table 3. Means and standard deviations of each training set and t-test on difference of means

Element	*Leichhardt Metamorphics*			*Argylla Formation*			*t score*	*df*	*Significance of Null Hypothesis*
	No.	*Mean*	*Std. Dev.*	*No.*	*Mean*	*Std. Dev.*			
SiO_2	14	70.59	0.98	14	70.55	1.14	0.10	26	0.914
TiO_2	14	0.33	0.06	14	0.54	0.11	−6.27	20.1	0.000
Al_2O_3	14	13.76	0.86	14	12.14	0.41	6.36	18.6	0.000
Fe_2O_3	14	0.77	0.22	14	2.20	1.41	−3.75	13.6	0.002
FeO	14	2.46	0.66	14	2.68	1.55	−0.49	17.6	0.60
MnO	14	0.02	0.01	14	0.02	0.01	0.69	26	0.500
MgO	14	0.64	0.33	14	0.48	0.33	1.28	26	0.25
CaO	14	2.57	0.53	14	1.05	0.61	7.15	26	0.000
Na_2O	14	2.81	0.66	14	2.36	0.57	1.93	26	0.07
K_2O	14	4.51	0.55	14	6.31	0.94	−6.18	21.0	0.000
P_2O_5	14	0.11	0.03	14	0.13	0.05	−1.28	21.3	0.25
H_2O^+	14	0.64	0.17	14	0.71	0.41	−0.59	17.3	0.55
H_2O^-	4	0.14	0.09	7	0.18	0.07	−1.55	9	0.140
As	10	7.7	5.3	8	4.0	4.6	1.58	16	0.150
Ba	14	1135.0	190.0	14	1325.0	367.0	−1.72	19.5	0.110
Ce	11	129.0	15.0	11	138.0	50.0	−0.57	11.8	0.60
Co	14	6.5	3.25	13	6.3	3.8	0.15	25	0.15
Cr	14	48.0	45.0	10	47.0	22.0	0.07	18.9	0.95
Cu	14	14.2	24.3	14	8.4	9.9	0.83	17.2	0.43
La	10	67.4	10.4	6	78.6	20.8	−1.23	19.1	0.28
Nb	11	10.9	1.8	11	34.0	8.0	−9.34	11.0	0.000
Nd	2	60.0	2.8	2	53.0	23.0	0.43	2	0.707
Ni	12	3.8	1.5	9	3.0	2.0	0.97	19	0.344
Pb	13	11.5	6.9	12	12.1	19.9	−0.10	14.3	0.93
Rb	14	154.6	27.0	14	160.0	45.0	−0.39	21.3	0.70
Sn	11	4.7	5.7	9	6.0	3.1	−0.60	18	0.554
Sr	14	192.0	47.5	14	31.3	8.8	12.45	13.9	0.000
Th	11	23.0	3.4	11	31.2	3.0	−6.00	20	0.000
U	10	3.8	1.4	10	7.0	2.1	−4.01	18	0.000
V	9	17.1	3.0	6	15.7	13.7	0.25	5.3	0.809
Y	11	33.0	7.9	11	74.3	12.1	−9.48	20	0.000
Zn	14	24.9	18.9	13	12.4	8.1	2.26	13.9	0.04
Zr	11	254.0	60.6	11	583.0	88.0	−10.21	20	0.000

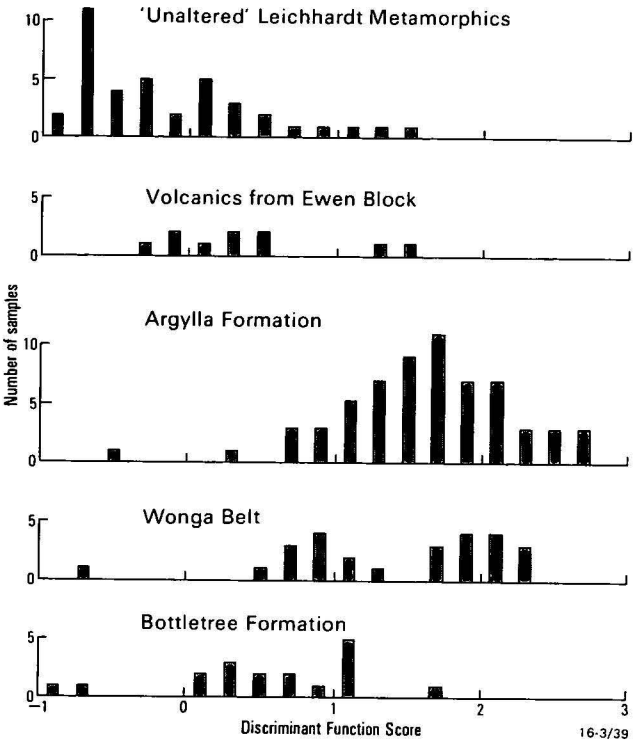

Figure 7. Histogram of discriminant function scores for the Leichhardt Metamorphics, Argylla Formation, Ewen Block, Bottletree Formation, and Wonga Belt.

Leichhardt Metamorphics and the Argylla Formation is obvious. About 80 per cent of the Ewen Block specimens are classified as Leichhardt Metamorphics and almost all the Wonga Belt specimens are classified as Argylla Formation. The Bottletree Formation scores occur mainly in the range where the Argylla Formation and Leichhardt Metamorphics cannot be distinguished.

Conclusions

The statistical treatment of chemical analyses of the Leichhardt Metamorphics and the Argylla Formation indicates that it is possible to distinguish between these formations by a variety of techniques, including histograms, variation diagrams, ratios, similarity coefficients, and discriminant analysis. When attempting to assign analyses from an unknown suite to either of these two formations, it must be stressed that the unknown suite may belong to a completely different unit. Examination of a large number of variables minimises the chance of mistaken correlation. For this reason a large number of histograms, variation diagrams, and simple ratios should be examined. Computer plotting and multivariate statistics such as similarity coefficients and discriminant analysis remove some of the tedium of such investigations.

Histograms, variation diagrams, and t-tests indicate which elements may be of use in the more elaborate discrimination tests. The similarity coefficient is relatively simple to compute and, because it is a non-parametric statistical function, it requires no particular element distribution pattern. It can easily compare a multi-element analysis of a single specimen with another individual specimen or with mean values from well-studied suites. This technique requires a relatively large range of accurately analysed elements. Discriminant analysis can discriminate units, but it requires extensive computation as well as a wide range of analysed elements. It has been possible to separate the Leichhardt Metamorphics and the Argylla Formation simply by accurate Nb determinations, but histograms of this element alone are unlikely to detect if a third unit is present. When a large body of test data is available, variation diagrams are easy to prepare and successfully distinguish between the Leichhardt Metamorphics and the Argylla Formation. All methods clearly indicate the affinities of the specimens from the Ewen Block to the Leichhardt Metamorphics and the Wonga Belt to the Argylla Formation. The Bottletree Formation shows some similarities to the Argylla Formation, but could represent a distinct unit.

References

Blake, D.H., 1980 — The early geological history of the Proterozoic Mount Isa Inlier, northwestern Queensland: an alternative interpretation. *BMR Journal of Australian Geology & Geophysics*, 5, 243–256.

Boneau, C.A., 1960 — The effects of violating of assumptions underlying the t-test. *Psychological Bulletin*, 77, 49–64.

Borchardt, G.A., Aruscavage, P.J., & Millard, H.T., 1972 — Correlation of the Bishop Ash, a Pleistocene marker bed, using instrumental neutron activation analysis. *Journal of Sedimentary Petrology*, 42, 301–306.

Burwash, R.A., & Kupricka, J., 1969 — Cratonic reactivation in the Precambrian basement of western Canada. 1. Deformation and chemistry. *Canadian Journal of Earth Sciences*, 6, 1381–1396.

Carter, E.K., Brooks, J.H., & Walker, K.R., 1961 — The Precambrian mineral belt of north-western Queensland. *Bureau of Mineral Resources, Australia, Bulletin* 51.

Chayes, F., 1964 — Variance–covariance relations in some published Harker diagrams of volcanic suites. *Journal of Petrology*, 219–237.

Condie, K.C., Viljoen, M.J., & Kable, E.J.D., 1977 — Effects of alteration on element distributions in Archean tholeiites from the Barberton Greenstone Belt, South Africa. *Contributions to Mineralogy and Petrology*, 64, 75–89.

Cooley, W.W., & Lohnes, P.R., 1971 — Multivariate data analysis. *Wiley & Sons, New York.*

Cox, K.G., Bell, J.D., & Pankhurst, R.J., 1979 — The interpretation of igneous rocks. *Allen & Unwin, London.*

Derrick, G.M., 1978 — Mount Isa–Cloncurry Project. *In* Geological Branch Summary of Activities 1977. *Bureau of Mineral Resources, Australia, Report* 208, 142–152.

Derrick, G.M., & Wilson, I.H., in press — Alsace, Queensland. *Bureau of Mineral Resources, Australia, 1:100 000 Geological Map Commentary.*

Derrick, G.M., Wilson, I.H., Glikson, A.Y., Hill, R.M., & Mitchell, J.E., 1977 — Geology of the Mary Kathleen 1:100 000 Sheet area, Queensland. *Bureau of Mineral Resources, Australia, Bulletin* 193.

Floyd, P.A., & Winchester, J.A., 1975 — Magma type and tectonic setting discrimination using immobile elements. *Earth and Planetary Science Letters*, 27, 211–218.

Green, D.H., Edgar, A.D., Beasley, P., Kiss, E., & Ware, N.G., 1974 — Upper mantle source for some hawaiites, mugearites, and benmoreites. *Contributions to Mineralogy and Petrology*, 48, 33–43.

Harker, A., 1909 — The natural history of igneous rocks. *Macmillan, New York.*

Hedberg, H.D., (editor), 1976 — International stratigraphic guide, *Wiley, New York.*

Jack, R.N., & Carmichael, I.S.E., 1968 — The chemical 'fingerprinting' of acid volcanic rocks. *California Division of Mines, Special Report* 100, 17–32.

Johnson, N.L., & Leone, F.C., 1964 — Statistics and experimental design in engineering and the physical sciences. Volume 1. *Wiley, New York.*

Jolly, W.T., & Smith, R.E., 1972 — Degradation and metamorphic differentiation of the Keweenawan tholeiitic lavas of Northern Michigan, U.S.A. *Journal of Petrology*, 13, 273–309.

Lepeltier, C.A., 1969 — A simplified statistical treatment of geochemical data by graphical representation. *Economic Geology*, 64, 538–550.

Nie, N.H., Hull, C.H., Jenkins, J.G., Steinbrenner, K., & Bent, D.H., 1975 — SPSS, Statistical package for the social sciences (2nd edition). *McGraw-Hill, New York*.

Page, R.W., 1978 — Response of U-Pb zircon and Rb-Sr total-rock and mineral systems to low-grade regional metamorphism in Proterozoic igneous rocks, Mount Isa, Australia. *Journal of the Geological Society of Australia*, 25, 141–164.

Pearce, J.A., & Cann, J.R., 1973 — Tectonic setting of basic volcanic rocks determined using trace element analyses. *Earth and Planetary Science Letters*, 19, 290–300.

Plumb, K.A., & Derrick, G.M., 1975 — Geology of the Proterozoic rocks of northern Australia. *In* Knight, C.L. (editor), Economic geology of Australia and Papua New Guinea. Volume 1 — Metals. *Australasian Institute of Mining and Metallurgy, Monograph* 5, 217–252.

Plumb, K.A., Derrick, G.M., & Wilson, I.H., 1980 — Precambrian geology of the McArthur River–Mount Isa region, northern Australia. *In* Henderson, R.A., & Stephenson, P.J. (editors), The geology and geophysics of northeastern Australia. *Geological Society of Australia (Queensland Division), Brisbane*, 71–88.

Shaw, D.M., 1968 — A review of K-Rb fractionation trends by covariance analysis. *Geochimica et Cosmochimica Acta*, 32, 573–602.

Wilson, I.H., 1978 — Volcanism on a Proterozoic continental margin in northwestern Queensland. *Precambrian Research*, 7, 205–235.

Wilson, I.H., & Grimes, K.G., in press — Myally, Queensland. *Bureau of Mineral Resources, Australia, 1:100 000 Geological Map Commentary*.

BMR Journal of Australian Geology & Geophysics, 8, 119-128

ARCHAEAN AND PROTEROZOIC GEOLOGICAL RELATIONSHIPS IN THE VESTFOLD HILLS–PRYDZ BAY AREA, ANTARCTICA

J.W. Sheraton & K.D. Collerson[1].

The Archaean cratonic block of the Vestfold Hills, Princess Elizabeth Land is one of only three well-documented examples in East Antarctica. It is characterised by tectonically interlayered tonalitic to granitic orthogneisses (Mossel gneiss) and garnetiferous paragneisses (Chelnok supracrustal assemblage) as well as subordinate units of predominantly mafic granulite (Tryne metavolcanics). This sequence is cut by a second suite of orthogneisses (Crooked Lake gneiss), ranging in composition from gabbro-diorite to tonalite and granite, which was emplaced synchronously with the last major phase of deformation. Cutting the gneisses are several suites of Proterozoic tholeiitic dykes, including a high-Mg suite, which range in age from about 2350 Ma to 1300 Ma. Most dykes are unmetamorphosed, but, in the southwestern part of the Vestfold Hills, high-pressure garnet-bearing assemblages developed during a late Proterozoic (about 1100 Ma) thermal event. Granulite facies gneisses that crop out southwest of the Vestfold Block, along the coast of Prydz Bay, show the regional effect of this younger metamorphism and form part of an extensive late Proterozoic high-grade terrain, which makes up much of the East Antarctic Shield. Gneisses in the Rauer Group of Islands, within 30 km of the Vestfold Hills, are lithologically similar (predominantly orthogneisses) to those of the Vestfold Block, and contain metamorphosed relics of Vestfold dykes; however, they include only a minor component derived by remetamorphism of Archaean continental crustal rocks. In contrast, gneisses further to the southwest were mainly derived from aluminous sedimentary protoliths, and are quite different in composition to those of the Vestfold Block and Rauer Group. They do not appear to have been intruded by mafic dykes (mafic granulite is very rare) and apparently represent a Proterozoic cover sequence of similar age to metasedimentary sequences in MacRobertson Land. Intrusion of locally fayalite- bearing granitic rocks took place about 500 Ma ago.

Introduction

Several Archaean cratonic blocks have been recognised in the East Antarctic Precambrian Shield in recent years: they include the Napier Complex of Enderby Land (Grikurov & others, 1976; Sheraton & others, 1980), much of the southern Prince Charles Mountains of MacRobertson Land (Tingey, 1982), and the Vestfold Hills of Princess Elizabeth Land (Collerson & Arriens, 1979; Oliver & others, 1982a; Collerson & others, in press). The Archaean blocks are separated by an extensive late Proterozoic high-grade terrain (Fig. 1), but the extent to which these younger metamorphics comprise remetamorphosed Archaean is difficult to establish, in view of the poor exposure and limited isotopic data.

Rb-Sr and Sm-Nd dating has indicated ages of between about 2400 and 3000 Ma for granulite-facies gneisses in the Vestfold Block (Collerson & Arriens, 1979; Collerson & others, in press). Dolerite dykes that cut these gneisses have given ages of between about 2350 and 1300 Ma (Arriens, 1975; unpublished data). Most of these dolerites belong to the same suites as those that cut Napier Complex metamorphics in Enderby Land, almost 1000 km to the west (Sheraton & Black, 1981). Late Proterozoic metamorphic rocks that crop out to the southwest of the Vestfold Hills, along the coast of Prydz Bay (Fig. 2), are also of granulite facies, but are not cut by dolerites (Tingey, 1981). Only in the Rauer Group of Islands, about 30 km southwest of the Vestfold Block, can such dykes be recognised in a disrupted state, suggesting remetamorphism of Vestfold Block gneisses. This younger tectonothermal event has been dated by P.A. Arriens at 1073 ± 111 Ma (initial $^{87}Sr/^{86}Sr$ 0.7086 ± 0.0013) in felsic gneisses from Filla Island (Tingey, 1981). The contact between the Archaean and Proterozoic terrains is not exposed, being hidden under the Sørsdal Glacier, but transitional relationships can be observed on one island of the Rauer Group immediately south of the Sørsdal Glacier. In the southwestern part of the Vestfold Block, both country rocks and dykes were extensively recrystallised under high-grade conditions during the Late Proterozoic event, although there was only limited associated deformation (development of shear zones).

An extensive sampling program was undertaken in the Vestfold Hills–Prydz Bay area during December 1980 and January 1981 with the object of comparing the chemical and petrographic features of the Archaean rocks of the Vestfold Hills with those of the late Proterozoic metamorphics to the southwest. In this paper, metamorphic and lithological relationships of the two terrains are compared and contrasted. The chemical and isotopic characteristics will be considered elsewhere.

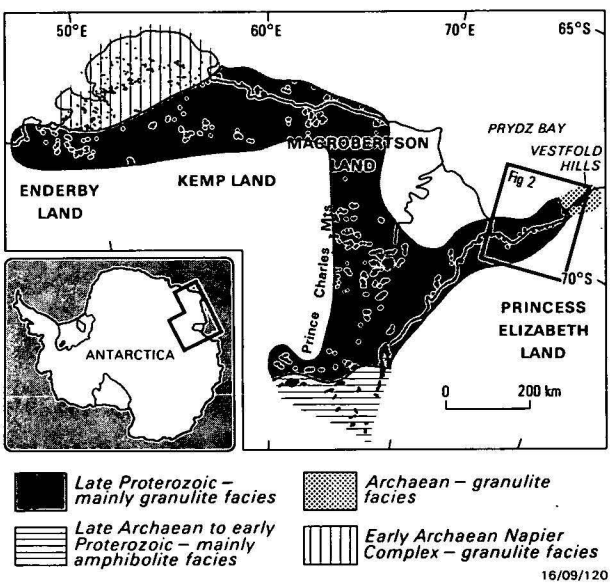

Figure 1. Map of part of East Antarctica, showing metamorphic complexes and outcrops (black).
Late Proterozoic metamorphics in the northern part of the southern Prince Charles Mountains are greenschist to amphibolite facies: metamorphic rocks of this age in Enderby Land are classified as Rayner Complex. All complexes except the late Proterozoic are intruded by abundant essentially undeformed tholeiite dykes.

Archaean metamorphics

Archaean metamorphics of the Vestfold Block were subdivided by Oliver & others (1982a) into 4 major units: layered 'grey gneiss', layered paragneiss, and two types of felsic orthogneiss (homogeneous, and with a diffuse layering). This classification was subsequently revised by Collerson & others (in press), who erected a relative chronology based on

[1] Research School of Earth Sciences, Australian National University, GPO Box 4, Canberra, ACT 2601

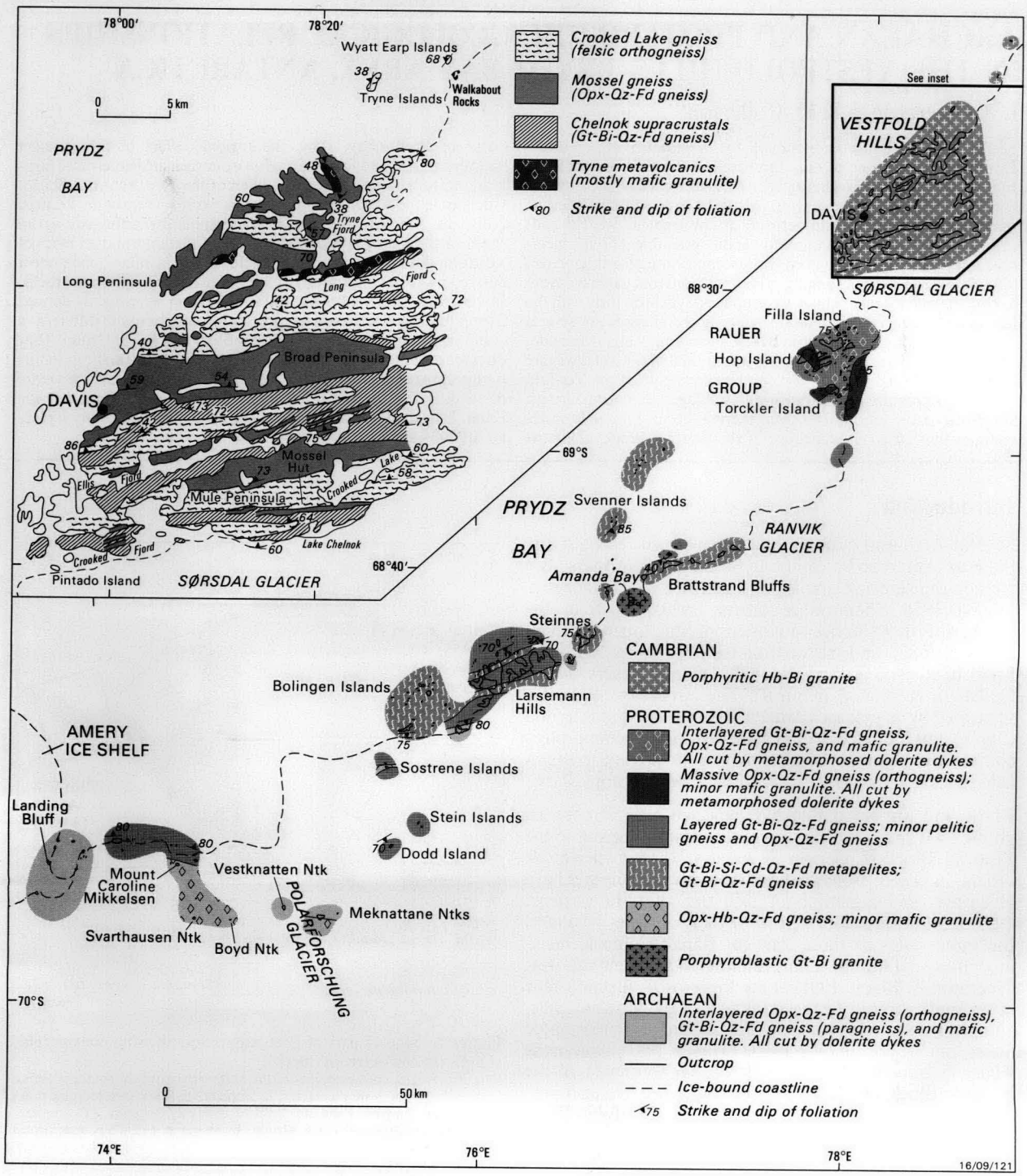

Figure 2. Geological map of the Vestfold Hills and Prydz Bay coast.

field relationships (Table 1), which is used in the following brief descriptions. Details of the structural evolution of the Vestfold Block have been given by Oliver & others (1982a) and Parker & others (1982), and of the conditions of metamorphism by Collerson & others (1983).

Mafic rocks (Tryne metavolcanics and subordinate mafic units within the Chelnok supracrustal assemblage).

The Tryne metavolcanics are the oldest, predominantly mafic, rocks recognised in the Vestfold Block. They occur in different states of preservation, as mappable units up to 0.5 to 1 km wide (Fig. 3), as boudinaged xenoliths or tectonic intercalations within the felsic Mossel gneiss (Fig. 4), and as xenoliths within the Crooked Lake gneiss (Fig. 5). They are medium to fine grained and commonly exhibit a layering defined either by deformed primary (felsic to mafic) compositional variations or by predominantly tonalitic (using the classification of Streckeisen, 1976) partial melts (Fig. 6). Although most of the mafic units were probably derived from volcanic protoliths, minor fragmented occurrences of pyroxenite, metagabbro, and metaleucogabbro suggest the presence of differentiated plutonic bodies within the sequence (Fig. 7). Mafic granulite layers consist of orthopyroxene (10–25%), clinopyroxene (5–30%), greenish-brown hornblende (up to 30%), reddish-brown biotite (up to 10%), plagioclase (50–60%), opaque minerals (up to 3%), and

Table 1. Geological history of Vestfold Hills–Prydz Bay area.

Event	Metamorphism	Approx. age (Ma)
1. Extrusion of protoliths of Tryne metavolcanics; deposition of Chelnok supracrustals; intrusion of mafic bodies.		> 3000?
2. High-grade metamorphism and deformation (D_1): partial melting of Tryne metavolcanics and formation of Mossel gneiss (mostly tonalitic).	Granulite facies	about 3000
3. Intrusion of mafic dykes.		
4. Emplacement of dioritic to granitic intrusives (Crooked Lake gneiss) and localised partial melting of older units; deformation (D_2).		2400–2500
5. Formation of steeply-dipping shear zones (D_3).		
6. Intrusion of high-Mg tholeiitic dykes.		about 2350
7. Intrusion of dolerite dykes.		about 1850
8. Deposition of sediments; emplacement of granitic intrusives.		
9. Intrusion of abundant dolerite dykes of at least two distinct suites.		about 1300
10. Deposition of sediments, including pelitic and psammitic types.		
11. Emplacement of tonalitic to granitic intrusives; deformation and high-grade metamorphism in rocks of the Prydz Bay coast; localised high-pressure metamorphism in southwestern part of Vestfold Hills, but only minor deformation.	Granulite facies	about 1100
12. Intrusion of granitic pegmatites.		
13. Emplacement of hornblende-biotite granite (Landing Bluff and Polarforschung Granites).		500
14. Intrusion of alkaline dykes, including lamprophyres.		

minor quartz, apatite and K-feldspar. A sample (81285364) from east of Pintado Island, in the extreme southwest of the Vestfold Hills, contains secondary garnet rimming pyroxene. Felsic layers are commonly of tonalitic composition, and contain up to 30 per cent quartz in addition to plagioclase, clinopyroxene, orthopyroxene, and minor hornblende, biotite, and Fe-Ti oxides.

Layered paragneiss (Chelnok supracrustal association).

Paragneiss is widespread in the southern half of the Vestfold Block (Fig. 2), where it forms tectonic units of variable thickness, interlayered on a regional and local scale with Mossel gneiss (Fig. 8). The most abundant, commonly migmatitic, varieties are semi-pelitic in composition, and include biotite-garnet-quartz-feldspar gneiss and biotite-orthopyroxene-garnet-quartz-feldspar gneiss. Unlike the Mossel and Crooked Lake gneisses, most contain abundant perthite, although a few have more sodic compositions. Garnet commonly makes up less than 10 per cent of the gneiss, but in a few layers, reaches 60 per cent (Fig. 9). Reddish-brown biotite (3–10%) is widespread, but other aluminous minerals (cordierite, sillimanite, and spinel) are rare, in marked contrast to the late Proterozoic metasediments of the Prydz Bay coast. Sapphirine-bearing assemblages have been reported by Collerson & others (in press), but, unlike those in Enderby Land, do not include either quartz or osumilite (cf. Sheraton & others, 1980). Oliver & others (1982a) and Collerson & others (in press) have reported the localised occurrence of orthopyroxene-cordierite-quartzite, calc-silicate (scapolite + diopside + quartz ± sphene) gneiss, marble, and quartz-magnetite rocks.

Superimposed, late Proterozoic metamorphism in the southwestern Vestfold Hills is reflected in the development of secondary garnet around orthopyroxene grains, and in extensive recrystallisation of quartz and feldspar.

Layered orthopyroxene-quartz-feldspar gneiss (Mossel gneiss).

This unit forms a major part of the layered gneiss complex in the Vestfold Block (Fig. 2, 10). It is composed of a number of components, including layered quartzo-feldspathic orthogneiss with intrafolial folds, sheets of homogeneous orthogneiss, boudins of mafic granulite, and discordant pegmatite veins, which contain blue quartz, plagioclase, and orthopyroxene. It has been shown by Collerson & others (in press) that part of the felsic component of Mossel gneisses formed by partial melting of Tryne metavolcanic mafic units. The latter show clear evidence of in situ anatexis (Fig. 11) and commonly occur as xenoliths in Mossel gneiss in areas of relatively low strain (Fig. 12).

The Mossel gneiss is predominantly biotite-orthopyroxene tonalite, with subordinate granodiorite and granite. Tonalitic gneiss contains orthopyroxene (4–14%), reddish-brown biotite (up to 7%), quartz (10–35%), plagioclase (45–70%) and minor perthite, opaque minerals, apatite, and zircon. Granitic gneiss contains abundant perthite, but less orthopyroxene and biotite. In contrast to the Crooked Lake gneiss, clinopyroxene and hornblende are generally present in only minor amounts.

Felsic orthogneiss (Crooked Lake gneiss).

This unit intrudes all the previously discussed groups and is one of the most abundant in the Vestfold Hills (Fig. 2). It commonly has sharp, semi-concordant contacts (Fig. 13) and, according to Oliver & others (1982a) and Collerson & others (in press), was emplaced synkinematically with the period of deformation (D_2) that resulted in the development of macroscopic folds in the layered gneisses. In areas where the effects of this deformation are strong, i.e. Mule Peninsula and Broad Peninsula, the Crooked Lake gneiss shows a pronounced diffuse layering, a simple anastomosing schistosity, and variably developed elongation lineation (Fig. 14). However, elsewhere, particularly on Long Peninsula, where deformation was less intense, the gneiss appears more massive and commonly exhibits only a weak fabric (Fig. 15). Country rock (Fig. 5, 16) and cognate xenoliths are abundant near contacts, and commonly aligned parallel to the contacts.

The most abundant lithology is tonalitic, quartz dioritic, and dioritic orthogneiss; more potassic varieties (granite, granodiorite, monzonite, etc) are less common, and contain perthite, which locally approaches mesoperthite in composition. Both perthite and plagioclase (commonly antiperthite) locally form porphyroblasts. Orthopyroxene, clinopyroxene, green to greenish-brown hornblende, and brown to reddish-brown biotite each form up to 15 per cent of the most melanocratic orthogneiss. Hornblende is relatively more abundant in diorite, and clinopyroxene in diorite and tonalite; they tend to be present in only minor amounts in granite, in which orthopyroxene is the predominant mafic mineral. However, orthopyroxene commonly shows marginal alteration to biotite (with minor hornblende) and quartz. Feldspar and quartz are locally recrystallised to a fine-grained granoblastic mosaic. Accessory minerals comprise opaque oxides (up to 2%), apatite, and zircon.

Figure 3. Tryne metavolcanics cut by Crooked Lake gneiss and dolerite dyke, Tryne Crossing.

Figure 4. Boudinaged Tryne metavolcanic layer in Mossel gneiss, Mule Peninsula.

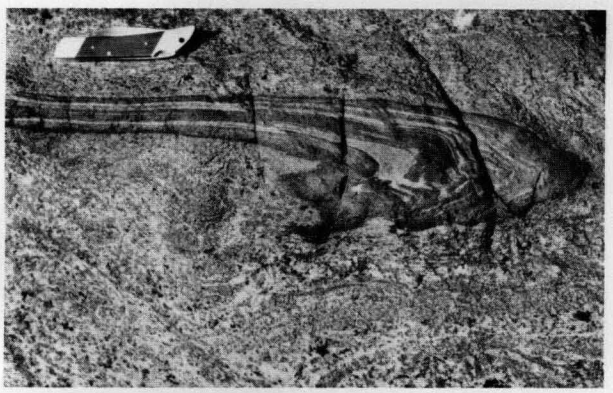

Figure 5. Folded Tryne metavolcanic xenolith in Crooked Lake gneiss, Mule Peninsula.

Figure 6. Migmatitic Tryne metavolcanics, Tryne Crossing.

Figure 7. Boudinaged metagabbro layer in Mossel gneiss, Long Peninsula.

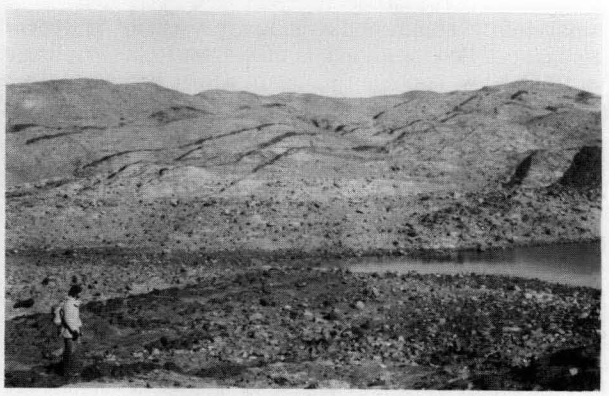

Figure 8. Contact between Chelnok supracrustals (light colour) and Mossel gneiss, cut by dolerite dykes, Broad Peninsula.

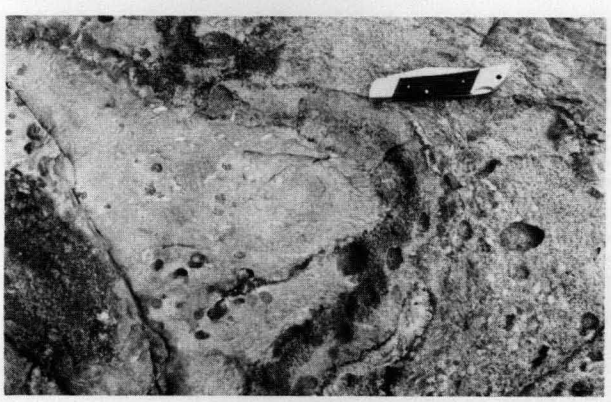

Figure 9. Primary layering in garnet-rich Chelnok metapelite, Mule Peninsula.

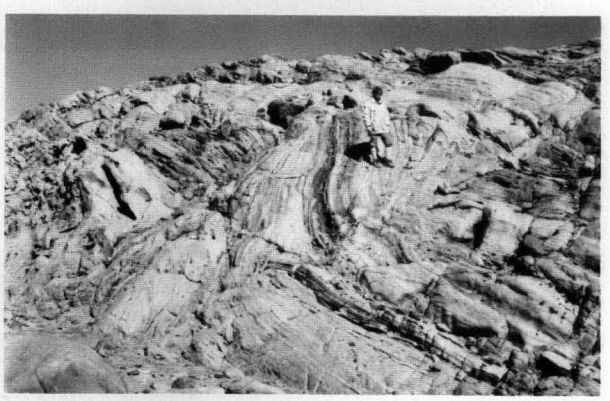

Figure 10. Monoclinal fold (F_3) in Mossel gneiss, Broad Peninsula.

Mafic dykes

Apart from a few early folded and metamorphosed mafic dykes (Fig. 17), the majority of dykes cutting Archaean gneisses of the Vestfold Block are essentially unmetamorphosed and form a dense swarm with a predominant north- south orientation (Fig. 18). Only in the southwestern part of the area do the effects of the late Proterozoic metamorphism become pronounced.

The most abundant are dolerites with subophitic to gabbroic textures. Clinopyroxene (augite or subcalcic augite: 30–40%), zoned reddish-clouded plagioclase (commonly An_{55-70}: 55–60%), and opaque minerals (ilmenite, magnetite, and rare pyrite, pyrrhotite, and chalcopyrite: 3–7%) are major constituents, and small amounts of dark green to greenish-brown hornblende, dark brown or reddish-brown biotite, quartz, and apatite are commonly present. One sampled dyke (81285246) contains about 5 per cent hypersthene with overgrowths of augite, and a few contain pigeonite; some quartz-free dykes contain minor rather altered olivine, and these are commonly porphyritic, with plagioclase phenocrysts. Preliminary Rb-Sr dating has indicated an age of about 1300 Ma for the majority of the dolerites, although one chemically distinct suite is significantly older (about 1850 Ma: unpublished data). The Amundsen Dykes of Enderby Land are petrographically similar, and one group has been dated at 1190 ± 200 Ma (Sheraton & Black, 1981).

Many dolerites show some degree of uralitisation of pyroxene, but in the southwestern part of the Vestfold Hills, particularly between Crooked and Ellis Fjords, all mafic dykes examined have been metamorphosed during the late Proterozoic event. Such metadolerites have granuloblastic textures and are generally fine-grained (about 0.1 mm), although relict igneous phases (e.g. clinopyroxene porphyroclasts) have locally survived. They contain pyroxene (orthopyroxene and clinopyroxene, up to 30%), dark greenish-brown hornblende (5–15%), reddish-brown biotite (up to 5%), plagioclase (35–55%), Fe-Ti oxides (2–5%), and minor quartz and apatite. Metadolerites in the extreme southwest (in and around Crooked Fjord) also contain up to 25 per cent garnet, which forms poikiloblastic aggregates 1–2 cm across associated mainly with clinopyroxene, surrounded by areas rich in hornblende, pyroxene, and plagioclase. However, its distribution is extremely patchy, some parts of individual dykes being full of garnet-rich spots, whereas others, a few metres away, are essentially garnet-free. Garnet development is not simply a function of degree of deformation, as many garnet-rich metadolerites show little evidence of deformation. A largely recrystallised hornblende pyroxenite dyke (81285368), from Kazak Island, chemically an olivine tholeiite, consists of clinopyroxene + orthopyroxene (50%), brown hornblende (40%), plagioclase (10%), and minor biotite and opaque oxides.

The other major group of mafic intrusives are high-Mg dykes, petrographically identical to a suite of tholeiites in Enderby Land; both have given Rb-Sr isochron ages of about 2350 Ma (Sheraton & Black, 1981; unpublished data), consistent with cross-cutting relationships that indicate that they predate the dolerite and hornblende pyroxenite dykes. The high-Mg dykes are characterised by abundant orthopyroxene (bronzite or hypersthene: 25–40%), together with augite (15–25%), andesine-labradorite (35–60%), reddish-brown biotite (up to 2%), and relatively uncommon (less than 2%) opaque minerals (magnetite, ilmenite, and traces of pyrite and chalcopyrite); minor olivine (up to 2%), quartz, and K-feldspar are present in some dykes, but primary hornblende is absent. Phenocrysts consisting of orthopyroxene with overgrowths of clinopyroxene are commonly present. Metamorphosed high-Mg dykes contain slightly less pyroxene, but more biotite (about 5%) and quartz; a few have secondary garnet.

Rare alkaline dykes show considerable, probably deuteric, alteration, and include ankaramite, alkali olivine basalt, and trachybasalt. They contain clinopyroxene and, in some cases, olivine phenocrysts in a fine-grained groundmass of biotite, reddish-brown amphibole, altered feldspar (albite + K-feldspar), and abundant (8–15%) opaque minerals (magnetite, ilmenite, and rare pyrite and chalcopyrite). Most of those examined have carbonate-rich ocelli. Other alkaline dykes include lamprophyres, composed of olivine, phlogopite, clinopyroxene, and rare plagioclase, carbonate, and amphibole, and carbonatitic pyroxenites.

Late Proterozoic metamorphics

Late Proterozoic metamorphics crop out on the south side of Prydz Bay, from the Rauer Group to Landing Bluff (Fig. 2). Rocks of similar age make up most of the outcrops on the east side of the Amery Ice Shelf, northern Prince Charles Mountains (Tingey, 1981, 1982), MacRobertson and Kemp Land Coast, and the western part of Enderby Land, where they are classified as the Rayner Complex (Sheraton & others, 1980) (Fig. 1). Over nearly all this area the predominant metamorphic grade is granulite facies, and nowhere are the rocks intruded by unmetamorphosed dolerite dykes. In the Prydz Bay area, the most abundant rock types are orthopyroxene and garnet-bearing gneisses and a variety of metasedimentary rocks, and there is minor mafic granulite. Granitic intrusives crop out at several places.

Orthopyroxene-quartz-feldspar gneiss

This is only abundant in the Rauer Group and Munro Kerr Mountains. Its composition, which ranges from granite to diorite, indicates that it is largely of igneous origin, although it is commonly interlayered with garnet-bearing gneisses and rarely with metasediments (Fig. 19). Apart from orthopyroxene (up to 12%), also commonly present are small amounts of reddish-brown biotite and, in some of the more melanocratic rocks, clinopyroxene and hornblende. Much of the gneiss (tonalite and subordinate quartz diorite and diorite) contains plagioclase, but little or no K-feldspar, whereas more potassic compositions (granodiorite to granite) have abundant perthite. Common accessory minerals are apatite, zircon, and opaque oxides.

Foliated intrusive rocks crop out at many places in the Rauer Group and include orthopyroxene-clinopyroxene granite at the eastern coastal outcrops, orthopyroxene-biotite tonalite near Hop Island, orthopyroxene granodiorite on Torckler Island (Fig. 20), and orthopyroxene-clinopyroxene-fayalite granite at the southernmost coastal outcrop of the Rauer Group. At the last locality, the granite gneiss is cut by variably deformed, metamorphosed mafic dykes.

Mount Caroline Mikkelsen, Svarthausen Nunatak, and Boyd Nunatak in the Munro Kerr Mountains are largely made up of relatively homogeneous orthopyroxene-quartz-plagioclase gneiss (tonalite). Variable, but generally small, amounts of perthite, clinopyroxene, dark greenish-brown hornblende, reddish-brown biotite, apatite, zircon, and opaque minerals are also present.

Figure 11. Partial melting of Tryne metavolcanics, Long Peninsula.

Figure 12. Mossel gneiss with restite Tryne metavolcanic xenoliths, Broad Peninsula.

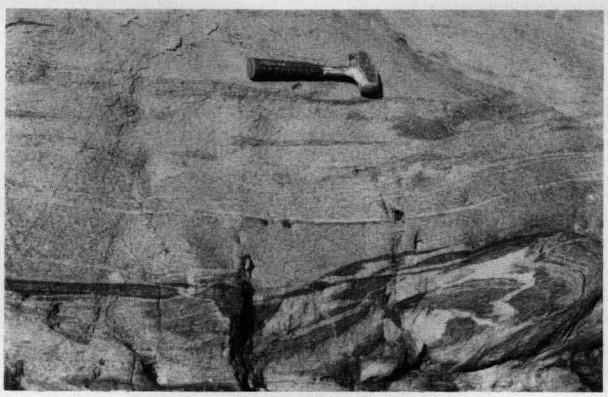

Figure 13. Contact between Crooked Lake gneiss and Tryne metavolcanics, Tryne Crossing.

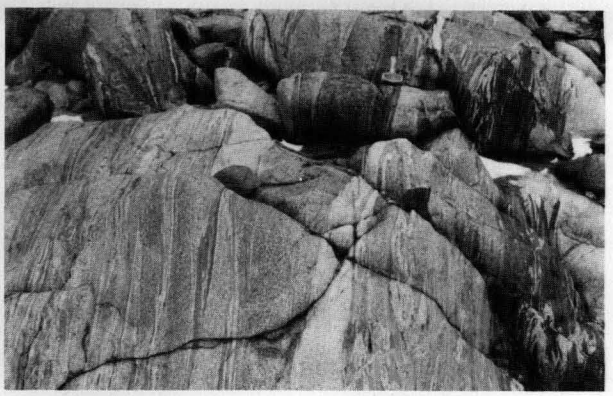

Figure 14. Strongly foliated Crooked Lake gneiss, showing effect of synkinematic emplacement, Long Peninsula.

Figure 15. Undeformed Crooked Lake gneiss, Long Peninsula.

Figure 16. Crustal xenoliths in Crooked Lake gneiss, Tryne Crossing.

Figure 17. Folded metabasic dyke cutting Chelnok supracrustals, Mule Peninsula.

Figure 18. Dolerite dykes cutting interlayered Mossel gneiss, Chelnok supracrustals, and Crooked Lake gneiss, Mule Peninsula; looking south with Sørsdal Glacier in background.

Garnet-quartz-feldspar gneiss

Garnet-bearing, generally migmatitic, felsic gneiss is common throughout the Prydz Bay area, particularly in the Larsemann Hills and coastal outcrops of the Munro Kerr Mountains. It is considerably more potassic than the orthopyroxene-quartz-feldspar gneiss, but K-poor, sodic gneiss crops out locally. In many places it shows evidence of partial melting (Fig. 21). Some is clearly of intrusive origin (granite) and forms homogeneous, subconcordant layers. Such granite gneiss typically contains up to 5 per cent garnet and 2–5 per cent reddish-brown biotite; orthopyroxene is present in a few samples from the Rauer Group. K-feldspar is commonly perthitic (orthoclase or microcline), and accessory minerals comprise apatite, zircon, opaque minerals, and rare monazite. More heterogeneous, strongly layered gneiss is commonly associated with metasediments and is probably, at least in part, itself of sedimentary origin. Garnet (mostly less than 10%), biotite (up to 10%), quartz (20–45%), plagioclase (commonly oligoclase, 15–50%), and K-feldspar (perthitic orthoclase or, rarely, microcline, 25–45%) are major constituents, and small amounts of cordierite, sillimanite, or spinel may be present. A few layers are particularly garnet-rich (up to 40%). Localised retrogressive effects include alteration of feldspar, and chloritisation of biotite.

Metapelites

Aluminous metasediments are common in the outcrops between the Ranvik Glacier and Bolingen Islands, including the Svenner Islands. However, they are much less common in the Rauer Group, where the only significant rocks of probable sedimentary origin are some of the garnet-bearing gneisses described above.

Metapelites in the area southwest of the Rauer Group are characterised by the presence of abundant garnet (up to 30%), sillimanite (rarely more than 10%), and cordierite (up to 25%). Reddish-brown biotite (mostly less than 5%), quartz (typically 20–50%), plagioclase (generally less than 10, but locally up to 50%), and perthite (up to 50%) are the other main constituents, together with small amounts of green spinel (up to 2%), opaque oxides, zircon, and rare apatite, monazite, and graphite. Some metapelites in the Brattstrand Bluffs area contain coexisting spinel and quartz, although in some cases the spinel is rimmed by sillimanite or cordierite. Cordierite is locally altered to pinnite. A marked foliation defined by aligned biotite grains, and lineation by oriented acicular sillimanite crystals may be present, but the are commonly deflected around garnet porphyroblasts; there is also evidence for both earlier (inclusions in garnet) and later (randomly oriented) crystallisation of sillimanite. K-feldspar and cordierite are commonly poikiloblastic. At a number of places, such as the Bolingen Islands, metapelites are interlayered with impure quartzite (up to 85 percent quartz).

Mafic rocks

Mafic granulite is only common in the Rauer Group. It is also present in minor amounts in the Sφstrene Islands–Larsemann Hills area, at Hovde Island, and in the Munro Kerr Mountains; elsewhere it is very rare.

Much of the mafic granulite in the Rauer Group represents metamorphosed mafic dykes, probable correlatives of the Vestfold Hills dolerites, although some may be remnants of the Tryne metavolcanics. Cross-cutting relationships are preserved in the northeastern Rauer Islands (Fig. 22); although the dykes are strongly folded and partly concordant, several distinct orientations are apparent (Fig. 23). Boudinaged, but not strongly folded dykes cut granitic gneiss at several places (e.g., Torckler Island and the coastal outcrop to the southeast), whereas elsewhere most mafic bodies are strongly deformed and essentially concordant (Fig. 24). Much of the granulite is rich in greenish-hornblende (15–25%) and also contains orthopyroxene (5–20%), clinopyroxene (5–15%), and plagioclase (45–60%), together with small amounts of opaque oxides (up to 3%), apatite, and, less commonly, biotite and quartz. Textures are commonly granuloblastic. Strongly deformed granulite from Filla Island contains hornblende (20–25%), reddish-brown biotite (15–20%), and quartz (about 10%), but no pyroxene. One sample (81285126) from Hop Island contains a little garnet with a reaction rim of orthopyroxene + plagioclase.

Granulite from further west is petrographically similar, although hornblende is rather less abundant (up to 15%), and biotite more so (up to 5%). Biotite flakes are commonly aligned, imparting a distinct foliation. None of the mafic granulite from this area shows evidence of derivation by metamorphism of mafic dykes, although the possibility cannot be discounted.

Ultramafic rocks are extremely rare, but hornblende pyroxenite crops out in the Sφstrene Islands and a pod of olivine-orthopyroxene hornblendite in the southwest Larsemann Hills.

Granitic intrusives

Apart from the more or less foliated orthopyroxene-bearing granitoids and subconcordant garnet-biotite granite gneiss mentioned above, undeformed cross- cutting granite and pegmatite veins are common throughout most of the area from the Rauer Group to the Polarforschung Glacier. White to pink quartz-feldspar pegmatites contain small amounts of garnet, biotite, and, locally, graphite. Larger bodies of even-grained granite at Steinnes and the eastern Larsemann Hills also contain reddish-brown biotite (up to 10%) and, less commonly, garnet, in addition to quartz, oligoclase, and orthoclase.

Possibly syn-metamorphic, pink to white porphyroblastic garnet-biotite granite makes up most of the outcrops in the southern part of Amanda Bay. It is somewhat foliated, owing to the alignment of K-feldspar porphyroblasts and gneiss inclusions, and is cut by pegmatite veins. Similar granite at Brattstrand Bluffs is interlayered with garnet-biotite gneiss. The granite contains perthite (50–55%), quartz (25–35%), plagioclase (10–15%), reddish-brown biotite (2–3%), garnet (1–3%), and minor opaque minerals (magnetite, ilmenite, and rare pyrite), apatite, zircon, spinel, and monazite. K-feldspar commonly shows partial inversion to microcline (wavy extinction) and feldspar and biotite are locally rather altered.

Younger post-orogenic pinkish-grey granite crops out around Sandefjord Bay (the Landing Bluff Adamellite of Tingey, 1981) and at Vestknatten and Meknattane Nunataks (Polarforschung Granite of Tingey, 1981). A Rb-Sr isochron age of 504 ± 17 Ma with an initial $^{87}Sr/^{86}Sr$ of 0.7184 was obtained by P.A. Arriens for the Landing Bluff Adamellite (Tingey, 1981). It is a porphyritic hornblende-biotite granite containing up to 5 per cent dark greenish-brown hornblende and up to 10 per cent dark brown biotite. The Polarforschung Granite has a slightly higher proportion (40–50%) of K-feldspar (microcline perthite), poikilitic phenocrysts of which, locally, have a preferred orientation. One sample (81285399) from Meknattane Nunataks contains about 1 per cent of fayalite. A distinctive and relatively abundant

Figure 19. Folded interlayered garnet-quartz-feldspar gneiss and orthopyroxene-quartz feldspar gneiss, Torckler Island, Rauer Group.

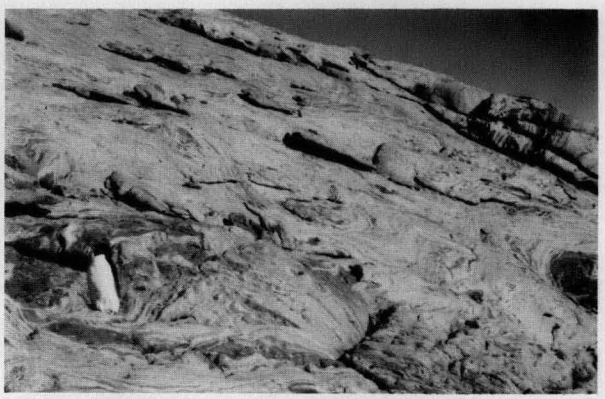

Figure 20. Partially melted orthopyroxene-quartz-feldspar gneiss, Torckler Island, Rauer Group.

Figure 21. Partially melted garnet-quartz-feldspar gneiss, Torckler Island, Rauer Group.

Figure 22. Intrusive relations of metadolerite dyke, Rauer Group.

Figure 23. Partially discordant metadolerite dykes, northeastern Rauer Group.

Figure 24. Subconcordant metadolerite dykes, northeastern Rauer Group.

accessory mineral suite, common to both intrusives, comprises magnetite, chalcopyrite, pyrite, ilmenite, apatite, zircon, sphene, metamict allanite, metamict chevkinite or perrierite, and fluorite. The granite is cut by white biotite aplite veins. Tingey (1981) reported that the contact with gneiss at Meknattane Nunataks is very sharp. A xenolith of clinopyroxene-orthopyroxene-biotite-quartz-plagioclase gneiss (81285400) at that locality contains unaltered pyroxene.

Discussion and conclusions

A tentative summary of the geological history of the Vestfold Hills–Prydz Bay area is given in Table 1. Events 1 to 7, 9, 11, and 14 have been recognised in the Vestfold Block, and are largely based on Oliver & others (1982a) and Collerson & others (in press). However, the relative ages of the oldest units (1) have not been conclusively established. Both the high-Mg dykes (6) and the main suite of dolerites (9) are,

petrographically, chemically, and isotopically, virtually identical to equivalent suites in Enderby Land (Sheraton & Black, 1981), but no analogues of the 1850 Ma Vestfold Block dolerites (7) have been found in the latter area. Rare alkali basalt and lamprophyre dykes (14) have not yet been dated, but, by analogy with dated alkaline intrusives in the Prince Charles Mountains (Walker & Mond, 1971; Sheraton & England, 1980; Sheraton, in press), may be of Phanerozoic age.

Rb-Sr and Sm-Nd isotopic data for gneisses from the Rauer Group indicate that only a minor proportion was derived by remetamorphism of Archaean continental crustal rocks, in spite of the general lithological similarity with Vestfold Block gneisses and the presence of metamorphosed mafic dykes (L.P. Black & M.T. McCulloch, personal communication, 1983). Most rocks have middle Proterozoic crustal formation ages (about 1600–1800 Ma), and apparently represent a younger suite of granitic intrusives (or extrusives) and subordinate semi-pelitic sediments (8). Such ages are consistent with the emplacement of abundant dolerites at about 1300 Ma, but are by no means sufficiently well constrained to show whether the gneiss precursors are predominantly older or younger than the 1850 Ma dolerites. Whereas much of the granitic orthogneiss, such as that in the southeastern Rauer Group, is cut by metadolerite dykes, there was also extensive syn-metamorphic intrusion of granitic magma. Thus, homogeneous orthopyroxene-quartz-feldspar gneiss containing xenoliths crops out at Torckler and Hop Islands, and foliated porphyroblastic garnet-biotite granite around Amanda Bay. In contrast, orthopyroxene-hornblende-quartz-plagioclase gneiss in the Munro Kerr Mountains is associated with minor mafic granulite and may predate the dolerite dykes. Geophysical (gravity and magnetic) data do not show any major change in crustal structure across the boundary between Archaean and late Proterozoic rocks (Wellman & Williams, 1982), but no data are available for the area to the southwest of the Rauer Group.

The extensive sillimanite and cordierite-bearing metapelites and associated garnetiferous gneisses of the Prydz Bay coast (10) are quite different in composition to all except a very minor proportion in the Vestfold Block and Rauer Group, and their age of deposition is not known with certainty. They were apparently not intruded by dolerite dykes (mafic granulite is very rare) and may have been deposited after the emplacement of such dykes in an older basement. Alternatively, the sediments may be older and dyke intrusion restricted to a deeper crustal level. Isotopic data indicate derivation of the metasediments from predominantly middle Proterozoic, rather than Archaean, precursors, but are consistent with weathering of middle Proterozoic rocks, such as the largely orthogneiss terrain of the Rauer Group (L.P. Black & M.T. McCulloch, personal communication, 1983). Relatively rapid deposition after dolerite dyke emplacement and before high-grade metamorphism at about 1100 Ma is our preferred interpretation. High-grade metasediments of generally similar composition and, possibly, similar depositional age crop out in the northern Prince Charles Mountains–Mawson Coast area of MacRobertson Land; greenschist-facies metasediments that postdate the emplacement of dolerite dykes in the southern Prince Charles Mountains may also be of similar age, but have a generally more calcareous composition (Tingey, 1982).

High-grade metamorphics of late Proterozoic age (1000–1100 Ma) extend for at least 2000 km west of Prydz Bay, and make up most of the northern Prince Charles Mountains and Mawson Coast of MacRobertson Land (Tingey, 1979, 1982). Kemp Land and western Enderby Land (Rayner Complex of Grikurov & others, 1976, and Sheraton & others, 1980), and Dronning Maud Land (Yoshida, 1979; Yoshida & others, 1982); slightly older ages (1300–1400 Ma) have been reported for amphibolite to granulite-facies gneisses of the Windmill Islands, 1400 km to the east (Compston & others, 1982; Oliver & others, 1982b). They are essentially coeval with metamorphics of a wide area of Gondwanaland, such as those formed during the Kibaran orogeny in southern Africa (Clifford, 1974), and the Vijayan gneisses of Sri Lanka (Crawford & Oliver, 1969). Regional correlations are discussed in more detail by James & Tingey (in press).

Gneisses of the Rayner Complex, within a few tens of kilometres of the Archaean Napier Complex in Enderby and Kemp Lands, appear on chemical and isotopic evidence, to be largely remetamorphosed Archaean rocks (Sheraton & Black, in press). In contrast, late Proterozoic gneisses in a wide area of MacRobertson Land include a high proportion with only a short previous crustal history, as well as some possibly derived from much older continental crust (Tingey, 1982). Many of the gneisses from this area were derived, either directly or by partial melting, from sedimentary protoliths (Sheraton & Black, in press). These relationships are thus analogous to those in the Vestfold Hills–Prydz Bay area, except that there Proterozoic reworking of the Archaean craton was apparently even more restricted. Furthermore, the development of relatively high-pressure (and lower-temperature) garnet + clinopyroxene-bearing assemblages in Archaean mafic rocks and Proterozoic tholeiite dykes immediately adjacent to late Proterozoic terrains has also been noted in the transitional zone between the Napier and Rayner Complexes in Kemp Land by Sheraton & others (1980). As in the southwestern Vestfold Hills, this late Proterozoic overprinting was not accompanied by major deformation, although, locally, in both the Vestfold Hills and Napier Complex garnet also crystallised in shear zones of probable similar age (Sheraton & others, 1980).

The granite at Landing Bluff is similar in age to pegmatites and granites, as well as minerals, (about 500 Ma) over wide areas of the East Antarctic Shield (Grew, 1978, 1982), notably the southern Prince Charles Mountains (Tingey, 1982) and can be correlated with the widespread 'Pan-African' orogeny (Clifford, 1974). Fayalite-bearing intrusives (including syenite, monzonite, and granite) have also been reported from Queen Maud Land and the Mirny area, and may be of similar early Palaeozoic age (Ravich & Kamenev, 1975).

Acknowledgements

The efforts of members of the Australian National Antarctic Research Expeditions at Davis were a major factor in ensuring the success of the field program on which this paper is based, and are gratefully acknowledged. Logistic support was provided by the Antarctic Division, Department of Science and Technology, Hobart. We thank N.G. Ware and K.J. Ellingsen for help with microprobe analyses, and R.J. Tingey for critically reading the manuscript.

References

Arriens, P.A., 1975 — The Precambrian geochronology of Antarctica. *1st Australian Geological Convention, Adelaide, Abstracts*, 97–8.

Clifford, T.N., 1974 — Review of African granulites and related rocks. *Geological Society of America Special Paper* 156.

Collerson, K.D., & Arriens, P.A., 1979 — Rb–Sr isotope systematics in high-grade gneisses from the Vestfold Hills, East Antarctica (Abstract). *Journal of the Geological Society of Australia*, 26, 267–268.

Collerson, K.D., Reid, E., Millar, D., & McCulloch, M., in press — Lithological and Sr–Nd isotopic relationships in the Vestfold Block: implications for Archaean and Proterozoic crustal evolution in the East Antarctic Shield. *4th International Symposium on Antarctic Earth Sciences, Adelaide, August, 1982.*

Collersen, K.D., Sheraton, J.W., & Arriens, P.A., 1983 — Granulite facies metamorphic conditions during the Archaean evolution and late Proterozoic reworking of the Vestfold Block, eastern Antarctica. *6th Australian Geological Convention, Canberra, Abstracts*, 53–54.

Compston, W., Williams, I.S., Collerson, K.D., Lovering, J.F., & Arriens, P.A., 1982 — A reassessment of the age of the Windmill Metamorphics, Casey area, East Antarctica. *4th International Symposium on Antarctic Earth Sciences, Adelaide, Abstracts*, 35.

Crawford, A.R., & Oliver, R.L., 1969 — The Precambrian geochronology of Ceylon. *Special Publication of the Geological Society of Australia*, 2, 283–306.

Grew, E.S., 1978 — Precambrian basement at Molodezhnaya Station, East Antarctica. *Bulletin of the Geological Society of America*, 89, 801–813.

Grew, E.S., 1982 — The Antarctic margin. *In* Nairn, A.E.M., & Stehli, F.G. (editors), The ocean basins and margins. Volume 6. *Plenum, New York*, 697–755.

Grikurov, G.E., Znachko-Yavorsky, G.A., Kamenev, E.N., & Ravich, M.G., 1976 — Explanatory notes to the geological map of Antarctica (scale 1:5 000 000). *Research Institute of the Geology of the Arctic, Ministry of Geology of the USSR, Leningrad.*

James, P.R., & Tingey, R.J., in press — The geological evolution of the East Antarctic metamorphic shield — a review. *4th International Symposium on Antarctic Earth Sciences, Adelaide, August, 1982.*

Oliver, R.L., James, P.R., Collerson, K.D., & Ryan, A.B., 1982a — Precambrian geologic relationships in the Vestfold Hills, Antarctica. *In* Craddock, C. (editor), Antarctic geoscience. *University of Wisconsin Press*, 435–444.

Oliver, R.L., Cooper, J.A., & Truelove, A.J., 1982b — Some petrological and zircon geochronological observations of gneisses from Herring Island, Wilkes Land and Commonwealth Bay, King George V Land. *4th International Symposium on Antarctic Earth Sciences, Adelaide (Abstracts)*, 130.

Parker, A.J., James, P.R., Mielnik, V., & Oliver, R.L., 1982 — Metamorphism and fabric development in Archaean gneisses of the Vestfold Hills, Antarctica. *4th International Symposium on Antarctic Earth Sciences, Adelaide, Abstracts*, 134.

Ravich, M.G., & Kamenev, E.N., 1975 — Crystalline basement of the Antarctic platform. *Wiley, New York.*

Sheraton, J.W., in press — Geochemistry of mafic igneous rocks of the northern Prince Charles Mountains, Antarctica. *Journal of the Geological Society of Australia.*

Sheraton, J.W., & Black, L.P., 1981 — Geochemistry and geochronology of Proterozoic tholeiite dykes of East Antarctica: evidence for mantle metasomatism. *Contributions to Mineralogy and Petrology*, 78, 305–317.

Sheraton, J.W., & Black, L.P., in press — Geochemistry of Precambrian gneisses: relevance for the evolution of the East Antarctic Shield. *Lithos.*

Sheraton, J.W., & England, R.N., 1980 — Highly potassic mafic dykes from Antarctica. *Journal of the Geological Society of Australia*, 27, 129–135.

Sheraton, J.W., Offe, L.A., Tingey, R.J., & Ellis, D.J., 1980 — Enderby Land, Antarctica — an unusual Precambrian high-grade metamorphic terrain. *Journal of the Geological Society of Australia*, 27, 1–18.

Streckeisen, A.L., 1976 — To each plutonic rock its proper name. *Earth-Science Reviews*, 12, 1–33.

Tingey, R.J., 1979 — East Antarctica — the key piece of Gondwanaland (abstract). *Journal of the Geological Society of Australia*, 26, 275.

Tingey, R.J., 1981 — Geological investigations in Antarctica 1968–1969: the Prydz Bay–Amery Ice Shelf–Prince Charles Mountains area. *Bureau of Mineral Resources, Australia, Record* 1981/34.

Tingey, R.J., 1982 — The geological evolution of the Prince Charles Mountains — an Antarctic Archaean cratonic block. *In* Craddock, C. (editor), Antarctic geoscience. *University of Wisconsin Press*, 455–464.

Walker, K.R., & Mond, A., 1971 — Mica lamporphyre (alnoite) from Radok Lake, Prince Charles Mountains, Antarctica. *Bureau of Mineral Resources, Australia, Record* 1971/108.

Wellman, P., & Williams, J.W., 1982 — Extent of Archaean and late Proterozoic rocks under the ice cap of Princess Elizabeth Land, Antarctica, inferred from geophysics. *BMR Journal of Australian Geology & Geophysics*, 7, 213–218.

Yoshida, M., 1979 — Tectonics and metamorphism of the region around Lutzow-Holmbukta, East Antarctica. *Memoirs of the National Institute of Polar Research, Tokyo, Special Issue*, 14, 28–40.

Yoshida, M., Kizaki, K., Kojima, H., Shirahata, H., & Suzuki, M., 1982 — Tectonic and metamorphic history of the crystalline rocks of Lutzow-Holm Bay, East Antarctica. *4th International Symposium on Antarctic Earth Sciences, Adelaide, Abstracts*, 185.

BMR Journal of Australian Geology & Geophysics, 8, 129-137

Rb-Sr GEOCHRONOLOGY OF PROTEROZOIC EVENTS IN THE ARUNTA INLIER, CENTRAL AUSTRALIA

L.P. Black, R.D. Shaw, & A.J. Stewart

Rb-Sr data reveal a long and complex Proterozoic history for the Arunta Inlier of central Australia. The first event was a widespread, dominantly granulite-facies episode, known as the Strangways Event, at 1790 ± 35 Ma. Five relatively precise ages from metamorphic and granitic rocks give an estimate between 1650 and 1700 Ma for widespread deformation and metamorphism during the Aileron Event. Two granites in the northern Arunta Inlier were probably emplaced at about 1500 m.y. Deformation and low-grade metamorphism during the Anmatjira Event are dated by generally imprecise isochrons at about 1400 Ma. Four isochrons, documenting both primary events and resetting, are in accord with an age of 900–1050 Ma for the Ormiston Event. The Rb-Sr data do not define the time of initial crust formation in the Arunta Inlier.

Introduction

This paper reports detailed Rb-Sr ages for the Arunta Inlier (Fig. 1), adding to data previously published by Marjoribanks & Black (1974), Black (1975), Shaw & others (1979), and Stewart & others (1980). The samples were collected between 1972 and 1975, during reconnaissance mapping of the Arunta Inlier and before of Black & others (1978, 1979) showed the need for detailed structural analysis to accompany sampling of complexly deformed and metamorphosed areas. However, sampling of each rock suite was kept within 1 m^3 of rock, which is likely to have remained in isotopic equilibrium during penetrative schistosity-producing events (Black & others, 1978, 1979). The significance of the isotopic data was judged from the petrography of the samples, the quality of each isochron, and the recurrence of particular ages in rocks from different areas.

Standard analytical procedures (Marjoribanks & Black, 1974; Page & others, 1976; Williams & others, 1976) were used for Rb-Sr analyses. All ages are reported or recalculated using the 1.42×10^{-11} y^{-1} decay constant for ^{87}Rb (Steiger & Jager, 1977).

Criteria and assumptions applied in geochronological interpretation

Black & others (1978, 1979) and Chopin & Maluski (1980) emphasised the importance of pervasive deformation in the

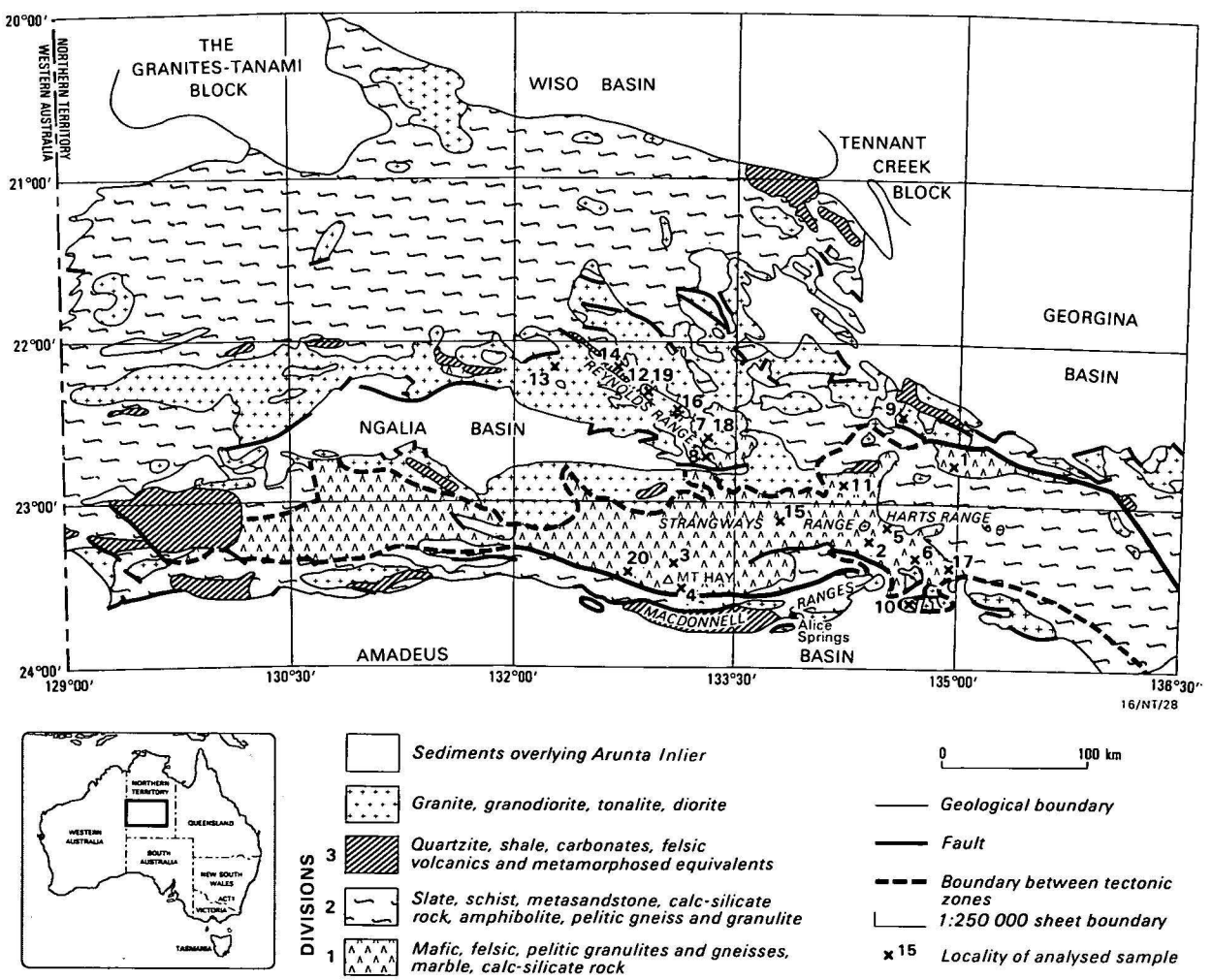

Figure 1. Geological map of the Arunta Inlier, showing major stratigraphic divisions, tectonic zones, and localities of analysed samples.

resetting of Rb-Sr total-rock isochrons. The formation of penetrative schistosity involves processes such as dislocation generation and migration, and grain-boundary sliding and migration, which are likely to enhance Rb and Sr diffusion. High partial pressures of the fluid phases should also assist isotopic equilibration. Without the development of penetrative schistosity, metamorphic recrystallisation tends to fill in pore systems, restricting fluid mobility and, consequently, restricting isotopic migration. Thus, in the high-grade metamorphic rocks of this study, Rb-Sr total-rock ages probably reflect deformation, even though the metamorphism appears in some cases to have outlasted the deformation. In general, it is assumed that if a rock is reconstituted during the formation of a new schistosity, the Rb-Sr total rock age will reflect the age of that schistosity.

Relict minerals from the previous metamorphic event are likely to contribute an older element to the total-rock age. If the older schistosity is dominant, but a new fabric is also evident, the Rb-Sr total-rock age will be a minimum age for the older schistosity. If the younger schistosity is dominant, the Rb-Sr total-rock age will approximate the age of the younger deformation and metamorphic event. In cases of uncertainty, a mineral–total-rock isochron may clarify the age of the deformational and metamorphic event, if the minerals selected for plotting are syntectonic with the dominant schistosity or fabric. In the Arunta Inlier, development of a younger foliation was commonly accompanied by retrograde metamorphism.

Because the nature of the fabric and the relative ages of minerals are important in the interpretation of Rb-Sr ages, the important petrographic features of each rock analysed are presented in an appendix.

Isotopic results

Our results are summarised in Tables 1–5 and isochron diagrams (Figs. 2–21). Petrographic data are given in Appendix 1. Isotopic data are available from the senior author.

Strangways Event

Several samples have Rb-Sr ages of about 1800 Ma (Table 1), which is considered to represent the age of the Strangways Event, a major granulite-facies metamorphic event, and the earliest event recognised in the Arunta Inlier.

Table 1. Strangways Event

Rock unit (sample no.)	*Age Ma*	*Initial ratio*	*Isochron model*	*MSWD**
Kanandra Granulite (72902009)	1790 ± 35	0.708 ± 0.002	2 (Fig. 2)	2.6
Cadney metamorphics (72913000)	1750 ± 33	0.712 ± 0.002	4 (Fig. 3)	14
Mount Hay granulite (73933007)	1768 ± 20	0.7085 ± 0.0006	2 (Fig. 4)	3.9
(73933006) Ongeva granulite	1728 ± 65	0.706 ± 0.001	3 (Fig. 5)	11
(73913006) (73913007)	1737 ± 68	0.716 ± 0.023	1 (Fig. 6)	—

* Mean Square of Weighted Deviates

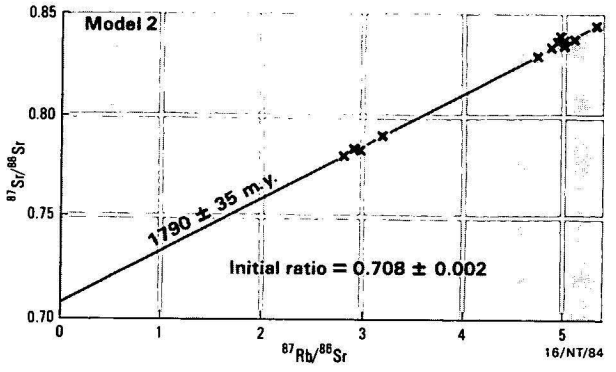

Figure 2. Rb-Sr isochron for the Kanandra Granulite (72902009).

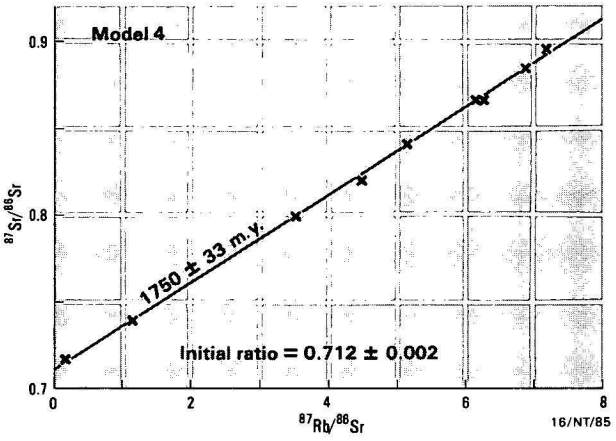

Figure 3. Rb-Sr isochron for the Cadney metamorphics (72913000).

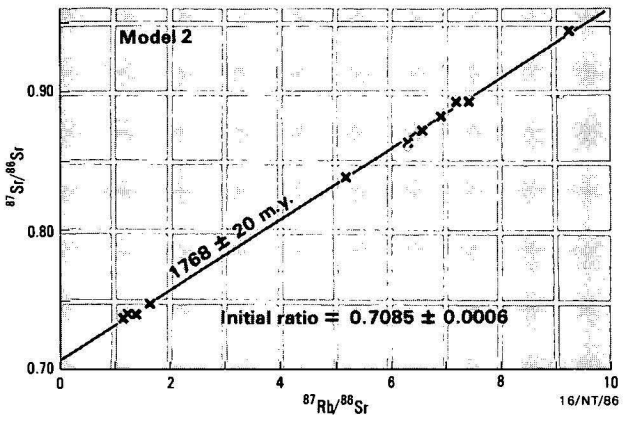

Figure 4. Rb-Sr isochron for granulite (73933007) at Mount Hay.

The **Kanandra Granulite,** which gave the greatest age, shows no post-crystallisation deformation, whereas most samples that gave younger ages do. The sample from the **Cadney metamorphics,** a mylonite gneiss, shows strong evidence of a second deformation, which makes its Rb-Sr age difficult to interpret. However, this is likely to be a minimum age for the Strangways Event, partly reset by mylonitisation.

A more complex metamorphic history is suggested for a sample (73933006) of the **Mount Hay granulites,** by grain growth of plagioclase megacrysts. 'Wetter' conditions may have allowed isotopic adjustment to continue during the waning stages of metamorphism and deformation.

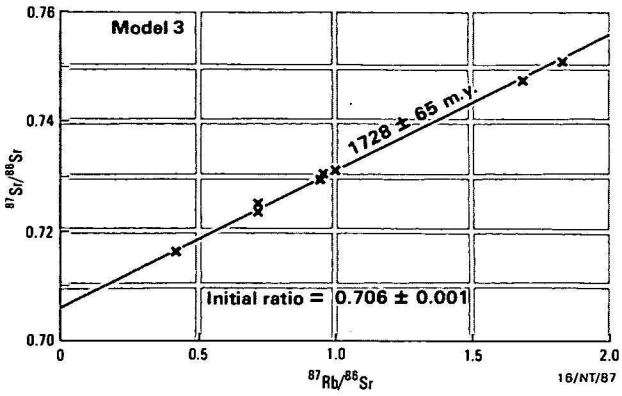

Figure 5. Rb-Sr isochron for granulite (73933006) at Mount Hay.

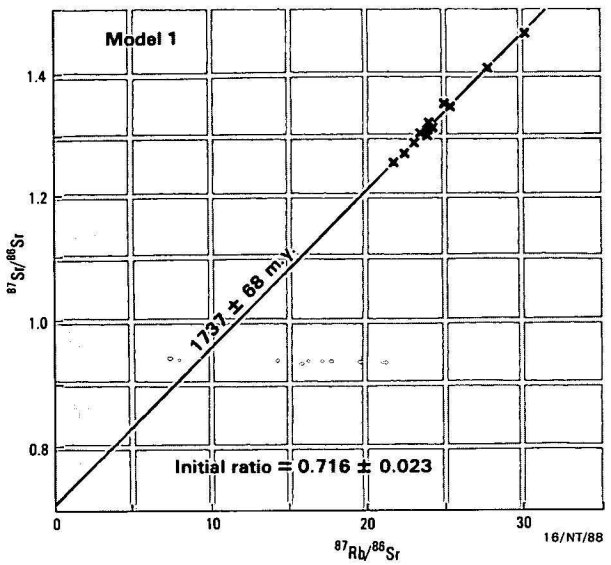

Figure 6. Rb-Sr isochron for the Ongeva granulite (73913006-7).

Retrogressive metamorphism has partly affected the **Ongeva granulite,** and this, together with the wide precision limits, has resulted in only an approximate age being obtained for the Strangways Event. We conclude that the best age for the Strangways Event is given by the Kanandra Granulite at 1790 ± 35 Ma.

Aileron Event

Five of six metamorphic and granitic rocks formed during or affected by the Aileron Event have given relatively precise ages in the range 1700–1650 Ma (Table 2).

Granitic gneiss (Cadney metamorphics) near Ambalindum

Although this gneiss occurs in a granulite terrain, its main features were formed by later deformation along a relatively narrow zone, probably under amphibolite-facies conditions, and it is this later event that the age records. Because of its intensity, it is likely that this event completely, rather than partly, reset the Rb-Sr system. It probably dates the event responsible for retrogression of the Ongeva granulite sample previously metamorphosed by the Strangways Event (sample 73913006).

Aileron metamorphics near Mount Boothby

Similar ages were obtained from two localities in the Aileron metamorphics, which include felsic and mafic granulite, and

Table 2. Aileron Event

Rock unit (sample no.)	*Age Ma*	*Initial ratio*	*Isochron model*	*MSWD*
Granitic gneiss near Ambalindum (72913001)	1686 ± 21	0.716 ± 0.001	2 (Fig. 7)	3.8
Aileron metamorphics				
(73921021)	1670 ± 87	0.715 ± 0.008	2 (Fig. 8)	7.6
(73921022)	1647 ± 65	0.808 ± 0.047	1 (Fig. 9)	—
Granite near Mount Ida (72902006)	1709 ± 36	0.61 ± 0.16	1 (Fig. 10)	—
Granite from Atnarpa Igneous Complex (73913009)	1651 ± 47	0.705 ± 0.001	1 (Fig. 11)	—
Migmatite complex (pEeg). *Mount Bleechmore area (72902013)*	1592 ± 66	0.713 ± 0.002	3 (Fig. 12)	4.4

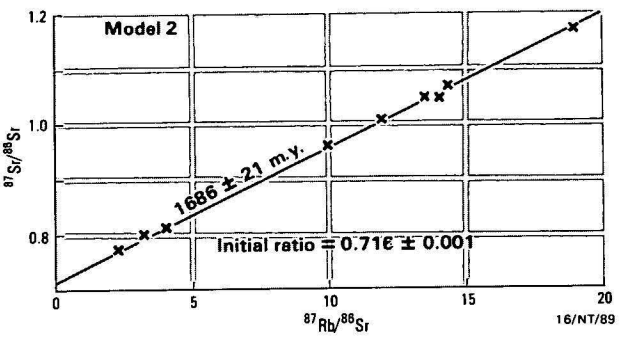

Figure 7. Rb-Sr isochron for retrogressed granulite (72913001) Ambalindum.

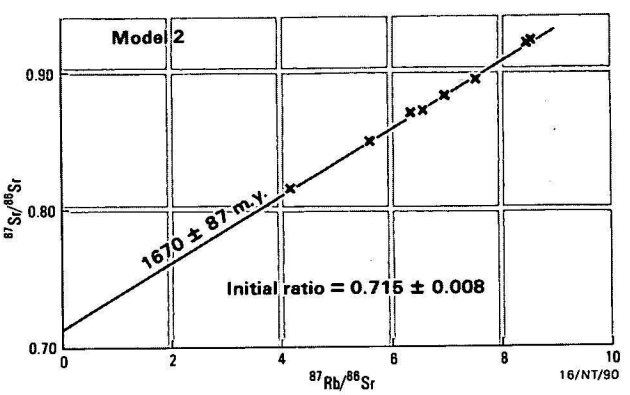

Figure 8. Rb-Sr isochron for Aileron metamorphics (73921021) near Mount Boothby.

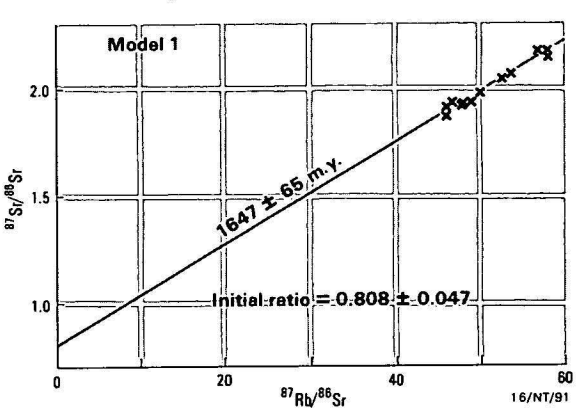

Figure 9. Rb-Sr isochron for Aileron metamorphics (73921022) near Mount Boothby.

subsidiary cordierite gneiss, garnet-biotite gneiss, calc-silicate rock, marble, sillimanite gneiss, and other metasediments. However, the samples differ in that one (73921022), containing hornblende and lacking hypersthene, is of amphibolite rather than granulite facies. Its high initial ratio of 0.808 ± 0.047 is strongly indicative of a reset isochron.

Granite near Mount Ida

The initial $^{87}Sr/^{86}Sr$ of this sample, 0.61 ± 0.16, is poorly defined, owing largely to a lack of samples with $^{87}Rb/^{86}Sr$ less than 100. The mean initial ratio is clearly untenable, but its large errors permit an acceptable value above 0.70, which gives an age in the lower part of the error range, at roughly 1670–1690 Ma. It is not clear from the data, however, especially with the imprecisely determined initial ratio, whether this age defines intrusion or a subsequent event.

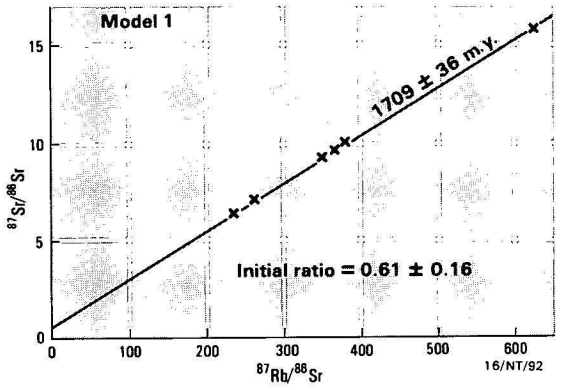

Figure 10. Rb-Sr isochron for granite (72902006) from near Mount Ida region.

Atnarpa Igneous Complex

Granite from the Atnarpa Igneous Complex gave a similar age to that from near Mount Ida, although $^{87}Rb/^{86}Sr$ ratios are much lower than those of that granite. Model 1 conditions are still preserved over the 1-m^3 scale of sampling. Again, it is not clear whether the isochron records emplacement or a later deformational event. The age is thus a minimum for the time of emplacement. A weak, variably oriented (± 15°) foliation, outlined by mica, is not a magmatic flow structure, for it cuts xenoliths (Shaw & others, 1979, p. 298). However, it may well be a syntectonic feature imposed during granite emplacement. If this is the case, the Rb-Sr age will approximate that of emplacement. The greenschist minerals (see Appendix) are likely to have formed during the Alice Springs Orogeny, but would have had a minimal effect on the age, because they are accessory in amount, patchy in distribution, and unoriented.

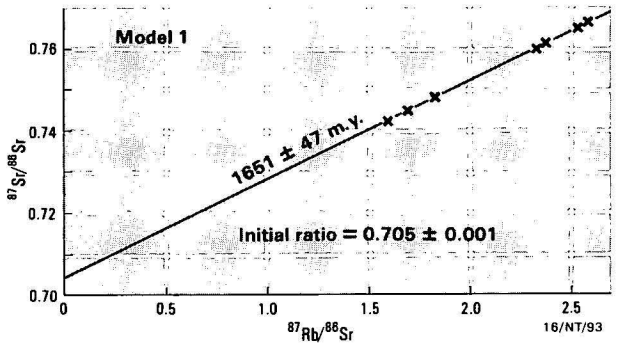

Figure 11. Rb-Sr isochron for granite (73913009) from the Atnarpa Igneous Complex.

Migmatite complex (pЄeg), Mount Bleechmore area

Only one reasonably defined total-rock isochron age of about 1600 Ma has been obtained in this study. This derives from a gneissic portion (72902013) of a generally massive homogeneous granitoid. The migmatitic gneiss is contiguous with quartzofeldspathic gneiss, migmatite, and basic granulite of the Mount Bleechmore Granulite (Shaw & others, 1975), a correlative of the Kanandra Granulite. Field evidence suggests that the migmatitic gneiss represents a more mobilised part of the granulite–migmatite complex of the Mount Bleechmore Granulite. However, it may represent a later granitoid. A second deformation accompanied by recrystallisation and retrogression of both hypersthene and garnet to biotite is evident in the analysed gneiss. The age, likely to approximate the time of emplacement of the migmatite complex, is similar to the 1586 ± 70 Ma determined by Majoribanks & Black (1974) for the Chewings Event. Relative imprecision of these 1600 Ma ages does not permit them to be unequivocally separated from the Aileron Event or the poorly defined 1500 Ma event.

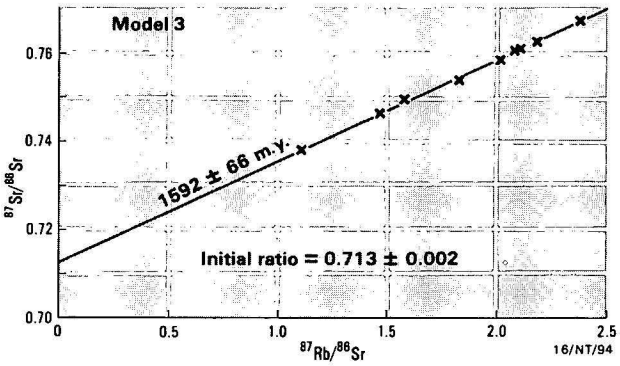

Figure 12. Rb-Sr isochron for migmatitic gneiss (72902013) from the Mount Bleechmore area.

Igneous event

Microgranodiorite in the Reynolds Range region, and Wangala Granite, northern Arunta Inlier

Two imprecise ages of about 1500 Ma have been obtained from granitic rocks in the Reynolds Range region (Table 3). The imprecision relates only to a limited spread in $^{87}Rb/^{86}Sr$, for, in both cases, model 1 conditions were satisfied. The age for the microgranodiorite xenolith in the Harverson Granite may define its original crystallisation. The Wangala Granite has escaped deformation, and retrogression is only slight. Hence, its total-rock isochron age is thought to record its emplacement. Muscovite and biotite Rb-Sr ages of 1361 Ma and 1166 Ma, respectively, probably record slight isotopic disturbance during the incipient retrogression.

Table 3. Igneous event

Rock unit (sample no.)	*Age Ma*	*Initial ratio*	*Isochron model*	*MSWD*
Microgranodiorite xenolith in Harverson Granite (72921006)	1497 ± 146	0.82 ± 0.07	1 (Fig. 13)	—
Wangala Granite (72921010)	1490 ± 100	0.76 ± 0.07	1 (Fig. 14)	—

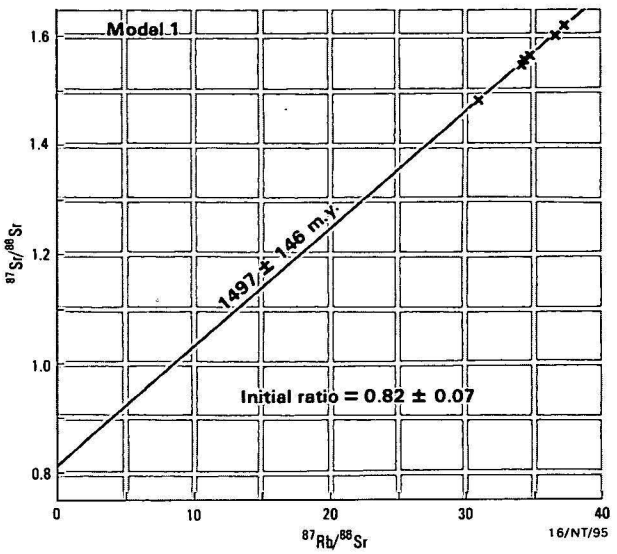

Figure 13. Rb-Sr isochron for large xenolith (72921006) within the Harverson Granite.

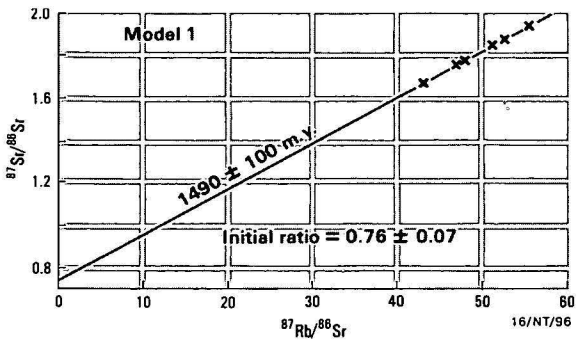

Figure 14. Rb-Sr isochron for the Wangala Granite (72921010).

Anmatjira Event

Three ages have been obtained with mean values close to 1400 Ma (Table 4).

Table 4. Anmatjira Event

Rock unit (sample no.)	*Age Ma*	*Initial ratio*	*Isochron model*	*MSWD*
Lander Rock beds (73921024)	1390 ± 180	0.72 ± 0.08	2 (Fig. 15)	3.3
Wuluma granitoid (75913020)	1426 ± 81	0.722 ± 0.005	1 (Fig. 16)	—
Deformed granitic rock, Anmatjira Range (72921004)	1424 ± 58	0.745 ± 0.005	1 (Fig. 17)	—

Lander Rock beds

The Lander Rock beds are the most widespread unit in the northern part of the Arunta Inlier, and are generally composed of weakly metamorphosed sandstone, siltstone, and shale, locally metamorphosed to granulite facies. The Rb-Sr age obtained is particularly imprecise, owing to a limited range of $^{87}Rb/^{86}Sr$ values. However, the MSWD of the isochron, at 3.3, is low. The age probably dates the low-grade progressive regional metamorphism of the Lander Rock beds.

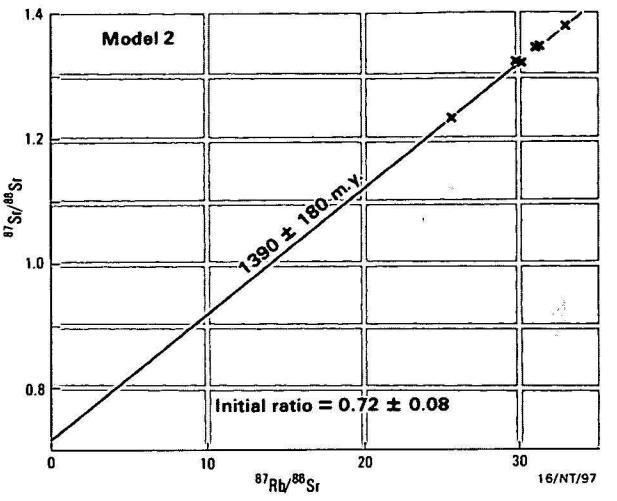

Figure 15. Rb-Sr isochron for the Lander Rock beds (72921024).

Wuluma granitoid

The Wuluma granitoid was thought by Langworthy (*in* Shaw & others, 1979) to have been emplaced at the close of the Strangways Event, because it grades into the Ingula migmatite suite, which, in turn, has a transitional contact with granulite of the Erontonga metamorphics. However, the Wuluma granitoid also locally intrudes the Erontonga metamorphics. Hence, it should be younger, if only slightly, than the granulites of the Strangways Event. The age obtained is undoubtedly a minimum age and, from textural evidence (Appendix 1) of recrystallisation, moderate strain, some grain growth during subsequent metamorphism, and slight deformation, it is likely to significantly postdate emplacement.

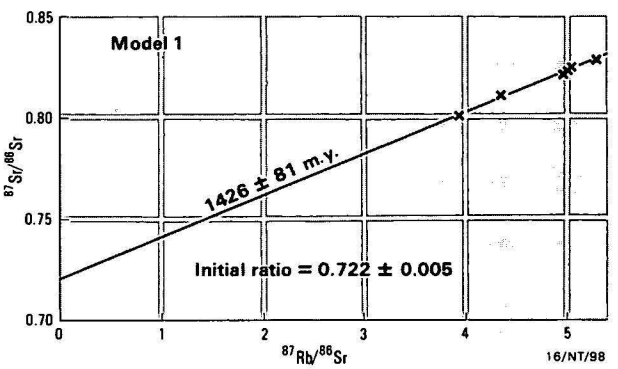

Figure 16. Rb-Sr isochron for the Wuluma granitoid (75913020).

Deformed rock — Anmatjira Range

A deformed granitic rock adjacent to a major shear zone in the Anmatjira Range, has given a similar age to that obtained from the Wuluma granitoid. K-feldspar, garnet, and hypersthene in nearby samples from the same granite mass are typical of granites correlated with the approximately 1700–1650 Ma high- grade Aileron Event. However, the isochron age probably dates the subsequent pervasive deformation of the rock during biotite growth. The biotite foliation is evident over a strike width of at least 500 m. Alternatively, the age may be only partly reset by the deformation, for which it would provide only a maximum age.

Iyer & others (1976) reported similar ages of 1439 ± 60 Ma and 1400 ± 60 Ma for felsic granulites from two localities in

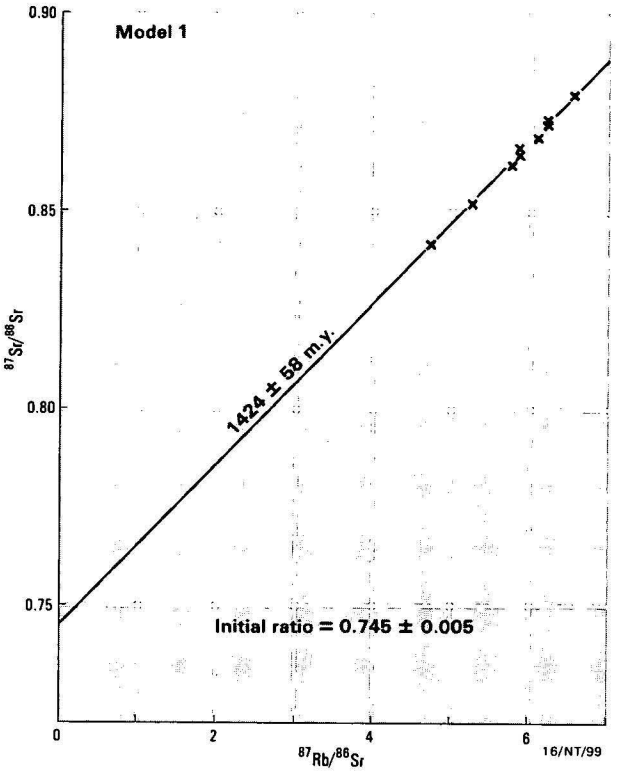

Figure 17. Rb-Sr isochron for deformed granitic rock (72921004) in the Anmatjira Range.

the Strangways Range. On petrological grounds these rocks were ascribed to a second granulite-facies event. The new ages reported above support the presence of a tectonothermal event at that time. However, they also suggest that if this event reached granulite grade in some areas, such rocks have a limited distribution.

Ormiston Event

Four ages have been obtained for rocks affected by the Ormiston Event (Table 5).

Table 5. Ormiston Event

Rock unit (sample no.)	*Age Ma*	*Initial ratio*	*Isochron model*	*MSWD*
Amphibolite, Black Cone area (72913002)	1040 ± 38	0.7045 ± 0.0002	1* (Fig. 18)	
Boothby Orthogneiss (73921020)	925 ± 153	0.764 ± 0.011	2 (Fig. 19)	24
Harverson Granite (72921005)	930 ± 190	0.92 ± 0.04	2 (Fig. 20)	5
Big-feldspar gneiss at Mount Hay 4(73933003)	893 ± 67	0.757 ± 0.004	3 (Fig. 21)	3.5

* internal mineral isochron

Amphibolite (Bungitina metamorphics), Black Cone area

Rocks in the Black Cone area were initially metamorphosed to transitional amphibolite–granulite facies, and then underwent extensive amphibolite-facies retrogression. The analysed sample is similar to plug-like basic bodies emplaced after the Strangways Event.

Samples, even from the restricted 1 m³ sampling volume, exhibit marked scatter. This and limited spread in $^{87}Rb/^{86}Sr$ precluded the derivation of a total-rock isochron age. However, a model 1 internal mineral isochron gave an age of 1040 ± 38 Ma. Should this isochron document a secondary event, it must have been particularly intense to produce the perfect analytical alignment. The age is indistinguishable from that derived by Marjoribanks & Black (1974) for the Ormiston Event, a period of extensive migmatite and granite formation in much of the southern Arunta Inlier. The amphibolite facies retrogression results from shearing along the Cadney Fault Zone (Shaw & others, 1979).

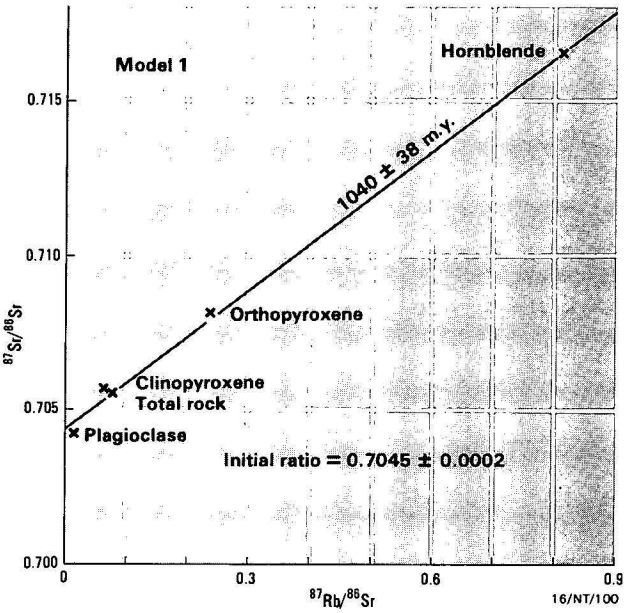

Figure 18. Rb-Sr mineral isochron for amphibolite (72913002) from the Black Cone area.

Boothby Orthogneiss

The Boothby Orthogneiss is a coarse-grained porphyroblastic granitic augen gneiss with subordinate porphyritic granite that crops out the southeast of Napperby 1:250 000 Sheet area. It intrudes and encloses large enclaves of Aileron metamorphics and intrudes the Lander Rock beds.

Rapakivi texture and the presence of garnet and sillimanite (see Appendix) favour correlation of the emplacement of this orthogneiss with emplacement of other porphyroblastic orthogneisses in the region. Other mineralogical and textural features such as recrystallisation, foliation, and saussuritisation of plagioclase suggest that the Rb-Sr total-rock age of 925 ± 153 Ma for this sample of the Boothby Orthogneiss documents a considerably later tectonothermal event. The MSWD of 24 is reasonably typical of such reset isochrons (Black & others, 1979). The initial $^{87}Sr/^{86}Sr$ ratio of 0.764 ± 0.011 is also consistent with this interpretation.

Harverson Granite

Another granitic body in the Reynolds Range yields a similar age, for which an entirely different interpretation is given. The Harverson Granite is massive, very coarse-grained, and porphyritic. It intrudes and metamorphoses the Lander Rock beds, and is intruded by a large number of quartz veins and a few dykes of aplite and tourmaline-bearing pegmatite. Its petrographic features, and the absence of mafic dykes, which are common in adjoining orthogneiss, indicate that the Harverson Granite is a typical late, post-orogenic 'wet'

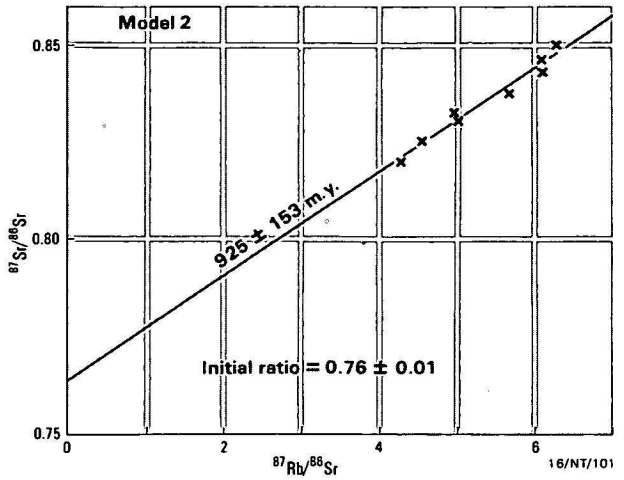

Figure 19. Rb-Sr isochron for the Boothby Orthogneiss (73921020).

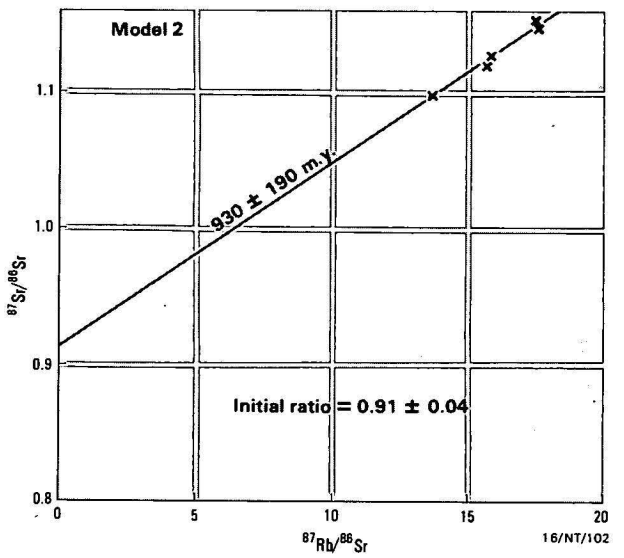

Figure 20. Rb-Sr isochron for the Harverson Granite (72921005).

granite, derived by melting of sedimentary rocks. Isotopic data are consistent with this conclusion. Although imprecise, the age clearly postdates that of the enclosed xenolith discussed above (1497 ± 146 Ma).

Big-feldspar gneiss at Mount Hay

The sample analysed is a granitic rock that intrudes the Redbank Deformed Zone (Marjoribanks & Black, 1974). The granite was deformed under low-grade amphibolite-facies conditions, and all minerals show various degrees of deformation and recrystallisation. Regression through total-rock analyses alone produced very wide precision limits from a restricted range of $^{87}Rb/^{86}Sr$. Five successive fractions from core to margin of a single microcline megacryst are, in essence, isotopically concordant, even though separated by up to 5 cm. Co-regression of microcline and total-rock samples (Fig. 21) reduced the MSWD to the total-rock isochron from 12 to 3.5, giving a model 3 isochron with age of 893 ± 67 Ma. This age should record the severe deformation under low-grade amphibolite-facies conditions that this rock has undergone, for the feldspar megacrysts are likely to be syntectonic with the foliation development. It provides a minimum estimate for the intrusion of this granitic body, and also represents a minimum age for uplift of the granulites in the Mount Hay region.

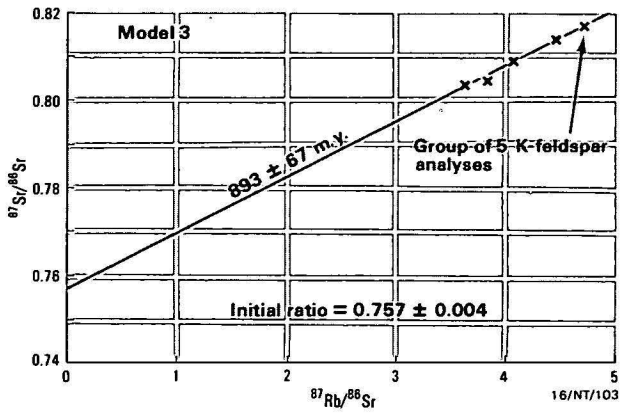

Figure 21. Rb-Sr isochron for big-feldspar gneiss (73933003) at Mount Hay.

Discussion

Two of the three mean ages of about 900 Ma presented above are not individually distinguishable from the 1050 Ma. Ormiston Event. Together, however, they are more diagnostic of a younger event, roughly contemporaneous with the 893 ± 67 Ma derived for the big-feldspar gneiss. Igneous activity in the Arunta Block at this time has been documented elsewhere: Allen & Black (1979) reported a Rb-Sr total-rock age of 990 ± 13 Ma for granite intruding the Harry Creek Deformed Zone; and Black & others (1980) presented a Rb-Sr mineral isochron age of 897 ± 9 Ma for dolerite from the Stuart Dyke Swarm in the Southern Tectonic Zone. This age represents an older limit for the unconformity separating the Arunta Block from the overlying Amadeus Basin sequence.

Conclusions

The ages reported above and in previous publications reveal a prolonged tectonothermal history for the Arunta Block. From the work of Black & others (1979), it is obvious that the oldest Rb-Sr ages are not primary, but have been reset during later high-grade tectonothermal events. Supporting evidence for this is provided by the relatively high initial $^{87}Sr/^{86}Sr$ ratios of the oldest isochron ages. Consequently, the Rb-Sr data provide only a minimum age estimate for sialic crust development. The region underwent widespread metamorphism at dominantly granulite facies at about 1800 Ma, and there is evidence for subsequent significant events at about 1700 Ma, 1600 Ma, 1050–900 Ma, and probably at about 1500 Ma, and 1400 Ma. Restricted emplacement of alkaline and carbonatitic rocks occurred at about 1200 Ma (Langworthy & Black, 1978) and 700 Ma (Black & Gulson, 1978), respectively.

The results illustrate some of the difficulties associated with the interpretation of isotopic ages in complex terrains. For example, the Cadney metamorphics give an older Rb-Sr total-rock age than the underlying Ongeva granulite, the result of imposition of a later deformation and consequent isotopic resetting at the particular sampled outcrop of the Ongeva granulite. For the same reason, many of the Rb-Sr total-rock ages, particularly those early in the history of the Arunta Block, have no direct stratigraphic significance, but are ages of metamorphism only.

Acknowledgements

Technical assistance in sample preparation and processing was provided by M.W. Mahon, T.K. Zapasnik, and J.L. Duggan. The manuscript was critically read in full by J.W. Sheraton and L.A. Offe, and parts of it were discussed with T.H. Bell and D.P. Windrim.

References

Black, L. P., 1975 -- Present status of geochronological research in the Arunta Block, N.T. *First Australian Geological Convention, 'Proterozoic Geology', Geological Society of Australia, Adelaide, May 1975, Abstracts*, 37.

Black, L. P., & Gulson, B. L., 1978 — The age of the Mud Tank Carbonatite, Strangways Range, Northern Territory. *BMR Journal of Australian Geology & Geophysics*, 3, 227–232.

Black, L. P., Bell, T. H., Rubenach, M. H., & Withnall, I. W., 1978 — The significance of Rb-Sr total-rock ages in a multiply deformed and polymetamorphic terrain. *In* Zartman, R. E., (editor), Short papers of the Fourth International Conference, Geochronology, Cosmochronology, Isotope Geology. *United States Geological Survey Open File Report* 78–701, 41–42.

Black, L. P., Bell, T. H., Rubenach, M. J., & Withnall, I. W., 1979 — Geochronology of discrete structural-metamorphic events in a multiply deformed Precambrian terrain. *Tectonophysics*, 54, 103–137.

Black, L. P., Shaw, R. D., & Offe, L. A., 1980 — The age of the Stuart Dyke Swarm and its bearing on the onset of Late Precambrian sedimentation in central Australia. *Journal of the Geological Society of Australia*, 27, 151–155.

Chopin, C., & Maluski, H., 1980 — ^{40}Ar–^{30}Ar dating of high pressure metamorphic micas from the Gran Paradiso area (Western Alps): evidence against the blocking temperature concept. *Contributions to Mineralogy and Petrology*, 74, 109–122.

Iyer, S. S., Woodford, P. J., & Wilson, A. F., 1976 — Rb-Sr isotopic studies of a polymetamorphic granulite terrane, Strangways Range, central Australia. *Lithos*, 9, 211–224.

Langworthy, A. P., & Black, L. P., 1978 — The Mordor Complex: a highly differentiated potassic intrusion with kimberlitic affinities in central Australia. *Contributions to Mineralogy and Petrology*, 67, 51–62.

Marjoribanks, R. W., & Black, L. P., 1974 — Geology and geochronology of the Arunta Complex, north of Ormiston Gorge, central Australia. *Journal of the Geological Society of Australia*, 21, 291–300.

Page, R. W., Blake, D. H., & Mahon, M. W., 1976 — Geochronology and related aspects of acid volcanics, associated granites, and other Proterozoic rocks in The Granites-Tanami region, northwestern Australia. *BMR Journal of Australian Geology & Geophysics*, 1, 1–13.

Shaw, R. D., Warren, R. G., Senior, B. R., & Yeates, A. N., 1975 — Geology of the Alcoota 1:250 000 Sheet Area. *Bureau of Mineral Resources, Australia, Record* 1975/100; *BMR Microform* MF107.

Shaw, R.D., Langworthy, A.P., Offe, L.A., Stewart, A.J., Allen, A.R., Senior, B.R., & Clarke, D.B., 1979 — Geological report on 1:100 000 scale mapping of the southeastern Arunta Block, Alice Springs 1:250 000 Sheet area, Northern Territory. *Bureau of Mineral Resources, Australia, Record* 1979/47.

Steiger, R. H., & Jager, E., 1977 — Subcommission on geochronology: convention on the use of decay constants in geo- and cosmochronology. *Earth & Planetary Science Letters*, 36, 359–362.

Stewart, A.J., Offe, L.A., Glikson, A.Y. Warren, R.G., & Black, L.P., 1980 — Geology of the northern Arunta Block, Northern Territory. *Bureau of Mineral Resources, Australia, Record* 1980/83.

Williams, I. S., Compston, W., Chappell, B. W., & Shirahase, T., 1976 — Rubidium-strontium age determinations on micas from a geologically controlled, composite batholith. *Journal of the Geological Society of Australia*, 22, 497–506.

Appendix 1. Details of dated samples

Kanandra Granulite

Sample 72902009 (Fig. 1, loc. 1).

Medium-grained granuloblastic gneiss intercalated with migmatite and basic granulite, and metamorphosed to upper amphibolite–granulite grade. The gneiss consists typically of perthitic K-feldspar (58%), quartz (25%), plagioclase (15%), brown biotite (2%) containing small opaque grains, garnet (trace) showing alteration along fractures to both brown and green biotite, traces of myrmekite and muscovite, and accessory zircon. Some of the fine-grained micas and the myremekite are secondary, as is the biotite within garnet fractures.

Cadney metamorphics

Sample 72913000, 5 km north of 'The Garden' (Fig. 1, loc. 2).

Partly mylonitised pelitic gneiss, which is interlayered with mafic rocks containing two pyroxenes and hornblende, consists of partly perthitic K-feldspar (54%), garnet (20%) enclosing biotite and sillimanite, sillimanite (10%), fine granular quartz (10%), biotite (4%), plagioclase (1%), magnetite (1%), and a trace of white mica and accessory spinel. A second deformation in the gneiss is indicated by bent and fractured K-feldspar grains, which are commonly rimmed by fine K-feldspar granules and thin lenses of recrystallised quartz, suggesting relict quartz ribbons. Retrograde reactions are the alteration of garnet to biotite and the chloritisation of biotite.

Mount Hay granulites

Sample 73933007, 3 km south of Valley Bore (Fig. 1, loc. 3).

Fine-grained slightly gneissic rock consisting of plagioclase (69%), hypersthene (9%), clinopyroxene (8%), quartz (6%), probable magnetite (4%), K-feldspar (2.5%), garnet (1.5%), and accessory hornblende and apatite. This sample is slightly more felsic than is typical for these granulites. The sparsity of hornblende suggests that drier conditions prevailed here than in much of the eastern part of the Arunta Block.

Sample 73933006 (Fig. 1, loc. 4).

The rock consists of plagioclase (64%) showing slight alteration to white mica and carbonate, clinopyroxene (12%), hypersthene (10%), green-brown hornblende (6%), quartz (5%), possible magnetite (2.5%) and accessory apatite. It is a fine to medium-grained granoblastic rock with a slight schistosity defined by granoblastic aggregates of mafic minerals, and also by the elongation of large quartz grains. A plagioclase megacryst has undergone later grain-growth. The schistosity, formed under hornblende-granulite-facies conditions, is stronger than in the nearby and previously discussed sample (73933007), but this may be due to 'wetter' conditions, suggested by the much greater hornblende content.

Ongeva granulite

Sample 73913006 (Fig. 1, loc. 5).

At this locality, granulite retaining granoblastic texture and consisting originally of hypersthene, garnet, K-feldspar, perthite, and cordierite has partly retrogressed to the assemblage biotite-garnet-cordierite-orthoclase-quartz.

Samples from a small pegmatitic (quartz-K-feldspar-garnet) segregation (73913007) are jointly regressed with this sample, because the combined grouping maintains model 1 conditions.

Granitic gneiss near Ambalindum

Sample 72913001 (Fig. 1, loc. 6).

This rock originally formed part of a sequence of felsic to mafic granulite, but has been strongly deformed and retrogressed along a relatively narrow zone. The gneiss consists of perthitic orthoclase (65%), quartz (25%), plagioclase (4%), biotite (4%), garnet (2%), and accessory hornblende, apatite, chlorite, and opaques. Orthoclase forms augen surrounded by thin rims of recrystallised feldspar.

Some orthoclase grains are bent and broken, and show internal recrystallisation. Much of the quartz is recrystallised or segmented into subgrains. Relict ribbon quartz grains suggest an earlier mylonitic fabric. Narrow folia contain fine to very fine recrystallised K-feldspar, quartz, and biotite. Garnet and opaque grains are interleaved with coarse biotite. Garnet is partly recrystallised.

Aileron metamorphics near Mount Boothby

Sample 73921021 (Fig. 1, loc. 7).

Medium-grained, slightly gneissic, granoblastic rock, consisting of quartz (25%), K-feldspar (62%), plagioclase (10%), brown and rare greenish biotite (2%), hypersthene (0.5%), and accessory green hornblende, myrmekite, apatite, sphene, ?allanite, and opaques.
Sample 73921022 (Fig. 1, loc. 8).

Medium-grained and granoblastic felsic gneiss with slight schistosity, containing orthoclase (50%), quartz (20%), plagioclase (21%), biotite (8%), green hornblende (0.5%), opaques (0.5%), rare myrmekite, and accessory apatite, and ?allanite.

Granite from near Mount Ida

Sample 72902006 (Fig. 1, loc. 9).

Foliated medium and even-grained granitoid, containing garnet and muscovite, and associated with veins and segregations of pegmatite, crops out 7 km north-northeast of Mount Ida. It has an allotriomorphic granular texture and shows no sign of later deformation. It may be a phase of the leucocratically comparable Mount Ida Granite.

Granite from Atnarpa Igneous Complex

Sample 73913009 (Fig. 1, loc. 10).

The granite is made up of subhedral oligoclase (40%) surrounded by partly recrystallised quartz (35%) and anhedral microcline (20%) and muscovite (2.5%), which both accompanies biotite (1.5%) and clinozoisite (1%) and is enclosed in oligoclase. A small proportion of biotite is altered to chlorite, and a trace of epidote is also present. Accessory minerals include apatite and opaque grains. Mild deformational features include bent micas and recrystallised quartz. Clinozoisite, chlorite, and sericite are retrograde minerals formed under greenschist-facies conditions.

Migmatite complex (pЄeg), Mount Bleechmore area

Sample 72902013 (Fig. 1, loc. 11).

This rock is a migmatitic gneiss made up of alternating palaeosome and leucosome layers (Mehnert, 1968). The palaeosome has a gneissic foliation and consists of plagioclase, quartz, perthitic microcline, hypersthene altered to biotite and opaques, and accessory apatite and zircon. The leucosome consists of perthitic microcline, quartz, garnet showing slight alteration to biotite, plagioclase, and opaque grains. A localised second foliation is outlined by biotite folia and finely recrystallised feldspar and garnet. Quartz, the bulk of which is concentrated in narrow layers, is largly recrystallised to a polygonal aggregate showing preferred dimensional and lattice orientation. Many feldspar grains are bent and fractured.

Microgranodiorite xenolith in Reynolds Range region

Sample 72921006 (Fig. 1, loc. 12)

A large microgranodiorite xenolith in the Harverson Granite contains ovoid to euhedral megacrysts of microcline (up to 5 cm), some of which are jacketed with plagioclase, which also occurs separately as small anhedral grains. Groundmass consists of plagioclase much altered to sericite, quartz, microcline, biotite, muscovite, a trace of clinozoisite, and accessory zircon, apatite, and opaques. The xenolith contains small darker xenoliths of fine biotite, quartz, and feldspar. These small xenoliths also occur in the host Harverson Granite, and are thought to be reconstituted metasediments from the adjoining Lander Rock beds.

Wangala Granite

Sample 72921010 (Fig. 1, loc. 13).

The Wangala Granite is a composite batholith, consisting of at least eight phases of foliated or massive granite. The dated sample is an even-grained muscovite adamellite. It has a hypidiomorphic granular texture, and consists of quartz, microcline (some of which poikiloblastically encloses quartz and plagioclase), plagioclase (An_{37-28}) showing slight alteration to sericite, large flakes of muscovite, biotite partly retrogressed to muscovite and chlorite, opaques, apatite, and rare green hornblende.

Lander Rock beds

Sample 73921024 (Fig. 1, loc. 14).

The analysed specimen consists of subangular to subrounded quartz grains, some plagioclase grains, rare pebbles of fine-grained micaceous sandstone, pelitic and quartzose rock fragments, and detrital tourmaline, in a schistose matrix of fine white mica, brownish green biotite, quartz, feldspar, and hematite. The schistosity is complex and consists of a weak slaty cleavage, which locally forms an anastomosing network.

Wuluma granitoid

Sample 75913020 (Fig. 1, loc. 15)

The granitoid is a coarse-grained homogeneous granular rock, enclosing rafts of mobilisate-rich biotite-quartzofeldspathic gneiss. It typically consists of quartz, microcline, which commonly poikiloblastically encloses some quartz, plagioclase showing alteration to sericite, slightly aligned biotite, and small amounts of muscovite, myrmekite, and opaques. In the dated sample, microcline (55%) and plagioclase (15%), showing extensive alteration to sericite and coarser white mica, form megacrysts, which are recrystallised at their edges and along fractures. The megacrysts occur in a fine-grained matrix of granular, recrystallised, partly aligned quartz grains (30%) and minor feldspar. A trace of biotite showing slight alignment is localised in patches.

Deformed granitic rock, Anmatjira Range

Sample 72921004 (Fig. 1, loc. 16).

The rock has a foliation outlined by narrow zones of high strain and patchy alignment of biotite. It is medium-grained, granular, and consists of strained quartz, polygonised into subgrains and cut by microfractures, strained microcline, fractured antiperthitic plagioclase with bent twin lamellae and some marginal myrmekite, bent flakes of (metamorphic?) biotite enclosing exsolved opaques, fractured garnet containing pale brown and green biotite, and accessory zircon and apatite. The biotite commonly occurs at plagioclase–microcline grain boundaries, but also along plagioclase twins and in fractures in plagioclase. It is commonly accompanied by fine retrograde epidote.

Amphibolite, Black Cone area

Sample 72913002 (Fig. 1, loc. 17).

A granoblastic rock containing plagioclase, hornblende, clinopyroxene, and hypersthene. The pyroxene grains have sutured boundaries, and some orthopyroxene grains are partly recrystallised and, in some cases, altered to actinolite, whereas the hornblende and plagioclase form elongate grains with smoothly curved or straight boundaries. The pyroxenes are considered to be relics of an earlier granulite metamorphism, whereas the hornblende and plagioclase outline a foliation formed during a later tectonothermal event.

Boothby Orthogneiss

Sample 73921020 (Fig. 1, loc. 18).

The analysed granitic gneiss sample contains recrystallised granular quartz, granular microcline (uncommon), secondary muscovite, and accessory myrmekite and carbonate. The foliation is outlined by muscovite and biotite folia, and probably dates from the time of quartz recrystallisation. Plagioclase is altered to clinozoisite,

muscovite and carbonate, and biotite shows localised alteration to chlorite. K-feldspar–plagioclase ratios commonly range from 2:1 to 3:1, but plagioclase-free variants also occur. In places, plagioclase rims microcline in typical rapakivi fashion. Quartz, biotite altering locally to chlorite and epidote, zircon, apatite, sphene, and probable ilmenite are also present. Some varieties contain hornblende. Apart from the gneissosity, there is generally little evidence of high-grade metamorphism, except in some areas where sillimanite and/or garnet indicate amphibolite-facies effects.

Harverson Granite

Sample 72921005 (Fig. 1, loc. 19).

The analysed sample consists of microcline megacrysts, plagioclase markedly altered to sericite and some clinozoisite, quartz, and minor biotite and muscovite. The rock is cut by veinlets of quartz and clinozoisite. The muscovite and clinozoisite are thought to be the products of deuteric alteration.

Big-feldspar gneiss at Mount Hay

Sample 73933003 (Fig. 1, loc. 20).

The analysed sample is a granitic gneiss, and consists of microcline and microperthite megacrysts, plagioclase, quartz, brown biotite, and accessory zircon, myrmekite, apatite, and opaques. Secondary minerals are mostly unstrained. They occur in narrow wavy anastomosing foliation zones, and include biotite, muscovite, nonperthitic microcline, garnet, blue-green hornblende reacting to biotite, carbonate, and sphene.

BMR Journal of Australian Geology & Geophysics, 8, 139-145

PROGRADE AND RETROGRADE SAPPHIRINE IN METAMORPHIC ROCKS OF THE CENTRAL ARUNTA BLOCK, CENTRAL AUSTRALIA

R.G. Warren

Sapphirine is a common mineral in silica-undersaturated rocks within the Mid-Proterozoic granulites of the Arunta Block in the northern Strangways Range, central Australia, and reactions involving sapphirine illustrate three episodes in the metamorphic evolution of the region. Prograde sapphirine-orthoclase-orthopyroxene assemblages occur as relics from the granulite stage (estimated P–T conditions 8 ± 1 kb, 850–920°C). In an early pervasive regional hydration, orthopyroxene-orthoclase-spinel assemblages reacted to form sapphirine-phlogopite or cordierite-phlogopite assemblages. As the rocks cooled from the abnormally high geothermal gradient to a 'normal' geothermal gradient, fine-grained intergrowths of orthopyroxene and sillimanite formed by reaction between sapphirine and cordierite.

Introduction

Granulite-facies assemblages, commonly partly retrogressed, are preserved over a considerable part of the Arunta Block, central Australia. Within the granulites, rocks containing sapphirine are also widely distributed (Warren, 1979). This paper is concerned principally with sapphirine-bearing rocks from the northern Strangways Range (Fig. 1) and the relationship between the metamorphic evolution of the rocks and various reactions involving sapphirine. These reactions provide some of the most important evidence for the early high-grade stages in the metamorphic evolution of this part of the Arunta Block. Also, because of the presence of precursor assemblages, the commonly reported textural association of sapphirine rimming spinel can now be recognised as the result of retrogressive hydration of the anhydrous assemblage orthoclase- orthopyroxene-spinel.

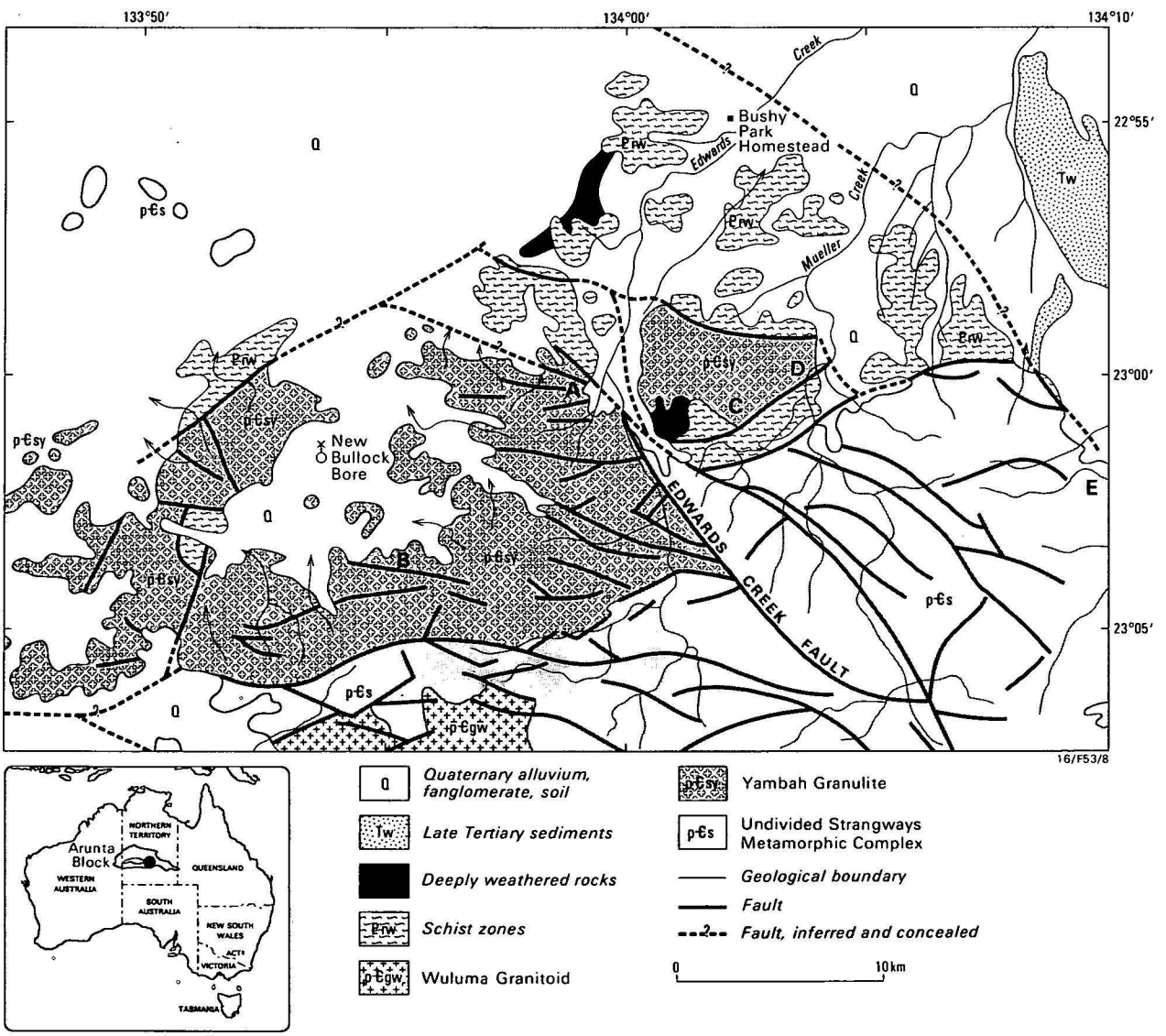

Figure 1. Generalised geology of the northern Strangways Range (after Shaw & Wells, in press, and Shaw & Warren, 1975).

Metamorphic evolution of the northern Strangways Range

The northern Strangways Range has had a protracted metamorphic history (Warren, 1982). The protolith probably formed shortly before 1850 Ma (L.A.I. Wyborn, BMR, personal communication, 1983), and was almost immediately metamorphosed to granulite facies, at about 1800 Ma (Black, 1975; Iyer & others, 1976; Black & others, 1983). This was followed by a regional hydration, isobaric cooling, and several episodes of hydration localised in shear zones transecting the granulite terrain. Amphibolite retrogression at about 1700 Ma (Black, 1975; Black & others, 1983) is correlated with the formation of gedrite and gedrite-kyanite assemblages.

The dry granulite stage was characterised by co-existing pyroxenes in mafic rocks, orthopyroxene-orthoclase in rocks of suitable bulk composition (either felsic or pelitic protoliths), and clinopyroxene-wollastonite-scapolite-calcite in calc-silicate rocks. Estimated pressure-temperature conditions for areas A and B from various geobarometers and geothermometers (Fig. 2) are 8 ± 1 kb, 850–920°C (Warren, 1982). The granulite metamorphism was followed by pervasive but incomplete regional hydration. Pargasitic hornblende formed from two-pyroxene-plagioclase assemblages in mafic granulites, and biotite formed by hydration of orthopyroxene-orthoclase-bearing assemblages.

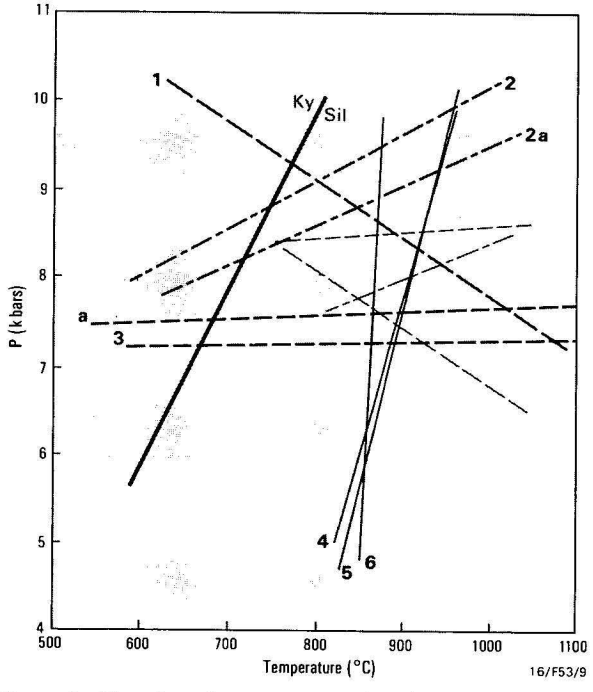

Figure 2. Plot of geothermometers and geobarometers calculated for specimens collected from area B.
1 — clinopyroxene-plagioclase-quartz (Ellis, 1980); 2 & 3 — garnet-plagioclase-orthopyroxene-quartz (Perkins & Newton, 1981, Harley & Green, 1982); 4 & 5 — Al_2O_3 exchange between garnet and orthopyroxene (Wood, 1974, & Harley & Green, 1982); and 6 — Fe-Mg exchange between garnet and orthopyroxene (Harley & Green, 1982). Limits are indicated for curves 1, 2a, and 3a. (After Warren, 1982).

The rocks then cooled under near-isobaric conditions to a 'normal continental' geothermal gradient. Clark & Ringwood (1964) considered the present-day steady-state continental geothermal gradient to be in the kyanite stability field, though higher geothermal gradients in the Precambrian were possible. The evidence from the retrogressive assemblages in the northern Strangways Range suggests the steady-state geothermal gradient was close to the kyanite-sillimanite boundary in the pressure range 6–9 kb. Subsequent periods of hydration were confined to shear zones. The earliest of these produced gedrite from orthopyroxene and gedrite-kyanite from cordierite. This hydration took place at similar pressures, but much lower temperatures, than the granulite-facies metamorphism. For areas C and D, where granulite-facies metamorphic conditions are estimated as 7.5 ± 1 kb, 795-850°C, the formation of kyanite-gedrite assemblages occurred at pressure-temperature conditions of 7.5–8.7 kb, 650–720°C (Warren, 1982).

Sapphirine-bearing assemblages

Sapphirine occurs in rocks with high MgO/FeO and low SiO_2, and which consist predominantly of K_2O, MgO, FeO, Al_2O_3 and SiO_2. The minerals found associated with sapphirine include spinel, cordierite, sillimanite, corundum, orthopyroxene, orthoclase, and phlogopite. Plagioclase, generally a sodic variety, is present in minor amounts in some specimens. In this paper, such rocks are referred to as silica-undersaturated rocks to emphasise the absence of free quartz and presence of silica-undersaturated mineral species. Sapphirine-bearing assemblages formed in both the granulite and early-hydration stages, and sapphirine was involved in additional reactions during the near-isobaric cooling.

Table 1. Abbreviations used in this report
Minerals: Cd — cordierite; Kf — orthoclase; Opx — orthopyroxene; Ph — phlogopite; Q — quartz; Sap — sapphirine; Sil — sillimanite; Sp — spinel
System: KFMASH — K_2O-MgO-FeO-Al_2O_3-SiO_2-H_2O

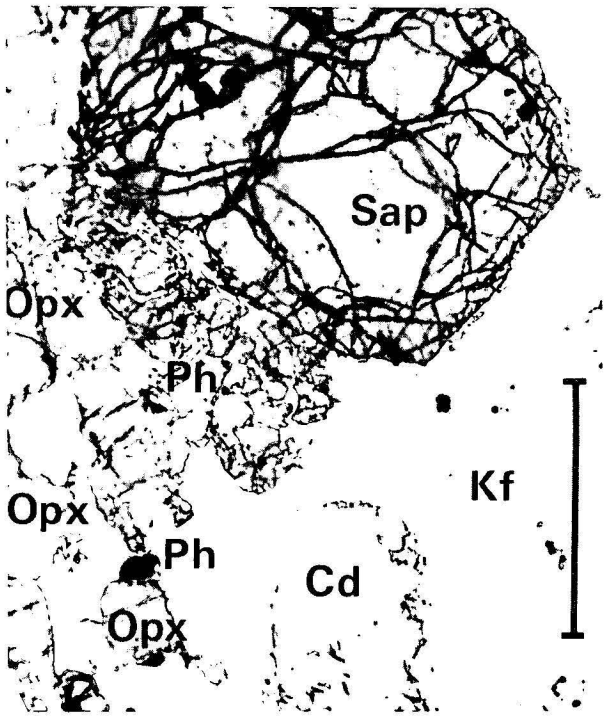

Figure 3. Granulite stage assemblage in a silica-undersaturated specimen (Area A, 80912785A), containing euhedral sapphirine, orthopyroxene, and cordierite.
Spinel, now partly mantled by sapphirine occurs elsewhere in the thin section. Note the phlogopite in the lower half of the photograph invading and partly replacing orthopyroxene. Scale bar 2 mm. Plane polarised light.

Prograde sapphirine occurs as idioblasts enclosed in feldspar, and is preserved in some specimens collected in the northern Strangways Range (Fig. 3): it can be distinguished texturally and by mineral association from retrograde sapphirine, which occurs as rims on spinel in the presence of abundant phlogopite, formed during the subsequent regional hydration. Relict anhydrous assemblages in the specimens from the northern Strangways Range enable recognition of the reaction by which the retrograde sapphirine formed. During near-isobaric cooling, cordierite and sapphirine reacted to produce fine-grained intergrowths of orthopyroxene and sillimanite. (The complex lower-temperature reactions that affected sapphirine-bearing rocks adjacent to the shear zones are not included in this report. On textural evidence these appear to have been sapphirine-out reactions.)

Sapphirine of the granulite stage

In rocks with bulk compositions in the KFMASH system, the index mineral association for the granulite facies is orthopyroxene-orthoclase. In silica-undersaturated rocks from areas A and B, sapphirine occurs with orthopyroxene and orthoclase; such rocks are characterised by spectacular, pegmatite-like patches of indigo-blue sapphirine euhedra enclosed in white orthoclase.

In the more magnesian, silica-undersaturated specimens from area A (e.g. BMR registered specimen 7791281A, mg of sapphirine = 100 x molecular MgO/MgO + FeO = 86–88), the divariant assemblage in the granulite stage was orthoclase-sapphirine-orthopyroxene-cordierite-spinel (cf. Figs. 3, 4a). In less-magnesian specimens collected from area B (e.g. 73914424, mg of sapphirine = 76–77), orthopyroxene and sillimanite are intergrown, so that these specimens appear to have contained the univariant anhydrous assemblage, orthoclase-sapphirine-orthopyroxene-sillimanite-cordierite-spinel (Figs. 4b, 5). Specimens containing the divariant assemblage, orthoclase-orthopyroxene-sillimanite-cordierite-spinel, have also been collected from area B.

In the pervasive hydration that followed the granulite stage phlogopite formed from orthoclase-orthopyroxene (e.g. Fig. 3). For silica-saturated rocks this reaction is presented by the equation: $H_2O + Kf + Opx \rightarrow Ph + Q$ . . . (1) (Table 1) so that, in silica-saturated rocks, quartz formed with the phlogopite. However in silica-undersaturated rocks, silica-deficient minerals were also involved in the phlogopite-forming reactions. In spinel-bearing rocks sapphirine rims formed on spinel through the reaction: $H_2O + Kf + Opx + Sp \rightarrow Sap + Ph$ . . . (2) (Figs.6, 7a,). Symplectites of spinel-orthopyroxene in specimens from areas A and B have been partly or wholly converted to intergrowths of sapphirine and orthopyroxene, concurrently with the formation of nearby phlogopite, also through reaction (2). Woodford & Wilson (1976) previously reported the association of sapphirine rims on spinel with abundant phlogopite in specimens from area E (Fig. 1), but, in the absence of the precursor assemblage, did not identify the reaction involved.

In granulites containing sapphirine-orthopyroxene-orthoclase, cordierite rims formed on sapphirine (Figs. 7b, 8) by the reaction: $H_2O + Kf + Opx + Sap \rightarrow Ph + Cd$ . . . (3) In the less-magnesian rocks from area B, two additional reactions may have occurred (Fig. 7c,d): $H_2O + Kf + Opx + Sp \rightarrow Ph + Sil$ . . . (4) and $H_2O + Kf + Opx + Sap \rightarrow Ph + Sil$ . . . (5).

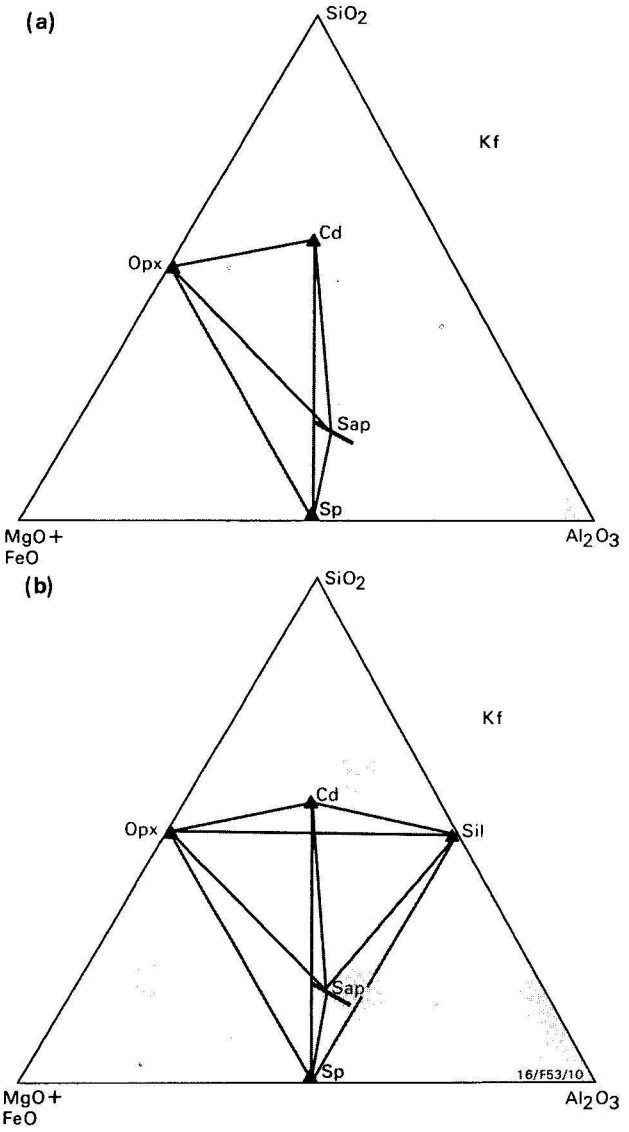

Figure 4. Granulite-stage assemblages in silica-undersaturated rocks from areas A & B, using the projection from $KAlSi_3O_8$ into the (F + M) AS triangle:
(a) the divariant assemblage Opx-Sp-Sap-Cd + Kf and (b) the univariant assemblage in 73914424, 73914426, and 73914429 from area B. The presence of the six phases orthoclase, orthopyroxene, sapphirine, spinel, cordierite, and sillimanite within single thin sectionsindicates conditions during the granulite metamorphism were close to the univariant curve linking all six phases.

Coarse-grained sillimanite intergrown with orthopyroxene or orthoclase (e.g. Fig. 5) is considered part of the granulite-stage assemblage in silica- undersaturated rocks from area B. However, sillimanite enclosed by phlogopite in the same specimens may be retrograde, formed by reactions (4) and (5).

Specimens containing orthopyroxene-orthoclase-quartz occur in areas C and D, and the textural relationships of sapphirine and cordierite to spinel in phlogopite-bearing undersaturated rocks are very similar to those observed in the partly hydrated silica-undersaturated rocks from areas A and B (Figs. 6, 9). Therefore, it is deduced that assemblages that had contained orthopyroxene-orthoclase-spinel hydrated to phlogopite-bearing assemblages, with either sapphirine or cordierite rimming spinel. Sapphirine is a comparatively rare mineral in silica-undersaturated rocks from areas C and D. It occurs only in the most magnesian rocks and the least magnesian sapphirine has mg of 96. In

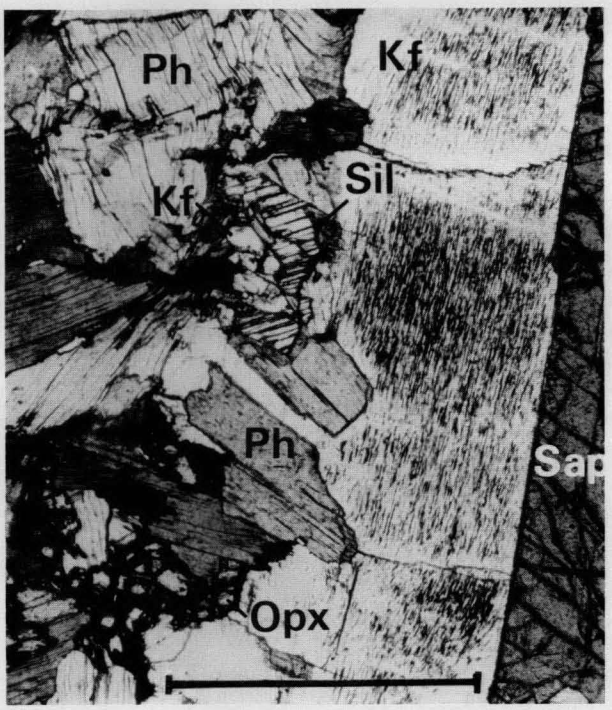

Figure 5. Relict granulite-stage assemblage of sillimanite, orthopyroxene, and cordierite, with later phlogopite (slide 12 of composite TS 75912657B, area B).
Scale bar 1 mm. Plane polarised light.

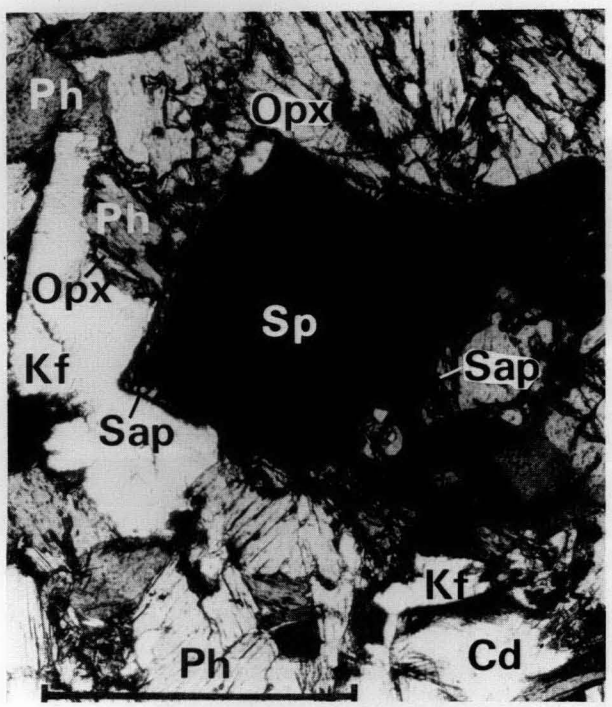

Figure 6. Rims of retrogressive sapphirine on spinel, formed by hydration of an orthoclase-orthopyroxene-spinel-cordierite assemblage (Area B, 73914426).
Scale bar 1 mm. Plane polarised light.

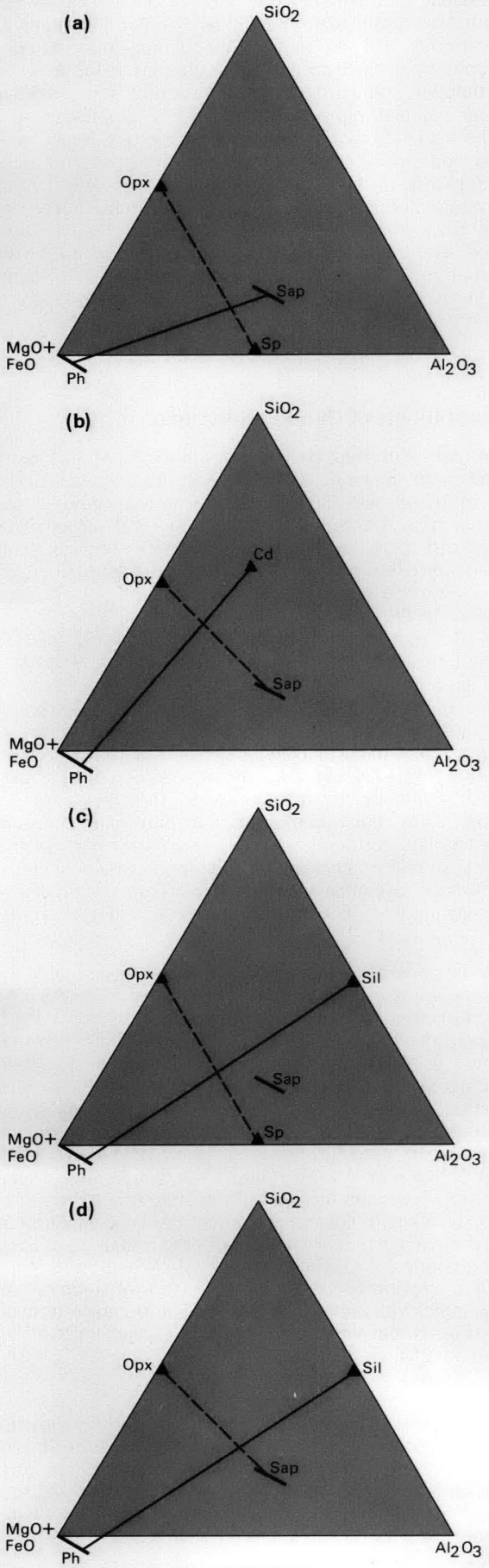

most silica-deficient rocks, cordierite encloses spinel in a distinctive enclave texture (Figs. 10, 11), even in those rocks in which garnet was present in the granulite-facies assemblage (Fig. 7e). The reaction for the formation of cordierite rimming spinel is represented by the equation: H_2O + Kf + Opx + Sp → Ph + Cd . . . (6).

The hydration reactions by which phlogopite formed should be more temperature-dependent than pressure-dependent (for constant P_{H_2O}). Comparison of coexisting garnet and cordierite, and geothermometers and geobarometers based on coexisting pyroxenes, clinopyroxene-plagioclase-quartz, and garnet-orthopyroxene (Warren, 1982) indicates that conditions of metamorphism were 0.5 kb and 50°C lower in areas C and D than in areas A and B. However, the presence of relict orthopyroxene-orthoclase-quartz shows that P_{H_2O} was similar and low in all areas. The different assemblages formed in silica-undersaturated rocks in areas C and D are, therefore, considered to reflect different pressure-temperature conditions in these areas.

The reaction between sapphirine and cordierite during isobaric cooling

During isobaric cooling, the cooling path may cross the divariant fields of reactions with low positive slopes, so that 'apparently high pressure' assemblages form by cooling. An important example of such a reaction is: Sap + Cd → Opx + Sil . . . (7). Newton & others (1974) calculated a low positive slope for this reaction in the MAS system (Fig. 12). In the FMAS system the reaction is divariant, and during the cooling the least magnesian sapphirine and cordierite react at the highest temperature. Therefore, in specimens from area B (e.g. 73914424, in which mg of sapphirine is 76–77) abundant fine-grained orthopyroxene-sillimanite occurs at cordierite-sapphirine boundaries (Figs. 6, 13), but in more magnesian specimens from area A (Fig. 8) the reaction between cordierite and sapphirine is less advanced.

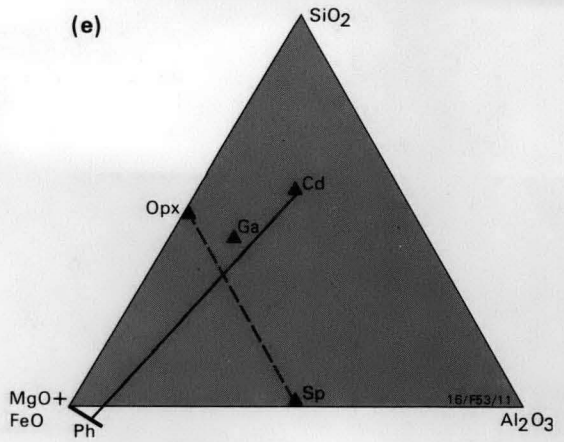

Figure 7. Hydration reactions in silica-undersaturated rocks, illustrated using the projection from $KAlSi_3O_8$ into the (F + M)AS triangle.
(a) H_2O + Kf + Opx + Sp → Ph + Sap (illustrated in Fig. 6); (b) H_2O + Kf + Opx + Sap → Ph + Cd (shown in Fig. 8); (c) H_2O + Kf + Opx + Sp → Ph + Sil (for conditions in which sapphirine is not stable); (d) H_2O + Kf + Opx + Sap → Ph + Sil; (e) H_2O + Kf + Opx + Sp → Ph + Cd (showing that, under conditions where cordierite and garnet are both stable, cordierite forms rims on spinel, as in Fig. 11).

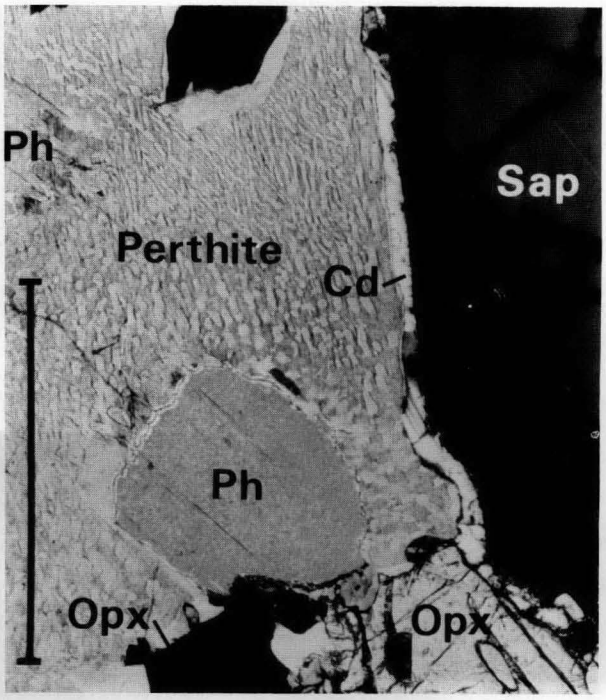

Figure 8. Cordierite rim on euhedral sapphirine. (Area A, 80912785B).
Scale bar 1 mm. Crossed nicols.

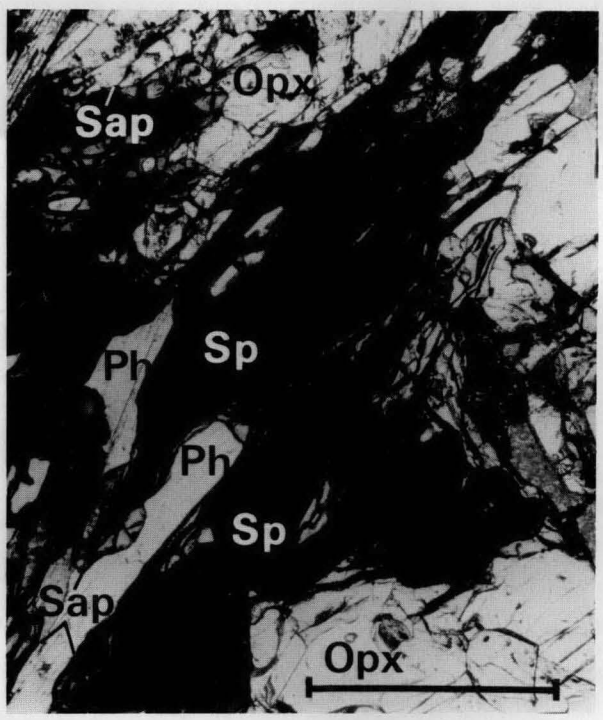

Figure 9. Sapphirine rims on spinel (Area D, 80900071A).
Scale bar 0.5 mm. Crossed nicols.

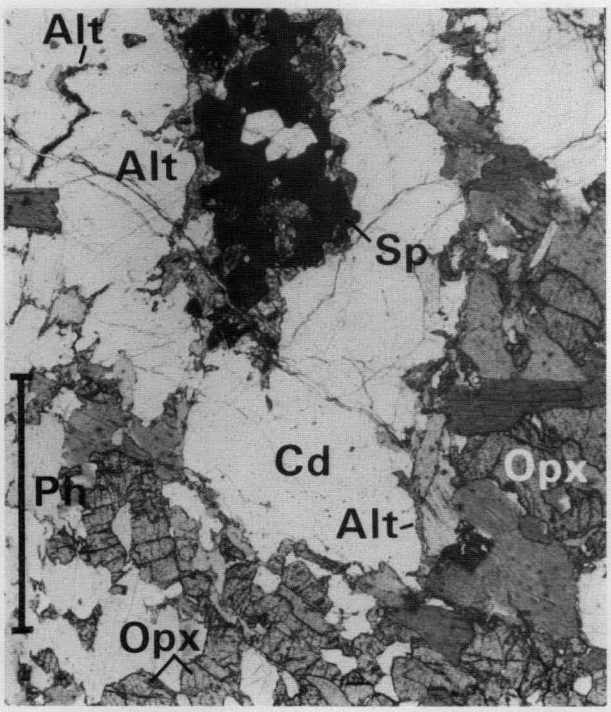

Figure 10. Enclave of spinel enclosed by cordierite within orthopyroxene-phlogopite, (Area C, 75912665).
Fine grained intergrowths, labelled ALT, at cordierite grain boundaries consist of phlogopite, sillimanite and gedrite. Scale bar 2 mm. Plane polarised light.

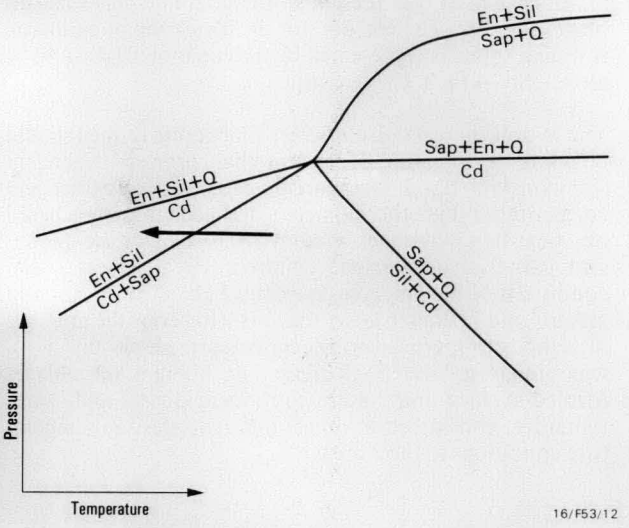

Figure 12. Schreinemakers' analysis for the phases enstatite (En), quartz, sillimanite, cordierite and sapphirine in the MAS system (Newton & others, 1974).
A near isobaric cooling path (shown by the heavy arrow) will cross to the 'high pressure' side of the reaction Cd + Sp → En + Sil as the temperature falls. Also, at still lower temperatures, cordierite in quartz-saturated rocks breaks down to enstatite-sillimanite-quartz.

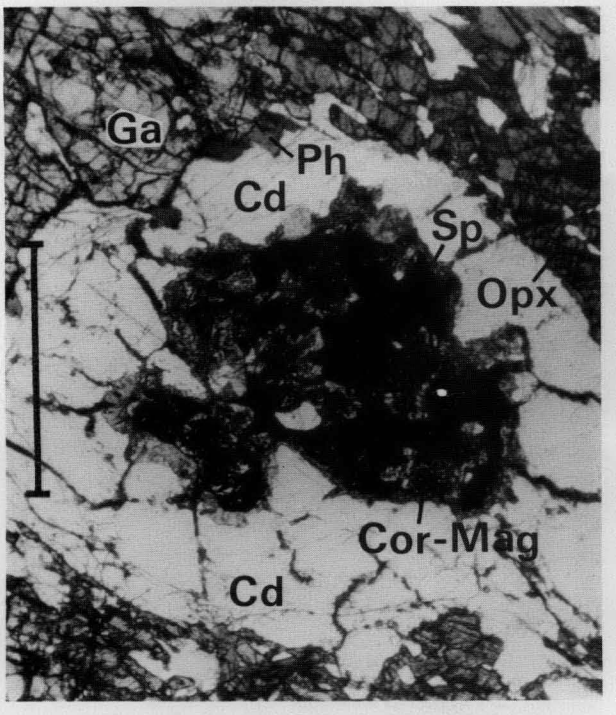

Figure 11. Retrogressive cordierite enclosing spinel (partly altered to later corundum-magnetite) (Area D, 73914523).
Cordierite formed from spinel-orthopyroxene-orthoclase despite the presence of garnet (Figure 7f). Scale bar 2 mm. Plane polarised light.

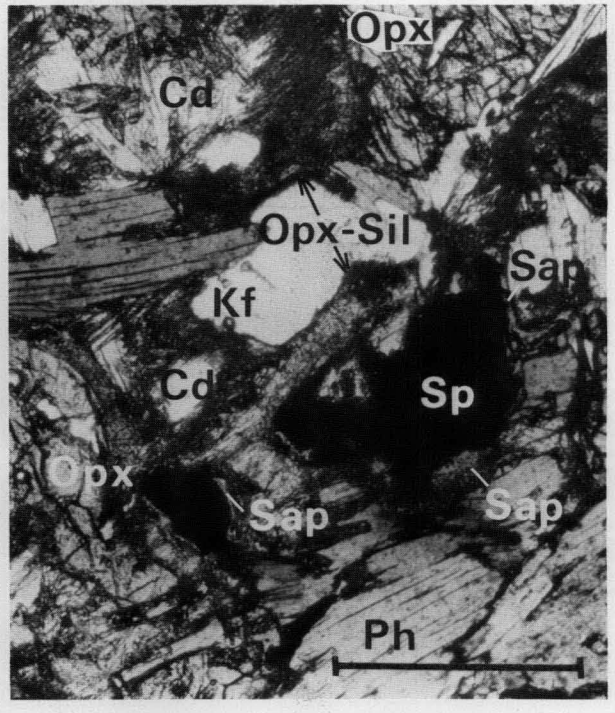

Figure 13. Fine-grained orthopyroxene-sillimanite formed by reaction between sapphirine and cordierite (Area B, 73914429) during isobaric cooling. Sapphirine rims on spinel away from cordierite have not been affected. Scale bar 0.5 mm. Plane polarised light.

Conclusions

Sapphirine-bearing assemblages in silica-undersaturated rocks from the northern Strangways Range have been invaluable for delineating the early stages in the metamorphic evolution of this area. Rocks containing sapphirine are widely distributed in the Arunta Block. Comparisons of the assemblages found in these rocks, using petrogenetic grids for the silica-undersaturated part of the KFMASH system (Hensen, 1983), should provide data on both the metamorphic evolution and relative pressure-temperature paths.

Acknowledgements

This paper is based on studies made as part of a Ph.D thesis prepared under the supervision of Dr B.J. Hensen at the University of New South Wales. The outcrop areas A, B, & D were discovered by A.P. Langworthy during the regional mapping program in the Arunta Block, and I am very appreciative of his generosity in suggesting I should study such petrologically interesting material. Drs D.J. Ellis, B.J. Hensen, and J.W. Sheraton made useful criticisms of drafts of this paper.

References

Black, L.P., 1975 — Present status of geochronological research in the Arunta Block. *First Australian Geological Convention, 'Proterozoic Geology', Geological Society of Australia, Adelaide, 1975, Abstracts*, 37.

Black, L.P., Shaw, R.D., & Stewart, A.J., 1983 — Rb-Sr geochronology of Proterozoic events in the Arunta Inlier, central Australia. *BMR Journal of Australian Geology & Geophysics*, 8 (this issue).

Clark, S.P., & Ringwood, A.E., 1964 — Density distribution and constitution of the mantle. *Reviews of Geophysics*, 2, 35–88.

Ellis, D.J., 1980 — Osumilite-sapphirine-quartz granulites from Enderby Land, Antarctica: PT conditions of metamorphism, implications for garnet-cordierite equilibria and the evolution of the deep crust. *Contributions to Mineralogy and Petrology*, 74, 201–210.

Harley, S.L. & Green, D.H., 1982 — Garnet-orthopyroxene barometry for granulites and peridotites. *Nature*, 300, 697–701.

Hensen, B.J., 1983 — Theoretical phase relations of ferromagnesian minerals in the silica-undersaturated portions of the systems FeO-MgO-Al_2O_3-SiO_2 (FMAS), FMASH (additional H_2O), and KFMASH (additional K_2O) for aluminous high-grade amphibolites and granulites. *Geological Society of Australia, Abstract Series*, 9, 63–64.

Holdaway, M.J., 1971 — Stability of andalusite and the aluminium silicate phase diagram. *American Journal of Science*, 271, 97–131.

Iyer, S.S., Woodford, P.J., & Wilson, A.F., 1976 — Rb-Sr isotopic studies of a polymetamorphic granulite terrane, Strangways Range, central Australia. *Lithos*, 9, 211-224.

Newton, R.C., Charlu, T.V., & Kleppa, O.J., 1974 — A calorimetric investigation of the stability of anhydrous magnesium cordierite with application to granulite facies metamorphism. *Contributions to Mineralogy and Petrology*, 44, 295–311.

Perkins, D. & Newton, R.C., 1981 — Charnockite geobarometers based on coexisting garnet-pyroxene-plagioclase-quartz. *Nature*, 292, 144–146.

Shaw, R.D. & Warren, R.G., 1975 — Alcoota, N.T. - 1:250 000 geological series, *Bureau of Mineral Resources, Australia, Explanatory Notes* SF/53–10.

Shaw, R.D. & Wells, A.T., in press — Alice Springs, N.T. (second Edition). — 1:250 000 geological Series, *Bureau of Mineral Resources, Australia, Explanatory Notes* SF/53–14.

Warren, R.G., 1979 — Volcanogenic and sedimentary origins to sapphirine-bearing rocks in the Arunta Block, central Australia. *Nature*, 278, 159–161.

Warren, R.G., 1982 — Metamorphic paragenesis in part of the Arunta Complex, Northern Territory. *Ph.D. thesis, University of New South Wales.*

Wood, B.J., 1974 — The solubility of alumina in orthopyroxene co-existing with garnet. *Contributions to Mineralogy and Petrology*, 46, 1–15.

Woodford, P.J., & Wilson, A.F., 1976 — Kornerupine in metasomatic zones, Strangways Range, central Australia. *Mineralogical Magazine*, 40, 589–594.

BMR Journal of Australian Geology & Geophysics, 8, 147-156

THE SEISMIC ZONE OF THE PAPUAN FOLD BELT

I.D. Ripper[1] & K.F. McCue[1].

Improved regional seismograph coverage in the 1970s has enhanced the resolution of the seismicity of the southern highlands of Papua New Guinea. Two zones can be defined. The Southern Highlands Seismic Zone follows the Papuan Fold Belt and extends from Kerema on the Gulf of Papua through the Star Mountains region into Irian Jaya. A second zone, the Mount Hagen Seismic Zone, plunges to the north-northeast from the Southern Highlands Seismic Zone south of Mount Hagen to intersect the intermediate-depth seismicity beneath the Ramu- Markham Valley. The southern highlands earthquakes reflect continuing Pliocene–Quaternary thrust faulting in the crust of the Indo-Australian Plate, brought about by the collision of the Indo-Australian and South Bismarck Plates over the sinking Solomon Sea Plate. Relief of compressive stress is through fracturing of the continental plate margin. The zone of fracture is now manifest in the Papuan Fold Belt. Seismic risk in the Southern Highlands Seismic Zone is less than that of the north coast, New Britain, and Bougainville, but is still high. The once-a-year largest earthquake is of magnitude 4.7, the ten-year earthquake magnitude 6.2, and the 30-year earthquake magnitude 6.9, which compare with the Californian figures of 5.7, 6.9, and 7.4, respectively. Large earthquakes are expected to occur along the zone in the future and their effects could be severe.

Introduction

On 19 January 1922, a magnitude 7.5 earthquake with its epicentre near Kikori occurred beneath the southern foothills of the central ranges of Papua New Guinea. The earthquake was felt strongly 200 km to the southwest. The Meteorological Observer at Daru reported that village houses were damaged in the southwest Papua region, that the sea was disturbed as if boiling, that at Sumai village (exact location not known) a six foot high wave swept over the village, and that people were terrified (see Fig. 1 for localities).

On 2 November 1931, a magnitude 6.5 earthquake occurred near Kerema. The Resident Magistrate reported that a number of village houses collapsed, trees crashed, and long cracks appeared in the ground.

On 3 March 1954, a magnitude 7 earthquake occurred in the Tari–Doma Peaks region, where it was felt at Modified Mercalli Intensity 7 (Dent, 1974; Everingham, 1979). The earthquake was felt from Daru on the south coast to Wewak in the north. A magnitude 5.5 earthquake in the same locality on 6 September 1977 caused landslides, which blocked the Tari–Margarima road.

On 25 June 1976, a magnitude 7.1 earthquake killed an estimated 420 people in Irian Jaya, near the border with Papua New Guinea (UNDRO, 1976). Landslides swept away or buried many villages and gardens. Fifteen small villages were completely destroyed and 70 more were damaged. The epicentre was 130 km northwest of the Star Mountains, and the area of destruction came to within about 60 km of the Papua New Guinea border near the Star Mountains. A second magnitude 7 earthquake occurred four months later, on 29 October 1976, killing many more people.

On 19 January 1981, another earthquake in Irian Jaya, 200 km west of the Star Mountains, was responsible for the deaths of over 300 people. The earthquake magnitude was 6.5. The devastated region was visited by H. Letz of the Freie University, West Berlin, in co-operation with the Indonesian Government, in February 1981 (Letz, personal communication).

These large earthquakes were not isolated events on the southern edge of the main seismic zone of northern New Guinea. Rather, they were events within a discrete seismic zone, here termed the Southern Highlands Seismic Zone. This zone coincides with the southern slopes of the central ranges and extends from the region of Kerema, on the Gulf of Papua, through the Star Mountains into Irian Jaya (Fig. 2; Ripper & McCue, 1982).

Papuan Fold Belt

The seismic zone coincides with the southern slopes of the central ranges, a region characterised by long northwest–southeast ridges of moderate relief, rarely more than 1500 m high, under heavy jungle cover, becoming more rugged in the west, and surmounted by several Quaternary stratovolcanoes (Dow, 1977). This region is part of a distinct geological structural unit, the Aure Tectonic Zone (Thompson & Fisher, 1965), which incorporates the Papuan Fold Belt (Bain, 1973). Bain described the Papuan Fold Belt as a belt of sub-parallel folds and faults, 50–70 km wide and 1000 km long, which bounds the northern and eastern limits of the Fly Platform. Broad synclines and tight, commonly faulted, anticlines in the northeast give way to overthrust anticlines in the southwest. Tertiary limestone has been considerably shortened by both folding and overthrusting from the north or, in the Aure Trough, from the east. Bain considered that some thrust faults clearly extend to considerable depth in the Mesozoic sequence and possibly into the Palaeozoic basement.

Jenkins (1974) interpreted the thrusts as resulting from gravity-induced horizontal sliding towards the southwest, away from an anticlinal uplift in the northeast. Davies (1979) rejected the gravity sliding mechanism for the development of the thrusts. He maintained that the thrusts are now recognisable as a classic foreland thrust belt, crustal shortening being north–south and northeast–southwest. According to Davies, thrusting commenced in the Pliocene and continued into the Quaternary, the axes of thrust activity and of uplift migrating southwards to the present location through the Star Mountains.

An essential difference between the two hypotheses is that Jenkins interprets the thrusts as being confined to depths above about 7 km, while Davies postulates that they extend to depths of about 25 km. Both hypotheses envisage the thrusting processes as continuing, as the existence of the seismic zone would seem to confirm.

Volcanism in the highlands and south of the highlands has continued from late Pliocene through the Pleistocene. Two volcanoes currently show signs of activity, Doma Peaks near Tari, and Mount Yelia near Menyamya (Mackenzie, 1976). Thus, the tectonic uplift and thrusting have occurred concurrently with the volcanism.

[1] Department of Minerals and Energy, Geological Survey, Geophysical Observatory, Box 323 Port Moresby, Papua New Guinea.

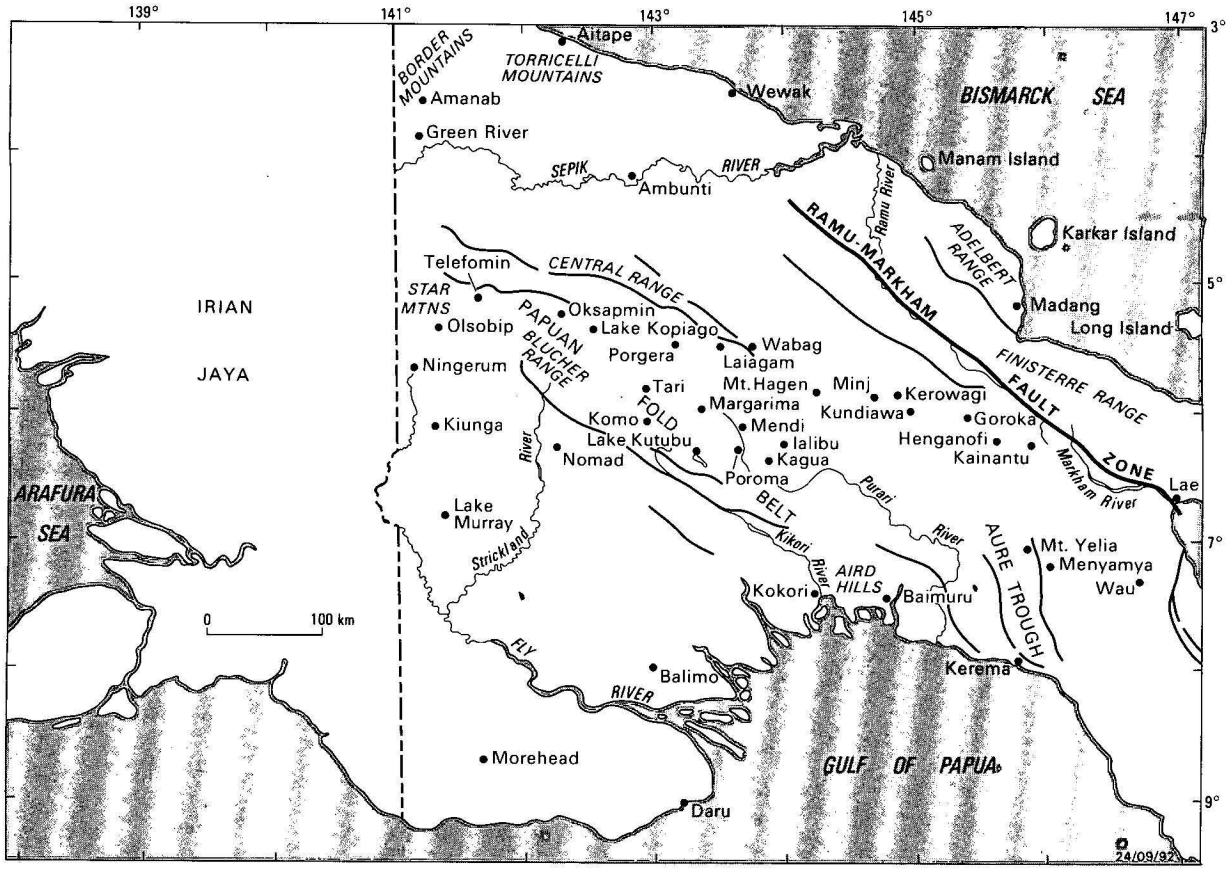

Figure 1. Central New Guinea localities and Pliocene–Quaternary fault zones, showing the Papuan Fold Belt.

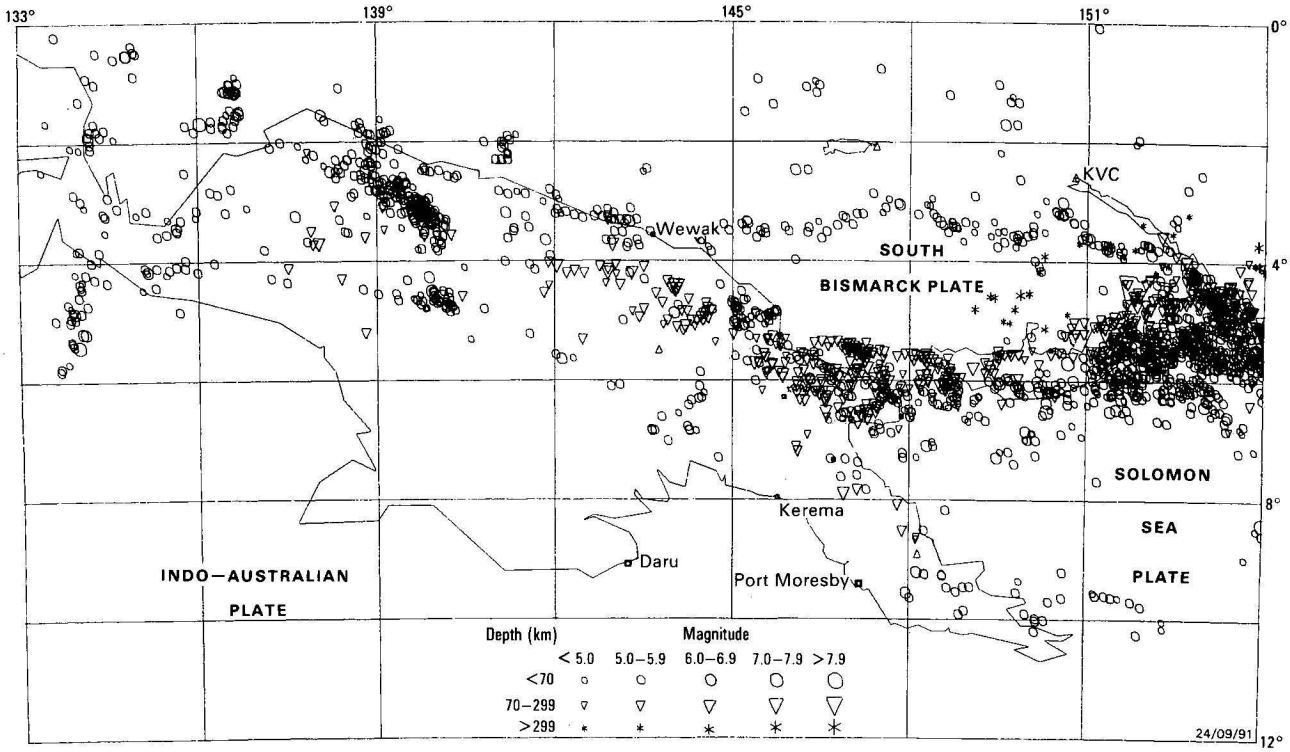

Figure 2. Seismicity of the New Guinea region, 1964–1980.
Fifteen or more stations used in the earthquake locations. The Southern Highlands Seismic Zone and the Mount Hagen Seismic Zone branching off it are clearly apparent.

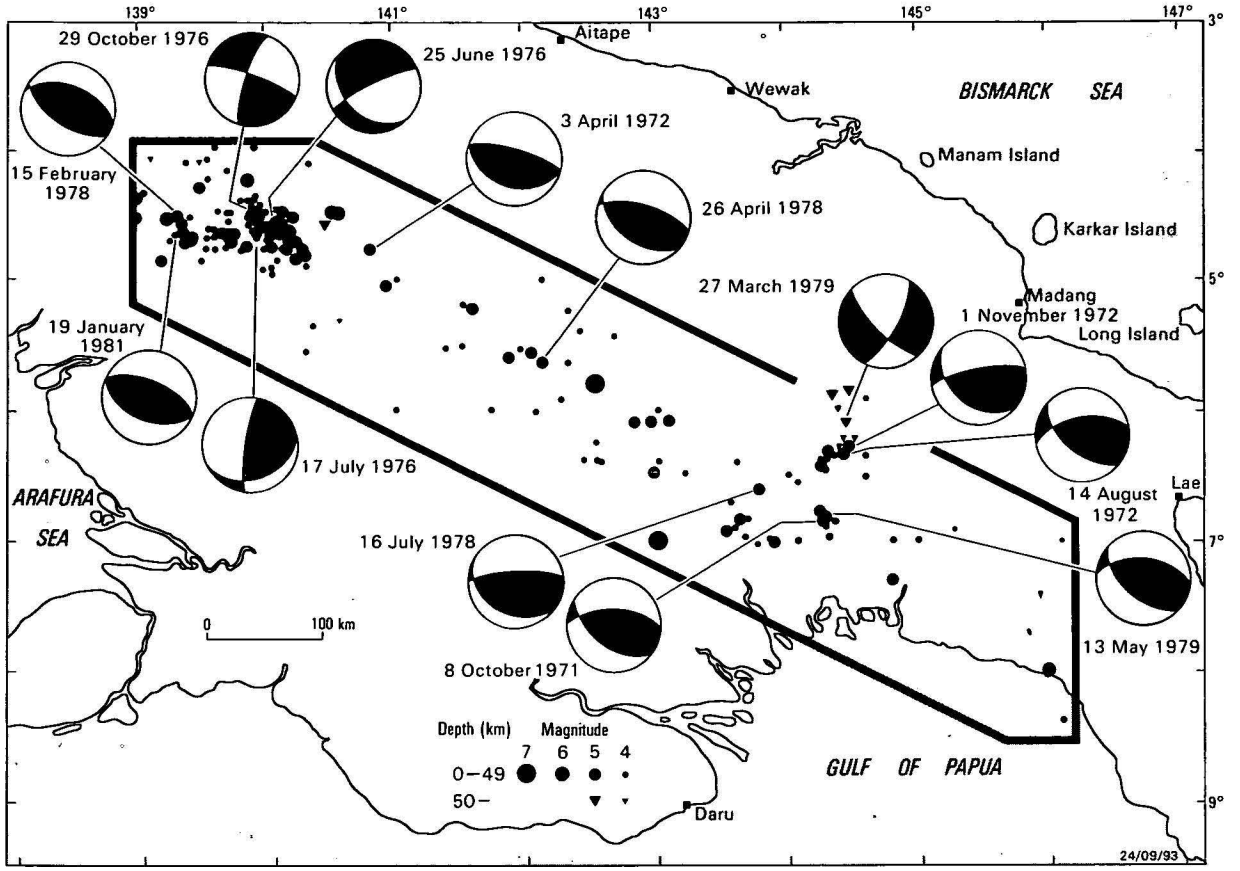

Figure 3. The Southern Highlands and Mount Hagen Seismic Zones.
The position of the NNE-trending Mount Hagen Seismic Zone is shown by the gap in the border around the Southern Highlands Seismic Zone. All known earthquake locations in the zones since 1900 are plotted. Earthquakes of the major seismic zones to the north have been omitted. Earthquake fault-plane solutions taken from Table 1 are superimposed. Solutions with 'black centres' — P-wave compressions — are overthrust; white centres — dip-slip normal; intersection in the centre — strike-slip.

The Southern Highlands Seismic Zone

The Southern Highlands Seismic Zone extends from Kerema on the Gulf of Papua, through the Star Mountains to about 4°S 139°E, and possibly further west-northwest to 136°E. The zone is at least 700 km long and up to 100 km across. The seismic zone is shown in detail in Figure 3. Most of the earthquake hypocentres have been taken from United States Geological Survey Bulletins (USCS, also previously USGS, USNOS, USERL) and International Seismological Centre Bulletins (ISC).

While the locations of earlier earthquakes in the zone may have an uncertainty of a degree or more, those of post-1970 earthquakes should be accurate to about 30 km. Most of the earthquake foci are at depths of less than about 35 km; for many of the depths given by USGS as 'normal, 33 km', the unrestricted computer depth computation was unsatisfactory, but shallow, and the solution was held by the reviewing geophysicist at 33 km. Depths other than 'normal' have either been determined from 'depth phases' (e.g., 13 May 1979) or have an uncertainty factor, normally plus or minus about 10 km. The computed depths would seem to indicate that, although earthquakes may be occurring in the top few kilometres of the crust, earthquakes are also occurring deep within the crust and possibly below it.

Most of the smaller (magnitude 5 or less) earthquakes in the zone, and which serve to define it, have occurred during the 1970s, reflecting not necessarily an increase in seismic activity in the 1970s, but an increased detection capability of the Papua New Guinea seismograph network, more sensitive overseas seismic stations, and improved earthquake location techniques by the USGS and ISC.

Gaps exist where large earthquakes have not recently occurred on the zone. One gap exists to the northwest of Kerema, and another in the Star Mountains region near the border between Papua New Guinea and Irian Jaya. Beyond Kerema, to the east-southeast, the zone either loses its identity or merges with a northerly seismic trend passing through the Wau region and joining the northern zone in the vicinity of Lae.

No earthquake has been correlated with a specific surface Pliocene/Quaternary fault, and no recent earthquake is known to have caused a surface fault scarp in the region. But such a scarp may well pass undetected in the heavy jungle cover or be masked by landslides.

A second earthquake zone, the Mount Hagen Seismic Zone, branches off the main Southern Highlands Seismic Zone at about 6.5°S 144°E, south of Mount Hagen. It trends approximately north-northeast past Mount Hagen, deepening to intersect the intermediate-depth seismicity beneath the Ramu and Sepik Valleys. The position of the zone in Figure 3 is shown by the break in the diagram border and a profile of the zone, showing the increase in depth of earthquakes to the north-northeast is shown in Figure 4. Most of the earthquakes located on the zone occurred in the 1970s and in a two-year period from mid-1971 to mid-1973, but some earlier earthquakes may not have been located. As the width

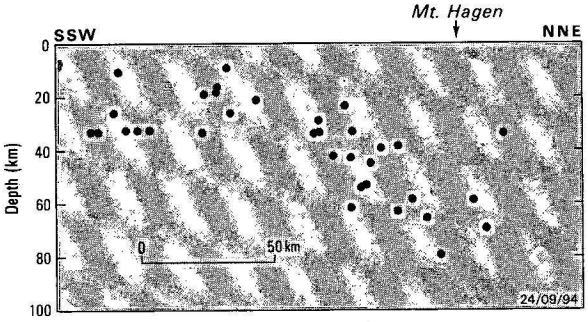

Figure 4. Depth profile of the Mount Hagen Seismic Zone.
The width of the profile is less than 70 km. Allowing for location uncertainty, the seismic zone is not a sloping plane, but rather resembles a plunging conduit. Earthquakes in the south-southwest of the diagram are part of the Southern Highlands Seismic Zone. Those of the centre and north-northeast define the Mount Hagen Seismic Zone.

of the zone is less than about 70 km, it is better described as a plunging conduit rather than a sloping plane or Benioff Zone.

Thirteen of the earthquakes on both zones were recorded at sufficient seismograph stations for fault plane solutions to be obtained. Solutions were obtained from P-wave first motions projected onto a Wulff stereographic projection. The first motions were obtained by examination of Papua New Guinea seismograms. Data from stations outside Papua New Guinea were extracted from International Seismological Centre Bulletins and individual station bulletins.

The P-wave first motion diagrams are shown in Figure 5 and the solution parameters in Table 1. The mechanism diagrams from Figure 5 are superimposed on Figure 3. All the first motion diagrams are adapted from Ripper & McCue (1981), and the 1976 and 1978 solutions are based on those by McCue (1981, 1982).

Of the thirteen solutions, nine are overthrusts on a general west-northwest strike. The depths computed for these earthquakes range from 16 km, through 'normal depth' to 45 km, and favour the Davies (1979) foreland thrust concept rather than the gravity-sliding hypothesis of Jenkins (1974).

The first motion diagram of the magnitude 7 Irian Jaya earthquake of 25 June 1976 indicates motion on a normal fault, not easily explained, but the 17 July aftershock appears to be a related 'backlash' event. The 29 October 1976 magnitude 7 earthquake in the same area was not an overthrust, but can be interpreted as a left-lateral fault movement on a west-northwest strike. Hence, neither of the two magnitude 7 Irian Jaya earthquakes had a thrust solution.

One fault plane solution has been obtained of an earthquake at intermediate depth (65 km) in the Mount Hagen Seismic Zone. The compressional stress axis is oriented at 355°, plunge 41°, that is, approximately parallel to the plunge of the seismic zone. The tensional axis of the solution is horizontal and approximately east–west.

Brief descriptions of the solutions

(1) 08 October 1971. Between Kikori and Mount Hagen. Depth 18 ± 7 km. Not a strong solution, but clearly an overthrust with the azimuth controlled by P-wave first motion compressions recorded at seismic stations Port Moresby (PMG) and Lae (LAT). In this solution, and in most of the solutions, PMG records a compression and is ideally positioned to orientate the thrust.

(2) 03 April 1972. Irian Jaya, adjacent to the Star Mountains. Depth 40 ± 13 km. Not a strong solution, there being only two dilatations, and the first motion at Momote seismic station (MOM) is anomalous. But the west-northwest-striking overthrust is essentially the only solution possible, despite the limited data.

(3) 14 August 1972. Southeast of Mount Hagen, on the Mount Hagen Seismic Zone. Depth 44 ± 6 km. An other-thrust solution, with pressure azimuth north-northeast controlled by the P-wave compressions at seismic stations Port Moresby (PMG) and Rabaul (RAB).

(4) 01 November 1972. Same location as the previous shock. Depth 35 ± 5 km. The solution is poor as there are several anomalous station readings, but clearly an overthrust.

(5) 25 June 1976. Irian Jaya, the damaging magnitude 7 earthquake. Normal depth. The solution is reasonable good, and differs significantly from the others. It is dip-slip normal, with the tension axis at shallow plunge to the north and pressure axis plunging steeply southeast. If the plane striking northeast is the fault plane, the southeast side moves relatively up on a normal fault.

(6) 17 July 1976. Aftershock of the 25 June earthquake. Normal depth. A reasonable solution. Fault movement is on either an almost vertical or almost horizontal plane. The polarity quadrants and stress axes are virtually opposite to those of the main 25 June shock, suggesting a backlash effect.

(7) 29 October 1976. A second magnitude 7 earthquake close to the 25 June shock in Irian Jaya. Normal depth. Although there are some anomalous station polarities, the

Table 1. Earthquake fault plane solution parameters.

Ref. No.	Date	Origin Time (UT)	Lat. (°S)	Long. (°E)	Depth (km)	Mag.	Nodal Planes Strike	Dip	Dip Az	Strike	Dip	Dip Az	B Axis Az	B Axis Pl	P Axis Az	P Axis Pl	T Axis Az	T Axis Pl
1	08 Oct 71	14 15 35.9	6.85	144.26	18±7	5.6	091	54	001	127	41	217	284	18	017	09	128	70
2	03 Apr 72	11 43 19.3	4.80	140.80	40±13	5.4	103	66	013	102	24	192	103	00	013	21	196	70
3	14 Aug 72	22 29 27.6	6.31	144.42	44±6	5.6	133	50	223	080	53	350	285	30	015	02	105	60
4	01 Nov 72	21 22 15.4	6.29	144.46	35±5	5.4	077	70	347	128	30	218	266	23	006	27	142	54
5	25 Jun 76	19 18 56.9	4.60	140.09	33	7.0	130	24	220	061	80	331	238	22	130	59	350	32
6	17 Jul 76	05 32 43.2	4.61	139.95	33	6.0	070	17	160	188	81	278	190	15	291	38	084	46
7	29 Oct 76	02 51 07.6	4.52	139.92	33	7.0	108	76	018	014	72	284	323	47	055	15	148	20
8	15 Feb 78	07 00 27.1	4.55	139.31	33	5.5	112	37	022	122	54	212	300	05	207	08	061	80
9	26 Apr 78	10 10 09.6	5.64	142.11	45±5	5.6	106	60	016	124	32	214	290	08	023	15	171	72
10	16 Jul 78	22 13 25.8	6.62	143.79	33	5.5	092	68	002	125	20	215	277	13	013	22	159	64
11	27 Mar 79	10 07 21.8	6.10	144.43	65±4	5.4	030	66	120	137	62	227	177	51	355	41	266	01
12	13 May 79	01 06 42.7	6.84	144.26	*16*	5.5	094	46	004	129	50	219	293	19	202	02	110	69
13	19 Jan 81	18 48 08.9	4.64	139.34	33	6.5	114	51	024	116	40	206	293	02	023	05	203	85

*Depth phases

Th — thrust; Nm — normal; Ss — strike-slip

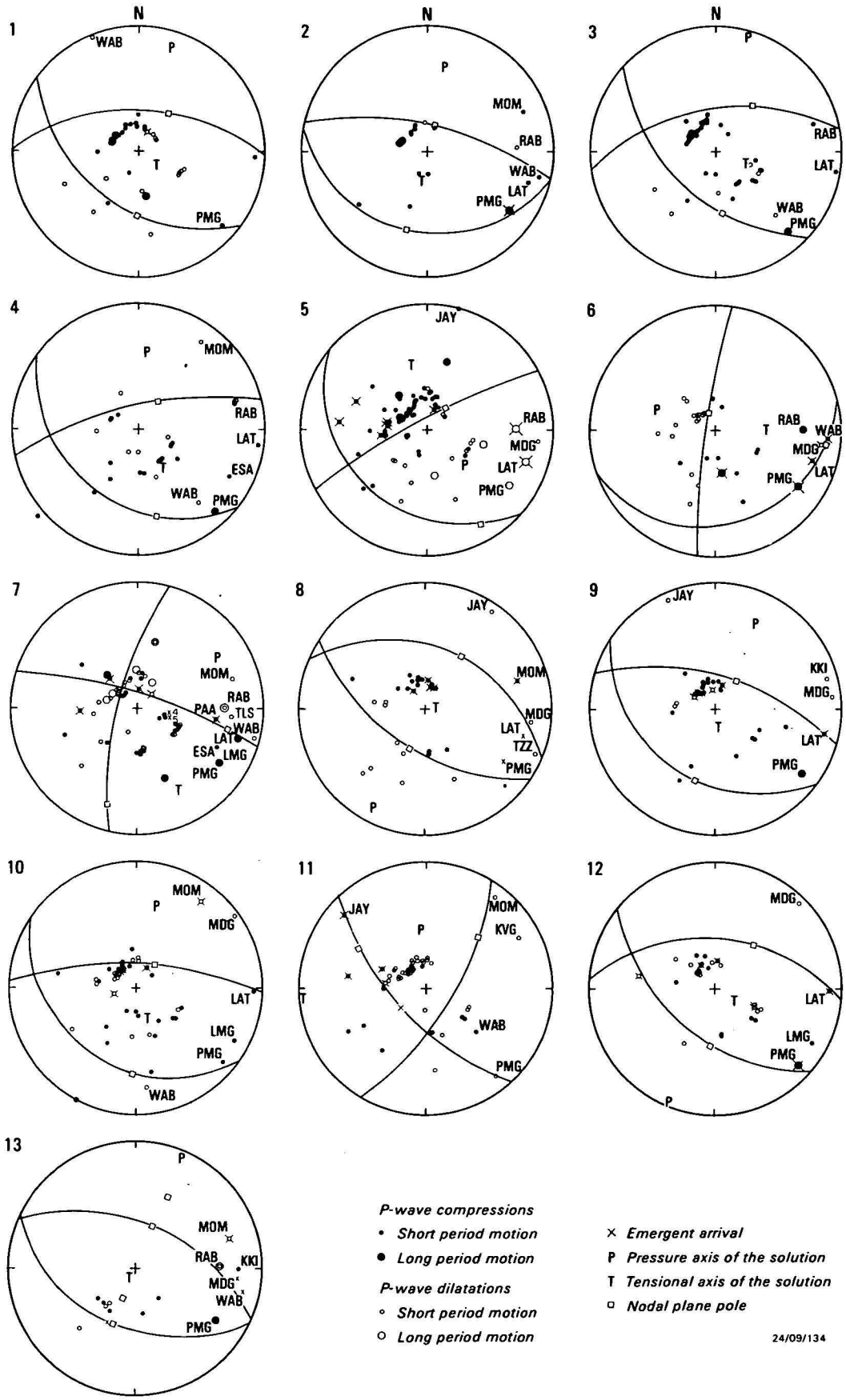

Figure 5. The P-wave first motion diagrams corresponding to the solutions shown on Figure 3.
The numbers correspond to the reference numbers given in the text and in Table 1. Local seismic stations are identified by their codes, ESA—Esa Ala, JAY—Jayapura, KKI—Karkar Island, KVG—Kavieng, LAT—Lae, LMG—Mount Lamington, MDG—Madang, MOM—Momote, PMG—Port Moresby, RAB—Rabaul, TLS—Talasea, TZZ—Tabubil, WAB—Wabag.

solution is strongly strike-slip, pressure axis northeast. If the west-northwest nodal plane is the fault plane, the motion is left lateral.

(8) 15 February 1978. Normal depth. Close to the 29 October 1976 Irian Jaya earthquake, but not an aftershock, since it occurred 16 months later. A west-northwest-striking overthrust, with the Tabubil (TZZ) station compression providing the azimuth control.

(9) 26 April 1978. Blucher Range/Strickland River region, east of the Star Mountains. Depth 45 ± 5 km. Again, a west-northwest-striking thrust, with seismic stations Port Moresby (PMG) and Lae (LAT) providing azimuth control.

(10) 16 July 1978. South of Mendi. Normal depth. A west-northwest-striking thrust, with seismic stations Port Moresby (PMG), Mount Lamington (LMG) and Lae (LAT) providing azimuth control.

(11) 27 March 1979. In the Mount Hagen Seismic Zone. Depth 65 ± 4 km. A reasonable solution, being a combination of strike-slip and dip-slip normal. The tension axis is horizontal, east–west, and the pressure axis plunges to the north.

(12) 13 May 1979. Southeast of Mt. Hagen. Depth 16 km (depth phases). A west-northwest-striking thrust, with azimuth control provided by seismic stations Port Moresby (PMG), Mount Lamington (LMG) and Lae (LAT).

(13) 19 January 1981. Irian Jaya. Normal depth. A west-northwest-striking overthrust with azimuth control provided by the Port Moresby (PMG) P-wave compression. The solution is similar to that issued by the United States Geological Survey Monthly Summary.

Tectonic setting

A simple model to explain the seismicity, faulting, uplift and volcanism of the Highlands is based on Davies' (1979) model of deep crustal thrusting and the collision of the South Bismarck and Indo-Australian Plates over the top of a sinking Solomon Sea Plate. The concept of the Solomon Sea Plate sinking beneath the Ramu-Markham Valley is based on the double-limbed seismic structure beneath the region (Ripper, 1980, 1982), which is preferred to the single-limb models of Jaques & Robinson (1977) and Johnson (1979). Seismicity at depths of greater than 100 km beneath the Ramu-Markham region is indicative of underthrust lithosphere (Denham, 1975). The tectonic model suggested here incorporates the Southern Highlands Seismic Zone into the plate collision pattern of the New Guinea region.

(1) In the middle Miocene, the Indo-Australian Plate was being subducted beneath an island arc system to the north or northeast of New Guinea and Australia (Page, 1976). Collision between the island arc and the margin occurred. The Outer Melanesian Arc, dormant since about the end of the Oligocene, was behind (north of) the island arc in the New Guinea region and not far from it (of the order of 200 km). The region between New Guinea and the Outer Melanesian Arc was to become part of the Solomon Sea Plate in the late Miocene.

(2) In the late Miocene, the Ontong Java Plateau margin of the Pacific Plate, of continental thickness, collided with the Solomon Islands (section of the Outer Melanesian Arc) and subduction of the Pacific Plate beneath the Solomon Islands region was terminated (Kroenke, 1972). Continued convergence of the Pacific and Indo-Australian Plates was accommodated by subduction of the Solomon Sea Plate beneath both major plates. As the plate margins were oblique to the azimuth of approach (plate margin trend approximately NW–SE; azimuth of approach approximately WSW–ENE), an anti-clockwise rotation was also induced into the Solomon Sea Plate, initiating subduction beneath New Britain.

(3) The New Britain subduction extended westward beneath the section of the arc north of New Guinea. The narrow strip of Solomon Sea Plate north of New Guinea was now being subducted northward beneath the Outer Melanesian Arc, and southwestward beneath New Guinea. Volcanism was occurring both in the arc and in New Guinea. The evolution of the northern New Guinea region from late Miocene is shown in Figure 6.

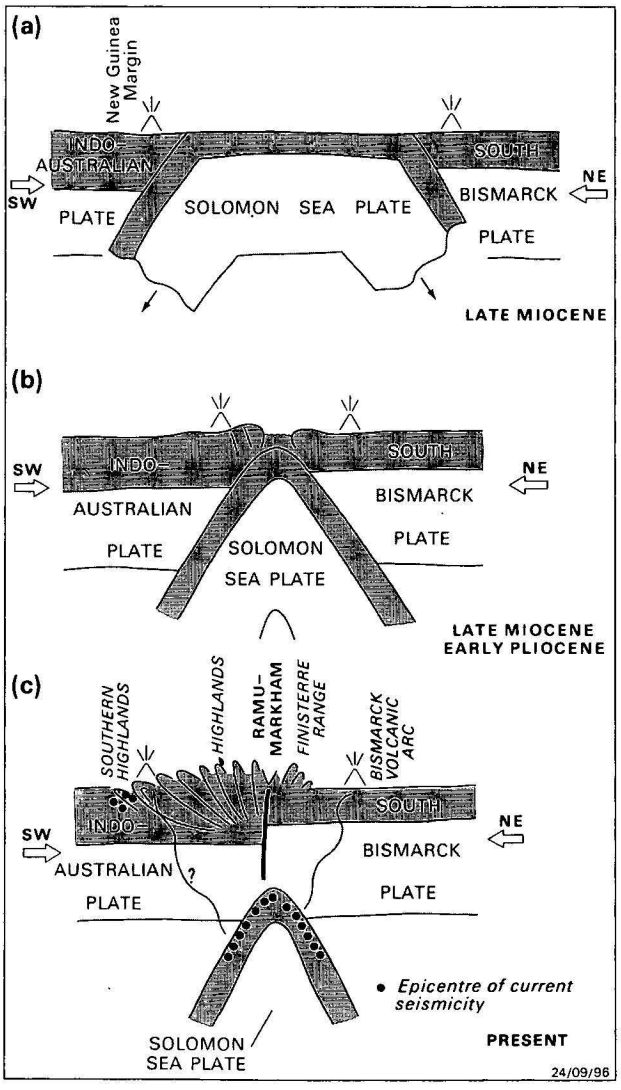

Figure 6. A series of three profile sketches illustrating the collision of the Indo-Australian Plate and the South Bismarck Plate, and the subsequent development of the highlands and southern highlands. (a) — Double subduction of the Solomon Sea Plate was initiated in late Miocene. (b) — Collision of the Indo-Australian Plate and South Bismarck Plate occurred almost immediately. The Solomon Sea Plate began to sink beneath the collision zone. (c) — Continued advance of the two plates applied a horizontal stress in the crystalline crust of the Indo-Australian Plate (northern New Guinea margin) causing faulting on near-vertical thrusts. The thrusting process has migrated away from the plate margin to the region of the southern highlands.

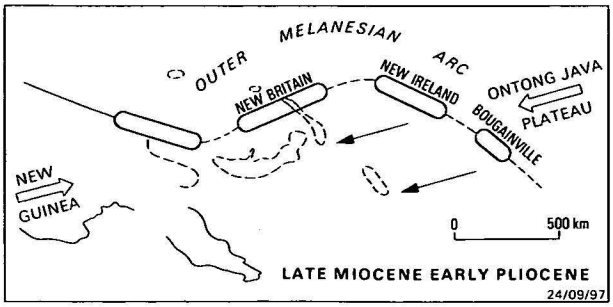

Figure 7. Sketch suggesting the approximate location of the Outer Melanesian Arc relative to New Guinea, at the time of its collision with the New Guinea margin of the Indo-Australian Plate, about late Miocene–early Pliocene.
The large arrows show the azimuth of Pacific/Indo-Australian Plate approach. The small arrows show the movement of New Ireland and Bougainville to their present positions (dotted). Although New Britain has not moved far with respect to New Guinea, its position with respect to New Ireland has changed significantly.

(4) Almost immediately (late Miocene–early Pliocene) the two subduction zones collided, first at the northwest, and progressively to the southeast. The Solomon Sea Plate now formed a suspended or hanging arch beneath the collision zone, whose surface expression is the Ramu-Markham Valley. Subduction slowed because each limb of the subduction zone was anchored to the other. The lithospheric arch was trapped above the aesthenosphere, and could only sink as aesthenosphere was displaced. Figure 6b illustrates this stage of the collision, and Figure 7 sketches the approximate relative positions of the New Guinea mainland and the relevant section of the Outer Melanesian Arc at the time of collision. Mackenzie (1975) suggested a similar sinking double-limbed subduction system, the limbs of which collided earlier, at the end of the early Miocene, and which was not identified as the Solomon Sea Plate.

(5) Convergence between the Indo-Australian and Pacific Plates continued, maintaining subduction of the Solomon Sea Plate at the Solomon Islands margin, and rotation of the Solomon Sea Plate. The virtual cessation of Solomon Sea Plate subduction southwest beneath New Guinea and northward beneath the arc in turn retarded subduction beneath southeast Papua and New Britain. The anti-clockwise plate rotation demanded continued subduction beneath New Britain, however, and this was then accommodated by the initiation of a southeast advance of New Britain past New Ireland (with respect to New Ireland), and associated 'back-arc' spreading behind (northwest of) New Britain. The back-arc spreading New Britain. The back-arc spreading has been described, for example, by Connelly (1976), Taylor (1979), and Johnson & others (1979).

(6) The collision of the arc and northern New Guinea continued. The arc and the New Guinea margin came into direct contact above the sinking Solomon Sea Plate, and compressive stress built up in the continental plate margin and the crystalline continental crust behind the margin. The development of a seismic zone across the Bismarck Sea enclosed a sub-plate, which has been termed the South Bismarck Plate (Fig. 2). The northern New Guinea collision then became a collision between the Indo-Australian Plate and the South Bismarck Plate over the sinking Solomon Sea Plate.

(7) Response to collisional stress was now transmitted to the continental front of the Indo-Australian Plate (Fig. 6c). The continental margin faulted on near-vertical thrusts, north-northeast side up. The thrusting process in the crust has since expanded to the southwest, and is now manifest in the Southern Highlands Seismic Zone and the Papuan Fold Belt. Rapid uplift of the Finisterre Range has occurred above the collision contact.

(8) The Quaternary southern highlands volcanism may originate in the crustal thrusts or deeper down in the Solomon Sea Plate, or as a combination of both. The Solomon Sea Plate is still lying at a depth of about 100 km beneath the Ramu-Markham Valley and is probably the origin of the West Bismarck volcanism (Ripper, 1982).

(9) The intermediate-depth seismicity beneath northwest Ramu Valley and the Sepik Valley (Ripper, 1982) possibly occurs in fragments of the old Solomon Sea Plate (see also Denham, 1975).

To summarise, the southern highlands seismicity, the Papuan Fold Belt, the highlands uplift, and the Finisterre uplift are manifestations of the Indo-Australian/South Bismarck Plate collision over the top of the sinking Solomon Sea Plate. The highlands volcanism may also be associated.

Seismic risk

Gaull (1979) investigated the seismic risk to 20 large towns in Papua New Guinea, and extrapolated his results to include rural areas. He listed the expected effects at each town of all known potentionally damaging earthquakes in Papua New Guinea for the period 1900–1979. He calculated the mean return period for Modified Mercalli Intensities 6 and higher for each town, and then contoured his results for the whole country. Using an empirical relationship, Gaull related intensities to peak ground acceleration. For the towns of Mendi and Kerema on the southern side of the highlands, Gaull obtained return periods of 45 and 55 years, respectively, for intensity 7. His contoured map (Gaull, fig. 23) of estimated maximum intensities for any 50-year period suggests that the Star Mountains should experience intensity 7 about once every 50 years, as for Mendi. Gaull obtained a return period of 60 years for an acceleration of 0.1g peak ground acceleration at Mendi.

It is likely that all New Guinea magnitude 7 or greater earthquakes since 1900 are documented (Everingham, 1974). Recording of earthquakes in the magnitude range 5–7 improved in the early 1960s with the installation of World Wide Standardised Seismographs at Port Moresby, Rabaul, Honiara in the Solomon Islands, and Charters Towers in northern Australia. Combining the two sets of Southern Highlands Seismic Zone data, the 22-year set of largest annual earthquakes 1960 to 1981, and the subset of the magnitude 7.0 or greater earthquakes in the 82 years from 1900 produces a reasonable sample for the analysis of seismic risk. Richter magnitudes measured on the Port Moresby (PMG) Wood Anderson seismographs are used in the magnitude range less than 6, and Surface Wave magnitudes measured world-wide, for the magnitude range 6 and over; above 6, the two scales are virtually equivalent (McGregor & Ripper, 1976).

Figure 8a shows the Type 1 or Gumbel Extreme Magnitude Distribution obtained for the Southern Highlands Seismic Zone, incorporating the two data sets. The method has been described by many workers, including Lomnitz (1974). A Type 1 or Gumbel distribution G(M) is fitted to the set of largest annual values magnitude M. The distribution is given by $P = \exp\{-\alpha e^{-\beta M}\}$ or $-\ln(-\ln(P)) = \beta m - \ln\alpha$ . . . (1), where P is the probability that the largest magnitude in any year is less than M, and α & β are constants.

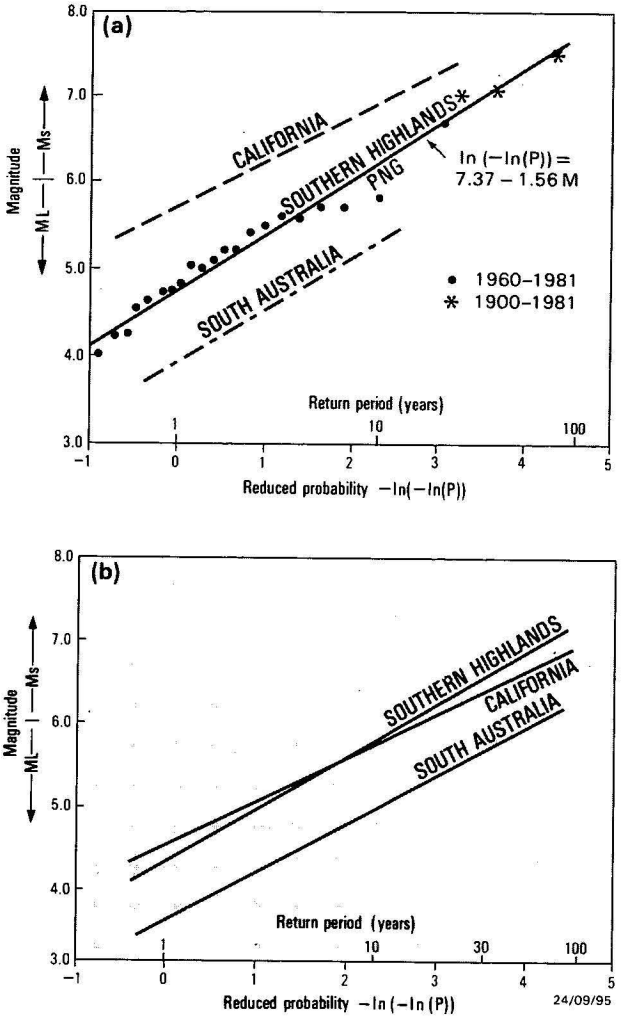

Figure 8. (a) — Southern Highlands Seismic Zone, largest annual earthquakes, 1900–1981 (magnitude 7 only) and 1960–1981.
The magnitude is shown as a function of return period. Also shown are the corresponding plots for California (Lomnitz, 1974) and South Australia (McCue, 1975).
(b) — For a direct comparison of seismic levels, the three seismic zones are normalised to a common area of 100 000 km².
The levels of California and Southern Highlands zones become virtually identical.

The return period T is defined by: $T = 1/(1 - P)$ . . . (2), which is approximated by Lomnitz (1974) as $T = \{ \exp(M) \} / \alpha$ . . . (3). Least squares analysis of the Southern Highlands data gives $\ln\alpha = 7.37$ and $\beta = 1.56$.

The slope of the familiar recurrence relation 'b' is related simply to β by $\beta = b \ln 10$ which gives a 'b' value of 0.7, lower than usual, indicating a higher than average ratio of large to small earthquakes. Wyss (1973) has suggested that a low 'b' value is symptomatic of high tectonic stress, which is in keeping with the thrust type focal mechanism obtained for earthquakes on the zone.

Return periods computed using equation (3) are compared (Table 2) with those given by Lomnitz (1974) for earthquakes in California, USA, and by McCue (1975) for South Australia. The first column (a) gives magnitudes computed directly from the relevant magnitude/frequency relationship, whilst those in the second column (b) are normalised to a unit area of 100 000 km².

Table 2. Earthquake return periods for the Southern Highlands Seismic Zone compared with those for California and South Australia.

	Magnitude					
Return period	*Southern Highlands*		*California*		*South Australia*	
T (years)	*(a)*	*(b)*	*(a)*	*(b)*	*(a)*	*(b)*
1	4.7	4.3	5.7	4.5	4.4	3.9
10	6.2	5.7	6.9	5.7	5.3	4.9
30	6.9	6.5	7.4	6.3	5.8	5.6

The once-per-30-year earthquake of the Southern Highlands Seismic Zone is magnitude 6.9, which would cause intensity 7 over a radius of about 80 km (an area of about 20 000 km²), and the 10-year earthquake, magnitude 6.2, intensity 7 over a radius of about 30 km (about 3000 km²).

The effect of comparing the risk per unit area is shown in Figure 8(b). The Californian and Southern Highlands curves are virtually inseparable. The consequences for a building code are clear, since California is rated Zone 3 on the United States Uniform Building Code (U.B.C.) and South Australia is Zone 2 (McCue, 1975). (Zone levels increase from Zone zero, which corresponds to a sufficiently low level of risk that no seismic load need be considered in normal building design). The Southern Highlands zone should be rated at least equivalent to Zone 2 and probably Zone 3 of the U.B.C.

Lomnitz (1974) has defined earthquake risk R_D as the probability of occurrence of an earthquake of magnitude M or more in a D year period, as $R_D(M) = 1 - \exp(-\alpha D e^{-\beta M})$ . . . (8). For example the risk that magnitudes 6 and 7 earthquakes will occur somewhere in the Southern Highlands Seismic Zone in the next 50 years are 99 per cent and 81 per cent, respectively. Although overshadowed by the more active seismic zones of the north coast, New Britain, and Bougainville, the Southern Highlands Seismic Zone is thus seen to have a significant seismic risk. Special precautions against future earthquake damage are warranted.

Gaps for magnitude 7 earthquakes in the zone exist in the border region between Irian Jaya and Papua New Guinea, and in the region between Kikori and Kerema. Gaps in the seismic zone are considered to be temporary and thus to have a better chance of being the site of a future large earthquake than the rest of the zone.

Strong motion data

An accelerogram is available of the 25 June 1976 magnitude 7 Irian Jaya earthquake, as recorded at the 'Hongkong' site in the Star Mountains. The duration of shaking exceeded the 43 seconds duration of the MO2 accelerograph recording. The MO2 retriggered, and the strongest shaking was in the second segment of record. The accelerogram is held at the Geophysical Observatory, Port Moresby.

The earthquake produced a maximum acceleration at the Hongkong site of 0.08g at frequency 1.5 hz. The earthquake woke everybody. People were unable to stand. Several landslides were caused, but no damage resulted. The Modified Mercalli Intensity is interpreted as 7. The distance of the Hongkong site from the earthquake epicentre was 135 km.

Conclusions

Two seismic zones are recognised in the southern part of the central ranges of Papua New Guinea. These are the Southern Highlands Seismic Zone, which coincides with the Papuan Fold Belt, and the Mount Hagen Seismic Zone, which branches off the Southern Highlands Seismic Zone south of Mount Hagen and trends north-northeast, deepening to intersect the intermediate-depth seismicity beneath the Ramu-Markham Valley. The Mount Hagen Seismic Zone has the form of a plunging conduit rather than an inclined plane.

Four large (magnitude 7) earthquakes have occurred in the Southern Highlands Seismic Zone this century, in 1922 and 1954 near Mendi, and two in 1976 in Irian Jaya. A magnitude 6.5 earthquake occurred at its eastern end, near Kerema in 1931. Gaps exist in the zone between Kerema and Kikori, and in the Star Mountains border region with Irian Jaya.

Fault plane solutions of earthquakes in the Southern Highlands Seismic Zone are mainly overthrusts that strike approximately parallel to the zone and have pressure axes trending approximately north-northeast–south-southwest. The solutions suggest that the earthquakes represent thrust fault movement in response to a north-northeast–south-southwest compressive stress. Two notable exceptions, however, were the magnitude 7 Irian Jaya earthquakes of June and October 1976, which were dip-slip normal and strike-slip, respectively.

Although no specific correlations between earthquakes and surface faults have been made, the earthquakes presumably occur on the system of east- southeast–west-northwest-trending faults of the Papuan Fold Belt, active through the Pliocene–Quaternary. The very existence of the seismic zone indicates that the fault system is currently active.

Davies (1979) proposed that the Pliocene-Quaternary faults of the Papuan Fold Belt are south-facing thrusts, caused by a regional compressive stress. The concurrence of the seismic zone with the region of Pliocene–Quaternary faulting, and the overthrust earthquake fault plane solutions support this.

The seismic zone is here recognised as an expression of the current collision between the Indo-Australian and South Bismarck Plates in the broad tectonic framework of the Indo-Australian and Pacific Plate convergence. Until about late Miocene, the Indo-Australian and South Bismarck Plates were separated in the northern New Guinea region by the Solomon Sea Plate. Double subduction of the Solomon Sea Plate brought the plates into direct contact, with the two subducting limbs of the Solomon Sea Plate sinking beneath the collision (Ramu-Markham) zone in the form of a hanging arch (inverted 'V' shape). Plate approach and stress build-up in the plate fronts continued above the sinking Solomon Sea Plate, and stress relief occurred by the faulting of the continental crust of the Indo-Australian Plate margin in the New Guinea highlands region. The thrusting and uplift have migrated south-southwest into the southern highlands and are now manifest in the Southern Highlands Seismic Zone and the Papuan Fold Belt.

The Mount Hagen Seismic Zone links the intermediate-depth seismicity of the sinking Solomon Sea Plate with the seismicity of the southern highlands. It could well be associated with Quaternary highlands volcanism as it provides a direct link between the subducted Solomon Sea Plate and the zone of Highlands volcanoes.

Return periods, seismic risk parameters and the magnitude frequency relationship b-factor for the southern highlands were determined by an extreme magnitude Gumbel distribution technique. The once-per-year earthquake was found to be of magnitude 4.7, 10-years, 6.2, and 30-years, 6.9. The corresponding figures for California, USA, are 5.7, 6.9, and 7.4, respectively. If a correction is made for the difference in area, the seismic risk of the Southern Highlands is seen to be equivalent to that of California. As California rates Zone 3 on the USA Unified Building Code scale, the Southern Highlands Seismic Zone should rate at least 2 and probably 3.

Acknowledgements

This paper is published with the permission of the Secretary, Department of Minerals and Energy, Port Moresby, Papua New Guinea.

References

Bain, J.H.C., 1973 — A summary of the main structural elements of Papua New Guinea. *In* Coleman, P.J. (editor). The Western Pacific: Island arcs, marginal seas, geochemistry. *University of Western Australia Press, Perth.*

Connelly, J.B., 1976 — Tectonic development of the Bismarck Sea based on gravity and magnetic modelling. *Geophysical Journal of the Royal Astromonical Society*, 46, 23–40.

Davies, H.L., 1979 — Explanatory notes to accompany to Mianmin 1:250 000 Geological Map. *Geological Survey of Papua New Guinea Report* 79/27.

Denham, D., 1975 — Distribution of underthrust lithospheric slabs and focal mechanisms — Papua New Guinea and Solomon Islands region. *Bulletin of the Australian Society of Exploration Geophysicists*, 6, 78–79.

Dent, V.F., 1974 — Felt earthquake reports from the Southern Highlands, Western and Gulf Districts of Papua New Guinea, 1953–1973. *Geological Survey of Papua New Guinea Report* 74/31.

Dow, D.B., 1977 — A geological synthesis of Papua New Guinea. *Bureau of Mineral Resources, Australia, Bulletin* 201.

Everingham, I.B., 1974 — Large earthquakes in the New Guinea–Solomon Islands area, 1873–1972. *Tectonophysics*, 23, 323–338.

Everingham, I.B., 1979 — Papua New Guinea earthquake intensity data, 1953–1959. *Bureau of Mineral Resources, Australia, Record* 1979/41.

Gaull, B.A., 1979 — Seismic risk at the 20 principal towns of Papua New Guinea. *M.Sc. thesis, University of Papua New Guinea.*

Hamilton, W., 1979 — Tectonics of the Indonesian region. *United States Geological Survey Professional Paper* 1078.

Jaques, A.L., & Robinson, G.P., 1977 — The continent/island arc collision in northern Papua New Guinea. *BMR Journal of Australian Geology & Geophysics*, 2, 289–303.

Jenkins, D.A.L., 1974 — Detachment tectonics in western Papua New Guinea. *Geological Society of America, Bulletin*, 85, 533–548.

Johnson, R.W., 1979 — Geotectonics and volcanism in Papua New Guinea: a review of the late Cainozoic. *BMR Journal of Australian Geology & Geophysics*, 4, 181–207.

Johnson, R.W., Mutter, J.C., & Arculus, R.J., 1979 — Origin of the Willaumez–Manus Rise, Papua New Guinea. *Earth and Planetary Science Letters*, 44, 247–260.

Kroenke, L.W., 1972 — Geology of the Ontong Java Plateau. *Hawaii Institute of Geophysics Report*, 72-5.

Lomnitz, C., 1974 — Global tectonics and earthquake risk. *Elsevier, Amsterdam.*

Mackenzie, D.E., 1975 — Volcanic and plate tectonic evolution of central Papua New Guinea. *Bulletin of the Australian Society of Exploration Geophysicists*, 6, 66–68.

Mackenzie, D.E., 1976 — Nature and origin of late Cainozoic volcanoes in western Papua New Guinea. *In* Johnson, R.W. (editor). Volcanism in Australasia. *Elsevier, Amsterdam*, 221–238.

McCue, K.F., 1975 — Seismicity and seismic risk in South Australia. *University of Adelaide, Report* ADP 137.

McCue, K.F., 1979 — Seismicity of Papua New Guinea and neighbouring region for 1977. *Geological Survey of Papua New Guinea, Report* 1979/32.

McCue, K.F., 1981 — Seismicity of Papua New Guinea and neighbouring region for 1976. *Geological Survey of Papua New Guinea, Report* 1981/10.

McCue, K.F., 1982 — Seismicity of Papua New Guinea and neighbouring region for 1978. *Geological Survey of Papua New Guinea, Report* 1982/4.

McGregor, P.M., & Ripper, I.D., 1976 — Notes on earthquake magnitude scales. *Bureau of Mineral Resources, Australia, Record* 1976/56.

Page, R.W., 1976 — Geochronology of igneous and metamorphic rocks in the New Guinea Highlands. *Bulletin of Mineral Resources, Australia, Bulletin* 162.

Ripper, I.D., 1980 — Seismicity, earthquake focal mechanisms and tectonics of the Indo-Australian/Solomon Sea Plate boundary. *Geological Survey of Papua New Guinea, Report* 1980/5.

Ripper, I.D., 1982 — Seismicity of the Indo-Australian/Solomon Sea Plate boundary in the Southeast Papua region. *Tectonophysics*, 87, 355–369.

Ripper, I.D., & McCue, K.F., 1981 — The Southern Highlands and Mt. Hagen Seismic Zones of Papua New Guinea. *Geological Survey of Papua New Guinea, Report* 1981/14.

Ripper, I.D., & McCue, K.F., 1982 — Seismicity of the New Guinea region, 1964–1980, computer plots. *Geological Survey of Papua New Guinea, Report* 1981/10.

Taylor, B., 1979 — Bismarck Sea: Evolution of a back-arc basin *Geology*, 7, 171–174.

Thompson, J.E., & Fisher, N.H., 1965 — Mineral deposits of Papua New Guinea and their tectonic setting. *Proceedings of the 8th Mining and Metallurgical Congress, Australia/New Zealand*, 6, 115–148.

Undro, 1976 — Report of the United Nations Disaster Relief Coordinator on the earthquakes in Irian Jaya and Bali, Indonesia, June, July, 1976. *United Nations Disaster Relief Organisation, Case Report* 002.

Wyss, M., 1973 — Towards a physical understanding of the earthquake frequency distribution. *Geophysical Journal of the Royal Astronomical Society*, 31, 341–359.

BMR Journal of Australian Geology & Geophysics, 8, 157-159

THE POODYEA FORMATION: A POSSIBLE TERTIARY FLUVIAL UNIT IN THE TOKO SYNCLINE, GEORGINA BASIN, QUEENSLAND & NORTHERN TERRITORY

B.M. Radke[1], C.J. Simpson[1], & J.J. Draper[2]

The Poodyea Formation, comprising boulder conglomerate, cross-stratified sandy conglomerate and pebbly sandstone, crops out as narrow linear and sinuous belts of small outliers within and to the south of the Toko Range, in the Georgina Basin, western Queensland and Northern Territory. The outliers are confined to present-day narrow valleys in the Carlo Sandstone, corresponding closely to either the Toko Syncline axis or cross-cutting structures, and form low linear ridges over plains of Mithaka Formation. The Poodyea Formation is considered to be of probable Tertiary age, and represents a river-channel deposit derived from reworking of parts of the Mesozoic, Palaeozoic, and Proterozoic sequences. In the past, outcrops of the formation have been included in Palaeozoic units. The formation is discussed and defined.

Introduction

Difficulty in distinguishing poorly or non-fossiliferous conglomerate and sandstone in the Toko Range area of the northern Toko Syncline, Georgina Basin, has resulted in prolonged use of general stratigraphic terms and informal names. In particular, this has been the case with lithologies of the Cravens Peak beds and similar rock types.

During the earliest regional mapping in the Toko Range area, Reynolds (*in* Smith, 1965) defined the Cravens Peak beds to include all sandstone and conglomerate of apparent Paleozoic age overlying the Middle Ordovician Mithaka Formation. The Cravens Peak beds were then subdivided into lower and upper units by Gilbert-Tomlinson (1968), on the basis of fossils. Smith (1972) designated the unit as Siluro-Devonian. The same sequence was subsequently subdivided by Draper (1976) into four units: (1) A lower sandstone unit conformably overlying the Mithaka Formation, later defined as the Middle Ordovician Ethabuka Sandstone (Draper, 1980); (2) A limestone and calcareous siltstone unit of Early Devonian age, which was termed 'thelodont-bearing rocks'; (3) A conglomerate and sandstone unit of Middle to Late Devonian age, for which the name Cravens Peak beds was retained; and (4) A conglomerate and pebbly-sandstone unit of post-Devonian age, considered a relict valley-fill deposit unconformably overlying the Ordovician sequence (Mithaka Formation, Carlo Sandstone, Nora Formation) and cutting across major structure in the area. Units 2 and 3 correspond to the 'lower and upper Cravens Peak beds' of Johnstone & others (1967) and Gilbert-Tomlinson (1968), who implied a hiatus between them.

Turner & others (1981) redefined the Cravens Peak beds as comprising a basal calcareous unit (i.e. unit 2 above) conformably overlain by a conglomerate and sandstone sequence (unit 3, above). Unit 4 of Draper (1976) is the Poodyea Formation discussed in this note and defined in the Appendix.

The recognition by Draper (1976) that two conglomerate and sandstone units occurred in the region was a significant step, and helped to explain the difficulties experienced by earlier workers. However, the problem of field identification and separation of these units still remains.

Stratigraphic relations.

Following geological mapping on the Toko 1:100 000 Sheet area, the unit 4 of Draper (1976) was recognised during airphoto interpretation as a relatively young unit and was informally designated the 'Beattie Creek Conglomerate' on the preliminary map (BMR, 1979). That unit was renamed the Poodyea Formation on the special map, Geology of the South Georgina Basin (BMR, 1982).

In the Toko Range, the Poodyea Formation unconformably overlies the Early to Middle Ordovician Toko Group (Draper, 1980), occurring within the confines of valleys in the Carlo Sandstone and as subtle ridges over the Mithaka Formation and Ethabuka Sandstone. The Poodyea Formation has not been mapped along the Toko Syncline into the Abudda Lakes 1:100 000 Sheet area to the southeast, although Reynolds (1968) noted deposits there that have lithological similarity. Boulders, cobbles, and pebbles of silicified sandstone that flank the Toomba Range and form low hilly mounds in the trough of the Toko Syncline in the Mount Whelan 1:250 000 Sheet area, were described by Reynolds as possible Permian unconsolidated fluvio-glacials. Draper considers these to be a weathered residue from the Cravens Peak beds and the Late Proterozoic Yardida Tillite. During gravity modelling of the Toomba Fault, Harrison (1980) found a shallow low-density deposit, up to 250 m thick, on the western margin of the fault. This deposit is locally adjacent to, but topographically lower than, the Tertiary Austral Downs Limestone. Harrison interpreted the unit as probably Jurassic to Cretaceous fill. However, control on the distribution of this unit by the Toomba Fault indicates similarities to the Poodyea Formation elsewhere.

East of Poodyea Point (Fig. 1), a cover of variable composition, comprising quartzose and quartzitic cobble-boulder and gravelly sediments, overlies Nora and Kelly Creek Formation subcrop. These thin blanket-like deposits of gravel are probably Quaternary derivatives from unconsolidated Tertiary gravel-boulder deposits. If this is so, both this easterly cover and the boulder gravels in the Toomba Range area may be, in part, reworked from the Poodyea Formation.

Depositional environment

A palaeoenvironmental reconstruction of the Poodyea Formation is very speculative, as the unit has not been consistently mapped or photo-interpreted beyond the Toko 1:100 000 Sheet area. The narrow linear belts of outcrop, which regionally ascribed a sinuous trend (Fig. 1), are likely to be valley-fill deposits, as suggested by Draper (1976), in a fluvial system controlled by the axis and cross-faults of the

[1] Division of Continental Geology, Bureau of Mineral Resources, P.O. Box 378, Canberra, ACT 2601
[2] Geological Survey of Queensland, GPO Box 194, Brisbane, Queensland 4001

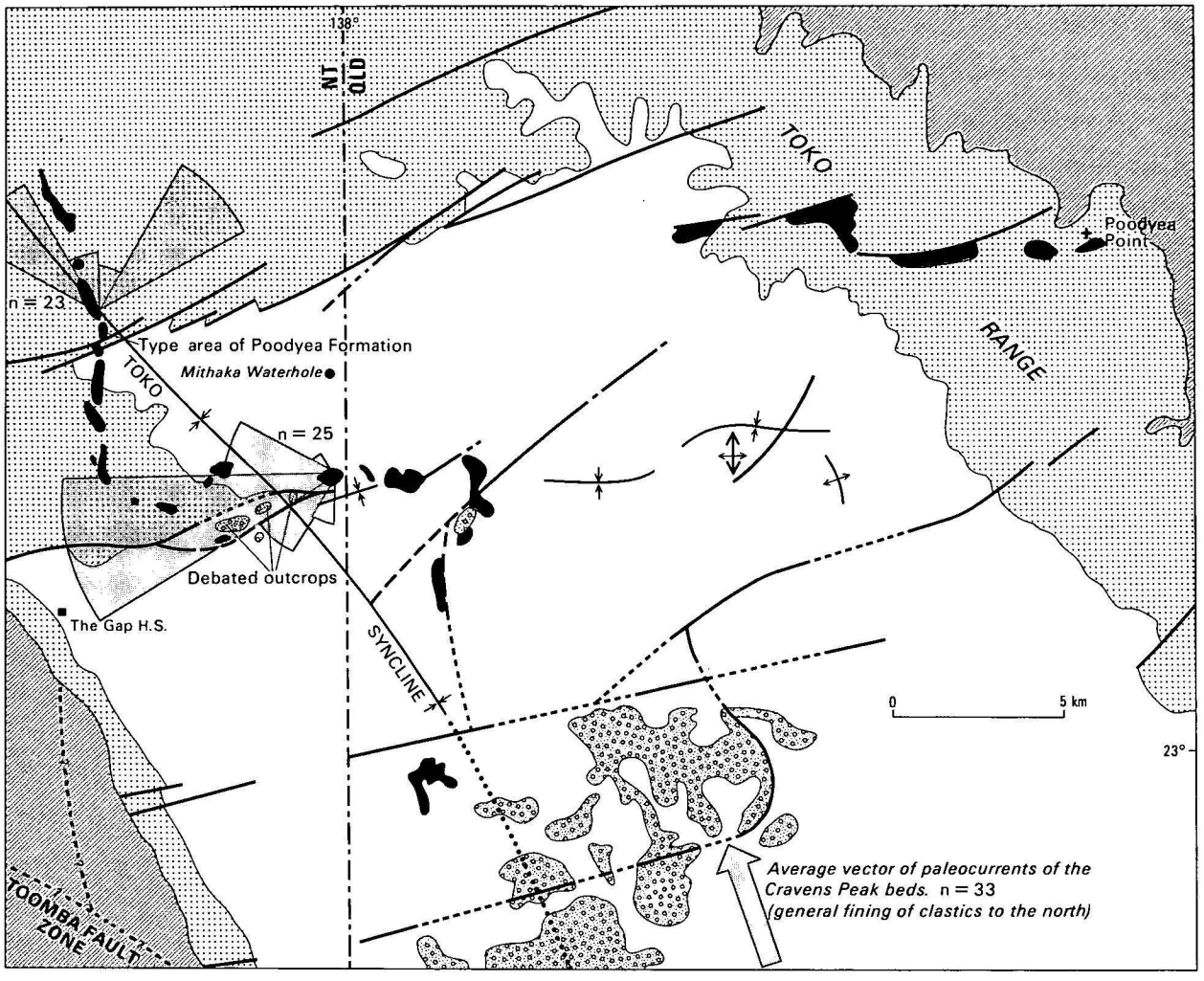

Figure 1. Generalised geology of the Toko syncline, Georgina Basin, showing presently established distribution of ?Tertiary Poodyea Formation in relation to regional structure (Mesozoic not shown).

Toko Syncline. Trough cross-stratification in the type area has a palaeocurrent pattern that indicates drainage to the north. The dominance of coarse detritus is suggestive of a braided stream system. This fluvial deposit was most likely derived from local erosion of the Cravens Peak beds and Mesozoic siliciclastics in and to the south of the Toko Range, and possibly from the Proterozoic Yardida Tillite to the southwest.

The extensive gravel and boulder debris east of the Toko Range may represent distal outwash fans at the abrupt change from incised valleys to very subdued topography. Similar distal outwash environments may have existed in the southern areas of the Mount Whelan Sheet area as scree from outcrops of Cravens Peak beds next to the Toomba Fault at that time.

Alternative interpretations of a problematic area

Distinguishing the various conglomerate and sandstone units remains a problem. One area of unresolved stratigraphy is located on the south side of an east-northeast-trending normal fault, 3 km south of Mithaka Waterhole (Fig. 1). On the South Georgina Basin 1:250 000 Special geological map (BMR, 1982), small (less than 1 km length), elliptical outcrops of both Poodyea Formation and Cravens Peak beds were differentiated. These outcrops had been

partly overlooked in previous work, though some had been mapped as Cravens Peak beds. On lithological, structural, depositional pattern, and palaeocurrent grounds, Draper believes all outcrops in that area to be Poodyea Formation and distinct from the Cravens Peak beds some 10 km to the southeast. Authors Radke and Simpson consider the mapping of some outcrops as Cravens Peak beds is justified because of reported Devonian fauna (Gilbert-Tomlinson, 1968), induration, weathering-enhanced intense jointing, and scattered distribution. The adjoining outcrops of Poodyea Formation, which are best distinguished by their characteristics on aerial photographs, display smooth rounded forms, subdued relief of outcrop, and a characteristic light pinkish tone on colour aerial photographs. The intense jointing of the Cravens Peak beds parallels the fault south of Mithaka Waterhole, and this is considered indicative of a pre-fault unit. In contrast, the Poodyea Formation outcrops have not been affected by the fault, but their distribution is controlled by it, probably the result of its morphological influence during Poodyea Formation deposition.

Lithologically, the Poodyea Formation is distinct in several ways from the major occurences of Cravens Peak beds to the south. The nearest outcrops of definite Cravens Peak beds are sandstones with rare pebbles, whereas conglomerate is dominant in the Poodyea Formation. Similarly, the largest grains in the Cravens Peak beds in the area are small pebbles, whereas the Poodyea Formation contains boulders up to 70 cm across. In fact, the largest clasts recorded in the Cravens Peak beds as a whole are less than 15 cm across (Draper, 1976), and the coarsest deposits are those most remote from the Poodyea Formation.

Depositional patterns and palaeocurrent data also show sedimentological differences between the Poodyea Formation and Cravens Peak beds. The Cravens Peak beds have a widely dispersed distribution, as befits a braided stream origin (Turner & others, 1981), whereas the Poodyea Formation has a narrow sinous pattern. Palaeocurrents for the Cravens Peak beds show variation but a pattern is discernible with an overall vector mean of 330°. In the Poodyea Formation, the palaeocurrents closely parallel the outcrop trends (Fig. 1).

Gilbert-Tomlinson (1968) described a fish fossil locality (her locality 26) from the area under discussion and authors Radke and Simpson cite this as one reason for mapping some outcrops as Cravens Peak beds. The fauna was found associated with aboriginal artifacts, and has been identified as the Devonian fish *Wuttagoonaspis* sp. (Ritchie, 1973). Draper (1976) suggested, from the presence of the artifacts and the fact that other data indicated a later age, that the sample had been carried there. Well-preserved *Wuttagoonaspis* are present at several localities in the Cravens Peak beds to the south (Turner & others, 1981). Wilson (*in* Gilbert-Tomlinson, 1968) pointed out that the rock was heavy and unlikely to have been carried far. Roth (1904), however, recorded that the Toko Range was a source for Aboriginal sandstone grinding-stones, and that well-developed trading routes existed, with slabs up to 45 cm long reaching the Leichhardt–Selwyn Ranges some 300 km to the northeast, and the 'middle Diamantina', a similar distance to the southeast, of the Toko Range. Roth (1904) found it 'almost incredible that some of these large slabs should be traded such distances, but then of course, the women were the beasts of burden, and even when shifting from camp to camp, the slab will be included in the swag carried on her back'. There was, therefore, a mechanism for the dissemination of large blocks of sandstone throughout the region. Subsequent surveys have failed to find any other fish fossils in the problematic area, despite considerable success in the Cravens Peak beds (Turner & others, 1981). The nearest known in situ localities of *Wuttagoonaspis* are 14 km to the southeast (Turner & others, 1981, Fig. 2).

Outcrops in the debated area are probably older than the most recent tectonic event, the Selwyn Uplift (Opik, 1960), which tilted Tertiary Basins in the Boulia area to the south (Paten, 1964), and which is dated as Pliocene or Pleistocene (Grimes, 1980). The fact that the Poodyea Formation crosses major structural elements without any deformation fixes its maximum age. The Cravens Peak beds were affected by the major structural deformation in the area, which is probably of Middle Devonian age (Draper, 1976). On this argument, the Poodyea Formation was deposited between the Late Devonian and Late Tertiary, a period when Jurassic, Cretaceous, and Tertiary deposits accumulated in the general area. The Poodyea Formation is considered Tertiary because of apparent lithological dissimilarity with the Mesozoic units.

Acknowledgements

J.J. Draper publishes with the permission of the Chief Government Geologist, Geological Survey of Queensland.

References

BMR. 1979 — Toko 1:100 000 Geological Series. Sheet 6452 (Preliminary edition). *Bureau of Mineral Resources, Australia.*

BMR. 1982 — Geology of the South Georgina Basin 1:250 000 Special Geological Sheet (Preliminary edition). *Bureau of Mineral Resources, Australia.*

Draper, J.J. 1976 — The Devonian rocks of the Toko syncline, western Queensland. *Bureau of Mineral Resources, Australia, Record* 1976/29.

Draper, J.J., 1980 — Ethabuka Sandstone, a new Ordovician unit in the Georgina Basin, and a redefinition of the Toko Group. *Queensland Government Mining Journal*, 81, 469–475.

Gilbert-Tomlinson, J., 1968 — A new record of *Bothriolepsis* in the Northern Territory of Australia. *Bureau of Mineral Resources, Australia, Bulletin*, 80, 191–226.

Grimes, K.G., 1980 — The Tertiary geology of North Queensland. *In* Henderson, R.A., & Stephenson, P.J. (editors). The geology and geophysics of northeastern Australia. *Geological Society of Australia (Queensland Division) Brisbane*, 329–347.

Harrison, P.L. 1980 — The Toomba Fault and the western margin of the Toko Syncline, Georgina Basin, Queensland and Northern Territory. *BMR Journal of Australian Geology & Geophysics*, 5, 201–214.

Johnstone, M.H., Jones, P.J., Koop, W.J., Roberts, J., Gilbert-Tomlinson, J., Veevers, J.J., & Wells, A.T., 1967 — Devonian of Western and Central Australia. *In* Oswald, D.H., (editor). International symposium on the Devonian System. *Alberta Society of Petroleum Geologists*, 1, 599–612.

Opik, A.A., 1960 — Cambrian and Ordovician geology of Queensland. *Journal of the Geological Society of Australia*, 7, 91–103.

Paten, R.J., 1964 — Tertiary geology of the Boulia region, Western Queensland. *Bureau of Mineral Resources, Australia, Report* 77.

Reynolds, M.A., 1968 — Mount Whelan, Queensland, 1:250 000 Geological Series. *Bureau of Mineral Resources, Australia, Explanatory Notes* SF/54–13.

Ritchie, A., 1973 — *Wuttagoonaspis* gen. nov., an unusual arthrodire from the Devonian of Western New South Wales, Australia. *Palaeontographica*, 143, Abt A, 58–72.

Roth, W.E. 1904 — Domestic implements, arts, and manufactures. *North Queensland Ethnography, Bulletin* 7 C.A. 56–1904.

Smith, K.G., 1965 — Tobermory, Northern Territory, 1:250 000 Geological Series. *Bureau of Mineral Resources, Australia, Explanatory Notes*, SF/53–16.

Smith, K.G., 1972 — Stratigraphy of the Georgina Basin. *Bureau of Mineral Resources, Australia, Bulletin* 111.

Turner, S., Jones P.J., & Draper, J.J., 1981 — Early Devonian thelodonts (Agnatha) from the Toko syncline, western Queensland, and a review of other Australian discoveries. *BMR Journal of Australian Geology & Geophysics*, 6, 51–69.

Appendix. Stratigraphic nomenclature

POODYEA FORMATION. This definition is based on field observations and subsequent airphoto interpretation.

Derivation of name. From Poodyea Point; grid reference 648148 (22°52'S, 138°13'E) Glenormiston 1:250 000 Sheet area.

Distribution. Southwest part of Glenormiston, southeast part of Tobermory, and the western area of Mount Whelan 1:250 000 Sheets. The unit occurs within the Toko Range and to the south as narrow discontinuous belts following the synclinal axis in part. Its total known extent is shown on the Geology of the South Georgina Basin 1:250 000 Special Map (BMR, 1982).

Type area. An unknown thickness (probably less than 10 metres) is exposed in the watershed dividing the upper tributaries of Beattie Creek and Linda Creek, 53K RQ 004666 on Toko 1:100 000 (Sheet 6452), 9 km north of Tobermory Outstation 'The Gap'. The outcrop has a low, subdued relief and is differentiated from the underlying Ordovician Carlo Sandstone by its light pinkish-brown appearance on colour aerial photography.

Lithology. Unconsolidated boulder conglomerate is most common, it consists of well-rounded clasts (up to 70 cm across) of quartzite, quartzose sandstone derived from the Carlo Sandstone, and milky quartz; cross-stratified sandy conglomerate and pebbly sandstone with parting lineation constitutes the bulk of the consolidated outcrop. The cross-strata comprise medium- to large-scale cosets of low-, medium- and high-angle trough cross-stratification. Planar lamination is present.

Thickness. Unknown, probably less than 10 m, but extremely varied locally.

Relationships and boundary criteria. Disconformably overlies the Lower to Middle Ordovician Carlo Sandstone, Ethabuka, Mithaka, and Nora Formations of the Toko Group (Draper, 1980), and the Lower to Middle Devonian Cravens Peak beds. It is overlain by unconsolidated Quarternary alluvium, colluvium and sand. Its relationships with the Jurassic-Cretaceous Hooray Sandstone and the Tertiary Austral Downs Limestone have not been established.

Age. There is no unequivocal evidence for the age of the unit, but it is post- Devonian, as it cuts across the major structural features of the area, which are Devonian in age (Draper, 1976; Harrison, 1980). It is considered Tertiary because: (1) of its apparent lithological dissimilarity to Mesozoic deposits in the area and its physiographic occurrence, in the Toko Range, in canyons incised below the Mesozoic level; (2) its outcrop trends are undisturbed by structures that have influenced erosional patterns of lateritised Mesozoic units; and (3) the unit is pre-Quaternary, being locally overlain by Quaternary cover, and outcrop trends indicate pre-existing valleys down the synclinal axis. Within the Toko Range, parts of these valleys have been followed by more recent post- Poodyea drainage, which has incised deeper into the Carlo Sandstone. To the southwest, in Ethabuka Sandstone and Mithaka Formation terrain, the more erosion-resistant Poodyea Formation remains as cappings.

Synonomy. Outcrops of the Poodyea Formation were previously considered part of the Silurian to Devonian Cravens Peak beds by Reynolds (*in* Smith, 1965) and Smith (1972). Unconsolidated pebble deposits in the Mount Whelan Sheet area were described by Reynolds (1968) and interpreted as Permian by Smith (1972); they were referred to as 'Unit 4 — post-Devonian rocks' by Draper (1976), mapped as the 'Beattie Creek Conglomerate' on Toko 1:100 000 Geological Sheet (BMR, 1979), and described as 'a post-Devonian valley-fill conglomeratic deposit' by Turner & others, (1981).

References.

BMR, 1979 — Toko 1:100 000 Geological Series, Sheet 6452 (Preliminary edition). *Bureau of Mineral Resources, Australia.*

BMR, 1982 — Geology of the South Georgina Basin 1:250 000 Special Geological Sheet (Preliminary edition). *Bureau of Mineral Resources, Australia.*

Draper, J.J., 1976 — The Devonian rocks of the Toko Syncline, western Queensland. *Bureau of Mineral Resources, Australia, Record* 1976/29.

Reynolds, M.A., 1968 — Mount Whelan, Queensland, 1:250 000 Geological Series. *Bureau of Mineral Resources, Australia, Explanatory Notes* SF/54–13.

Smith, K.G., 1965 — Tobermory, Northern Territory, 1:250 000 Geological Series. *Bureau of Mineral Resources, Australia, Explanatory Notes* SF/53–16.

Smith, K.G., 1972 — Stratigraphy of the Georgina Basin. *Bureau of Mineral Resources, Australia, Bulletin* 111.

Turner, S., Jones, P.J., & Draper, J.J., 1981 — Early Devonian thelodonts (Agnatha) from the Toko Syncline, western Queensland, and a review of other Australian discoveries. *BMR Journal of Australian Geology & Geophysics*, 6, 51–69.

BMR Journal of Australian Geology & Geophysics, 8, 161-163

DISCUSSION: A review of the Corella Formation, Mount Isa Inlier, Queensland

I.H. Wilson[1]

Blake (1982) has emphasised small differences between very similar sequences of metamorphosed and brecciated laminated calcareous siltstone, shale, limestone, and minor volcanics to establish his three zones in the Corella Formation. Variations in thickness and metamorphic grade within one unit could easily account for most of the differences. Erosion and preservation of an incomplete sequence in the faulted synclines in his Zone A could account for the thinner sequences and scarcity of volcanic rocks in this area. It should be noted that Blake acknowledges that large thickness variations occur within the individual unnamed members of the Corella Formation in Zone A (p. 113), but he uses differences in thickness of possibly incomplete sequences of the formation as evidence for different stratigraphic units.

Some of the lithological evidence Blake uses for zones in the Corella Formation is also debatable. He states that Zone B contains more volcanics than Zone A, and supports this (p. 115) with the conjecture that much of the Tommy Creek Microgranite, amphibolite, and 'dolerite' in the zone is extrusive. Volcanics are present in Zone A, but their extent is limited by erosion and the unconformable overlap of the Mount Albert Group (Wilson & others, 1977).

Blake states that the metasediments in Zone B are more calcareous than in Zone A and, although this is partly true for the east of Zone A, Derrick & Wilson (1981, p. 269) indicated an increase in the carbonate content to the west and northwest in Zone A, noting a change to dolomite. There is thus ample evidence that extensive facies variation occurs within Zone A, and facies variation is a likely explanation for the differences between Zone A and Zone B.

Resolution of stratigraphy in Zone B is difficult, because of intense structural deformation and facies variation, but it is important, as this zone contains the type sections of the Corella Formation. Major faults such as the Ballara–Corella River Fault Zone and the Cameron Fault have displacements of several kilometres, and effectively bound three distinct domains in Zone B. Within the western domain, a consistent stratigraphic sequence from the Ballara Quartzite to the basal Corella Formation has been mapped from near Mary Kathleen to Kajabbi (Wilson & others, 1977; Derrick, 1980). About 10 km northeast of Mary Kathleen, the central domain contains a tightly folded, but well-defined stratigraphic sequence, which I have reinterpreted for the second edition of the Cloncurry 1:250 000 geological map as the upper part of the Corella Formation and the overlying Knapdale Quartzite. Wilson & Hutton (1980) were able to locate the Corella Formation type section with reasonable certainty. It traverses the three domains of Zone B and includes a relatively complete sequence of the formation. Contrary to Blake (1982), sufficient facing evidence is available and the stratigraphic succession has now been firmly established.

Blake (p. 115) concludes that there were no tectonic events between 1870 and 1670 Ma, because bedding in rocks of these ages in the south of the inlier is concordant. This conflicts with the timing of the unroofing of the Kalkadoon and Ewen Granites, the onlap of the Haslingden Group sediments and volcanics onto the older basement (Wilson & others, 1977), and marked angular discordance beneath the Fiery Creek Volcanics, Surprise Creek Formation, and Mount Isa Group in the north of the inlier (Wilson & others, 1979). The apparent parallelism of bedding in the south has probably been imposed by intense folding during the main deformational event that accompanied the regional metamorphism about 100 Ma after deposition of the Mount Isa Group. The deformations that caused the angular discordances in the north of the inlier do not appear to have been associated with regional metamorphism.

The evidence that the rocks in the west of Zone B were deformed and metamorphosed before intrusion of the Burstall Granite resulted from the belief that the skarn alteration that replaces previously metamorphosed rocks in the Mary Kathleen mine and surrounding areas was caused by the Burstall Granite (Derrick, 1980). The skarn alteration is now known to replace dykes related to the Burstall Granite, and metasomatism has recently been dated near Mary Kathleen as several hundred million years younger than the granite (Page, 1981a). There is thus no evidence for an 'older' Corella Formation in Zone B. The evidence for a 'younger' Corella Formation in this zone depends on the interpretation of the field relationships of a felsic rock in the Milo mine area, which is dated at 1607 Ma (Page, 1981b). Blake contends that the felsic rock is an extrusive in a sequence unconformably overlying folded calc-silicate rocks intruded by 'Burstall-type' granite. My interpretation from field work and a re-examination of aerial photographs is that the felsic rock is discontinuous and possibly discordant; features which are more consistent with an intrusion. Also, the area in which Blake describes the unconformity, is poorly exposed; few rocks are in situ, they are near a granite contact, and they consist of laminated calc-silicate rocks that are commonly folded and brecciated in the region. The granite is mapped as Naraku Granite and has not been dated, but it is unfoliated and suspected of being younger than the Burstall Granite. Because of these observations, the proposed unconformable relationship is doubtful.

Discussion of the Corella Formation and its correlatives in Zone C is complicated by poorly resolved stratigraphic relations (Blake & others, 1981) and because numerous workers have studied small parts of the zone and reached incompatible conclusions. A maximum age for the Corella Formation in this zone is provided by the underlying Argylla Formation of the Duck Creek Anticline (1760 Ma, Page, 1981b). A further constraint on the base of the Corella Formation is provided by the Overhang Jaspilite, which underlies the Corella Formation in Zone B, and the Staveley Formation (Blake & others, 1981) and 'undivided' Corella Formation in Zone C (Derrick, 1980). The possibility of an unconformity at this stratigraphic level is raised by Blake. There is thus good evidence for the Corella Formation in Zones B and C commencing at similar times. The stratigraphic evidence is consistent with the correlation of the Corella and Doherty Formations. The latter formation contains a felsic volcanic dated at 1720 ± 7 Ma (Page, 1981b; Blake, 1982). Blake distinguishes the Staveley and Doherty Formations because of a slight change in the proportion of clastics and carbonates and differences in metamorphic

[1] Geological Survey of Queensland, GPO Box 194, Brisbane, Queensland, 4001. Published with the permission of the Director General, Department of Mines, Queensland.

grade. Neither of these criteria are reliable elsewhere in the region, and the validity of this distinction is doubted. The Roxmere Quartzite, which overlies the 'undivided' Corella and Staveley Formations in Zone C, is correlated with the Knapdale Quartzite in Zone B (Derrick & others, 1977). Both of these quartzites appear to overlie the Corella Formation unconformably. The Corella Formation and similar rocks in all three zones are thus confined between two unconformities.

In conclusion, there are no substantial reasons for renaming the Corella Formation in Zone A or subdividing the unit in Zone B. The sequence in the existing type section has a well-defined base and top and its stratigraphy *is* capable of resolution. The status of the Corella Formation should not be down- graded to beds. No real evidence has been presented for the existence of a younger sequence previously referred to the Corella Formation in Zone C, and the introduction of the name Doherty Formation is unnecessary.

References

Blake, D.H., 1982 — A review of the Corella Formation, Mount Isa Inlier, Queensland. *BMR Journal of Australian Geology & Geophysics*, 7, 113–118.

Blake, D.H., Bultitude, R.J., & Donchak, P.J.T., 1981 — Definitions of newly named and revised Precambrian stratigraphic and intrusive rock units in the Duchess and Urandangi 1:250 000 Sheet areas, Mount Isa Inlier, northwestern Queensland. *Bureau of Mineral Resources, Australia, Report* 233, *BMR Microform* MF164.

Derrick, G.M., 1980 — Marraba, Queensland. *Bureau of Mineral Resources, Australia, 1:100 000 Geological Map Commentary.*

Derrick, G.M., & Wilson, I.H., 1981 — The early geological history of the Proterozoic Mount Isa Inlier, northwestern Queensland: an alternative interpretation: Discussion. *BMR Journal of Australian Geology & Geophysics*, 6, 267–271.

Derrick, G.M., Wilson, I.H., & Hill, R.M., 1977 — Revision of stratigraphic nomenclature in the Precambrian of northwestern Queensland. VII Mount Albert Group. *Queensland Government Mining Journal*, 78, 113–116.

Page, R.W., 1981a — Timing of igneous activity and metasomatism, and its bearing on uranium mineralisation in the Mary Kathleen syncline. (Abstract). Joint Meeting on Mount Isa Geology. *Northwest Queensland Branch, Australasian Institute of Mining and Metallurgy.*

Page, R.W., 1981b — Mount Isa Inlier. *In* Geological Branch Annual Summary of Activities, 1980. *Bureau of Mineral Resources, Australia, Report* 230, 127–128.

Wilson, I.H., & Hutton, L.J., 1980 — Geological field work in Mount Isa District — August and September, 1980. *Geological Survey of Queensland, Record* 1980/34.

Wilson, I.H., & Derrick, G.M., Hill, R.M., Duff, B.A., Noon, T.A., & Ellis, D.J., 1977 — Geology of the Prospector 1:100 000 Sheet area, Queensland. *Bureau of Mineral Resources, Australia, Record* 1977/4.

Wilson, I.H., Hill, R.M., Noon, T.A., Duff, B.A., & Derrick, G.M., 1979 — Geology of the Kennedy Gap 1:100 000 Sheet area (6757), Queensland. *Bureau of Mineral Resources, Australia, Record* 1979/24.

REPLY

D.H. Blake

The discussion by Wilson highlights the subjectivity inherent in firstly observing and secondly interpreting geological field evidence. Differences in interpretation arise, inevitably, from the different experiences, interests, and pre-conceived ideas of the geologists involved. In this discussion, matters of opinion, rather than facts, are mainly in dispute, as was also the case in an earlier related discussion (Derrick & Wilson, 1981; Blake, 1981). Hence, on basically the same facts, differences in lithology, thickness, deformation, metamorphism, and internal and external stratigraphic relationships of the Corella Formation, the most extensive formation mapped in the Precambrian Mount Isa Inlier, are considered by Wilson to be of minor stratigraphic importance, whereas I have suggested that they are likely to be of major significance in stratigraphic correlations. Similarly, igneous rocks regarded by Wilson as probably intrusive are considered by me to be probably extrusive. Specific points raised by Wilson are discussed below.

Lithologic and other differences between the various parts of the Corella Formation, as previously mapped in my Zones A, B, and C, can be considered comparable to those in the Mount Isa Inlier between different units of sandstone (e.g., Mount Guide, Ballara, Mitakoodi, and Warrina Park Quartzites), or of felsic volcanics (such as those of the Leichhardt Volcanics/Metamorphics, Bottletree Formation, Argylla Formation, Corella Formation, and Carters Bore Rhyolite) or of mafic volcanics (such as those of the Bottletree Formation, Eastern Creek Volcanics, Magna Lynn Metabasalt, Marraba Volcanics, and Soldiers Cap Group).

Wilson acknowledges that the stratigraphy of the Corella Formation in Zone B is difficult to resolve because of intense structural deformation, but, unlike me, considers that the stratigraphic succession here is now firmly established. I also do not share his confidence that the original type section of the Corella Formation selected by Carter & others (1961) has been located with reasonable certainty and that the sequence in the type section area has a well defined base and top.

As stated previously (Blake, 1982, p.115), there is no evidence of a major tectonic event involving significant regional metamorphism during the period from about 1870 Ma to about 1670 Ma in the southern part of the Mount Isa Inlier. Wilson apparently agrees with this conclusion. However, there is abundant evidence of widespread volcanism, plutonism, uplift and erosion, down-warping and deposition, tilting, and faulting during this 200 Ma period, readily accounting for unroofing of granites, onlapping of sediments and volcanics, and local angular discordances between units of widely different to closely similar ages. The suggestion of Wilson that parallelism of bedding in this part of the inlier is a deformational effect is not in accord with the layer-cake stratigraphy convincingly documented by Derrick & others (1980) and discussed by me (Blake, 1980, 1981).

Evidence for Corella rocks in Zone B being deformed and metamorphosed before being intruded by 1720–1740 Ma Burstall Granite and similar granites to the south is based not only on the development of skarns in the vicinity of many of the granite bodies, as assumed by Wilson, but also on the

observation that dykes of granitic rock spatially, and probably genetically, related to the granites cut previously folded calc-silicate rocks. The dykes are deformed, but much less so than the rocks they intrude. The difference in age between dyke intrusion and earlier folding is conjectural — the dykes and associated granites may be more than 150 Ma younger than the folding, as I have suggested (Blake, 1980, 1981, 1982), but could conceivably be only slightly younger.

Wilson prefers to interpret as intrusive the felsic igneous rock dated by Page (in press–a) at about 1600 Ma from the Zone B Corella Formation near the Milo mine in the Tommy Creek area, because it is 'discontinuous and possibly discordant'. Such an interpretation is at variance with the expressed views of geologists who examined the sample site during an excursion in September 1981, following the joint meeting on Mount Isa geology conducted by the Australasian Institute of Mining and Metallurgy, BMR, and the Geological Survey of Queensland. The dated sample is a metamorphosed, fine-grained, flow-banded quartzofeldspathic rock, associated with felsic agglomerate and tuff of apparently similar composition, in a sequence containing several concordant bands of both felsic and mafic metavolcanics, together with interlayered biotite schist, black slate, and bedded calcareous metasediments. The sequence dips uniformly northwards and differs markedly in lithology and deformation from a sequence of highly contorted, thinly banded calc-silicate rocks, also mapped as Corella Formation, to the south. It is the strongly discordant contact between these two sequences, marked by a fragmentary zone, a few metres wide, aligned parallel to the bedding in the northern sequence and strongly discordant to the southern sequence, that is regarded by me (Blake, 1982, p.116), but doubted by Wilson, as a possible major unconformity.

In spite of the views expressed by Wilson, there is no good evidence for correlating the Corella Formation of Zone B with the Doherty Formation of Zone C. On the contrary, geochronological evidence is against such a correlation — Corella Formation rocks in Zone B are intruded by granite and gabbro dated at 1720–1740 Ma (Page, in press–b), whereas the Doherty Formation includes metarhyolite dated at 1720+ 7 Ma, a significantly (beyond experimental error) younger age. Wilson considers that the distinction of the Doherty Formation from the Staveley Formation on the basis of mappable differences in lithology and metamorphic grade is unreliable. However, in my view this distinction is probably significant stratigraphically, is better based than his correlation of the Roxmere Quartzite rocks overlying, apparently conformably, the Staveley Formation in Zone C with isolated outcrops mapped as Knapdale Quartzite in Zone B, and follows normal stratigraphic nomenclature principles (Hedberg, 1976).

Hopefully, many of the present problems concerning the status of the Corella Formation will be resolved in the near future, when results of proposed detailed structural and metamorphic studies in the Mount Isa Inlier by BMR and university geologists, supplemented by geochronological data, become available.

References

Blake, D.H., 1980 — The early geological history of the Proterozoic Mount Isa Inlier, northwestern Queensland: an alternative interpretation. *BMR Journal of Australian Geology & Geophysics*, 5, 243–56.

Blake, D.H., 1981 — The early geological history of the Proterozoic Mount Isa Inlier, northwestern Queensland: an alternative interpretation: Reply to discussion. *BMR Journal of Australian Geology & Geophysics*, 6, 272–4.

Blake, D.H., 1982 — A review of the Corella Formation, Mount Isa Inlier, Queensland. *BMR Journal of Australian Geology & Geophysics*, 7, 113–118.

Carter, E.K., Brooks, J.H., & Walker, K.R., 1961 — The Precambrian mineral belt of north-western Queensland. *Bureau of Mineral Resources, Australia, Bulletin* 51.

Derrick, G.M., & Wilson, I.H., 1981 — The early geological history of the Proterozoic Mount Isa Inlier, northwestern Queensland: an alternative interpretation: Discussion. *BMR Journal of Australian Geology & Geophysics*, 6, 267–71.

Derrick, G.M., Wilson, I.H., & Sweet, I.P., 1980 — The Quilalar and Surprise Creek Formations - new Proterozoic units from the Mount Isa Inlier: their regional sedimentology and application to regional correlation. *BMR Journal of Australian Geology & Geophysics*, 5, 215–23.

Hedberg, H.D. (editor), 1976 — International stratigraphic guide. *Wiley, New York*.

Page, R.W., in press a — Timing of superposed volcanism in the Proterozoic Mount Isa Inlier, Australia. *Precambrian Research*.

Page, R.W., in press b — Chronology of magmatism, skarn formation and uranium mineralization, Mary Kathleen, Queensland, Australia. *Economic Geology*.

BMR Journal of Australian Geology & Geophysics, 8, 163-165

DISCUSSION: A Proterozoic rift zone at Mount Isa, Queensland, and implications for mineralisation

I.P. Sweet

There are three main points in the paper by Derrick (1982) on which I will comment: (1) definition of the Leichhardt River Fault Trough (LRFT); (2) nature of the western margin of the LRFT; and (3) the extent of the Mount Gordon Arch.

Definition of the Leichhardt River Fault Trough

Derrick's paper perpetuates the confusion over the definition of the term Leichhardt River Fault Trough (LRFT), and of the geological character of the trough. As defined by Glikson & others (1976) the LRFT '. . . refers to the north-trending structurally complex area bounded to the east by the Gorge Creek–Quilalar Fault Zone . . . and the Kalkadoon–Leichhardt acid igneous complex and to the west by the Mount Isa and Mount Gordon Fault Zone . . .'. Although Glikson & others' definition states nothing about the timing of faulting, they conclude that 'early pre-depositional faulting took place along the eastern border of this trough'. Derrick (1982) has carried the conclusions further, and sees the LRFT as 'an 1800–1650 m.y. old intracontinental or continental margin rift structure'. He regards its western boundary as being *west* of the Mount Isa–Mount Gordon Fault Zone, because it 'also occurs within and extends beneath the Proterozoic Lawn Hill Platform'. The extent of the LRFT is based largely on magnetic and gravity anomalies caused by the effects of large volumes of basic volcanics in the region.

Derrick's rift-fill sequence is the Haslingden Group, which was 'deposited between about 1800 m.y. and 1740 m.y. ago'

(Derrick, p. 85). It is conformably overlain by the Quilalar Formation, considered by Derrick & others (1980) to be part of a blanket deposit that extended beyond the eastern boundary of the LRFT. Similarly, the Fiery Creek Volcanics and Bigie Formation, which overlie the Quilalar Formation, have correlatives beyond the LRFT to the west (Carrara Range Group — Hutton & Sweet, 1982) and northwest (Peters Creek Volcanics — Sweet & others, 1981). The youngest Proterozoic rocks preserved in the region under discussion are the Mount Isa Group, dated at around 1670 Ma (Page, 1981), and its correlative, the McNamara Group. The McNamara Group is even more extensive than the other formations overlying the Haslingden Group. The Quilalar Formation and Mt Isa/McNamara Groups are designated 'rift cover' in Derrick's figure 3, yet figures 4 and 5 clearly show them to be part of the LRFT. They cannot be both. If the LRFT is a rift, then it ceased to exist as a tectonic entity by about 1740 Ma, *before* deposition of the Quilalar Formation. Derrick presents no evidence that the Mount Isa Group was deposited in a rift structure.

Nature of the western margin of the LRFT

Following on from the above discussion it is apparent that the western margin of the LRFT is not satisfactorily defined. In the northwest the Haslingden Group forms the basement to the Lawn Hill Platform Cover (Hutton & Sweet, 1982). Here the Haslingden Group is at least 2800 m thick, suggesting that although it may have thinned westward, the thinning is gradual, not abrupt. No conglomerates are present in the west and there is no evidence of active faulting during deposition. The conclusion I draw is that a rift-type western margin for the LRFT cannot be seen, despite the indirect geophysical evidence for the extent of basalt fill. The more likely explanation is that the LRFT is a half graben with a faulted eastern margin and an unfaulted western one.

The extent of the Mount Gordon Arch

The stratigraphic and sedimentological evidence for the existence of a local high in the Mammoth area is convincing (Derrick, fig. 6), but the interpretation of an arch to the north of that area is questioned. It appears to be based on (i) the presence of a trachybasalt member in the Quilalar Formation; (ii) the amount of pre-Surprise Creek Formation deformation in the vicinity of the supposed arch; and (iii) on the thickness of the Surprise Creek Formation. I would counter these arguments thus: (i) the trachybasalt flows are thin, and would not be expected to extend over a huge area. Any lava flow must stop somewhere, and the existence of tuffs beyond the point of termination is not necessarily an indication of a topographic barrier to the lavas; (ii) evidence of erosion preceding deposition of the Surprise Creek Formation may well indicate warping and uplift south of Gunpowder (near locality d, Derrick, fig. 8), but there is no evidence of any such effect to the north; (iii) preserved thicknesses of the sandstone units in the Surprise Creek Formation (BMR, 1981) vary between 270 m and 800 m, but show no systematic variation relative to the site of the Mount Gordon Arch. On the contrary, the thickness is less in the northwesternmost outcrops, away from the site of the supposed arch.

Conclusions

Derrick's usage of the term LRFT differs from that of Glikson & others (1976), and his paper presents conflicting information on the younger limit of rift-related sedimentation. The western margin of the LRFT has not yet been recognised, and in fact it may not be a rift (faulted) margin at all. There is no evidence for the existence of the Mount Gordon arch in the Mount Oxide Region (i.e. north of Gunpowder).

Acknowledgement

I thank D.H. Blake for commenting on a draft for this discussion.

References

BMR, 1981 — Mount Oxide Region, Queensland, 1:100 000 Geological Special, Preliminary edition. *Bureau of Mineral Resources, Australia* (unpublished).

Derrick, G.M., 1982 — A Proterozoic rift zone at Mount Isa, Queensland, and implications for mineralisation. *BMR Journal of Australian Geology & Geophysics*, 7, 81–92.

Derrick, G.M., Wilson, I.H., & Sweet, I.P., 1980 — Quilalar and Surprise Creek Formations — new Proterozoic units from the Mount Isa Inlier: their regional sedimentology and application to regional correlation. *BMR Journal of Australian Geology & Geophysics*, 5, 215–224.

Glikson, A.Y., Derrick, G.M., Wilson, I.H., & Hill, R.M., 1976 — Tectonic evolution and crustal setting of the Middle Proterozoic Leichhardt River Fault Trough, Mount Isa region, northwestern Queensland. *BMR Journal of Australian Geology & Geophysics*, 1, 115–130.

Hutton, L.J., & Sweet, I.P., 1982 — Geological evolution, tectonic style and economic potential of the Lawn Hill Platform Cover, northwest Queensland. *BMR Journal of Australian Geology & Geophysics*, 7, 125–134.

Page, R.W., 1981 — Depositional ages of the stratiform base metal deposits at Mount Isa and McArthur River, Australia, based on U–Pb zircon dating of concordant tuff horizons. *Economic Geology*, 76, 648–658.

Sweet, I.P., Mock, C.M., & Mitchell, J.E., 1981 — Seigal, Northern Territory and Hedleys Creek, Queensland. *Bureau of Mineral Resources, Australia. 1:100 000 Geological Map Commentary.*

REPLY

G.M. Derrick

Definition of the Leichhardt River Fault Trough (LRFT)

The definition by Glikson & others (1976) of the LRFT reflected the limits of detailed geological mapping by the Bureau of Mineral Resources and Geological Survey of Queensland at that time. Glikson & others considered that the most characteristic feature of the fault trough was an abundance of basic volcanics, and their distribution clearly outlined a north-trending linear zone bounded by a partly faulted eastern margin; the Mount Isa–Mount Gordon Fault Zones appeared to be a satisfactory western margin because of the change in structural style across these faults, and an apparent absence of basic volcanics west of the fault system in parts of the Lawn Hill Platform.

More recently, it has been established that basic volcanics do occur in the cores of domal structures in the Lawn Hill Platform, and that they possess, everywhere, a pronounced magnetic signature. The latter appears to show a relatively linear western margin to the basalts in the subsurface. These factors were influential in my extending and redefining the LRFT from that discussed by Glikson & others. In so doing I have maintained the emphasis of earlier authors, viz. the basalt content is most characteristic. I also suggest the updated descriptions of the nature and extent of the LRFT are preferable to the introduction at this stage of yet another new name for this feature.

Sweet's comments regarding Figures 3, 4 and 5 of Derrick (1982) are pedantic. Figure 3 correctly distinguishes between 'rift fill' (Haslingden Group) and 'rift cover' (Quilalar Formation, Surprise Creek Formation, Mt. Isa and McNamara Groups). Figure 4 clearly shows Quilalar Formation as an open-ended sheet transgressing the eastern margin of the LRFT. Figure 5 likewise shows the same phenomena for Mount Isa–McNamara Group deposition. Quilalar Formation is described (p. 81) as being of 'region-wide' distribution, and as extending across 'much of the Mt. Isa Inlier' (p.85).

In discussion on evolution of the LRFT (Derrick, 1982, fig. 12) it is clearly stated that post-Haslingden Group sedimentation 'extended far beyond the limits of (Haslingden Group) rift fill'; the younger sequences are schematically shown as occupying broad basins 130 km wide, compared with stated LRFT widths of about 65 km.

I contend that these quotations are sufficient to conclude that the Mount Isa and McNamara Groups were not deposited in a rift structure — rather they were deposited *on* a rift structure and beyond. Yet the Mount Isa and McNamara Groups are inextricably linked to the earlier-formed rift fill (1800–1750 Ma) by virtue of reactivation of older rift structures, e.g. the Mount Gordon Arch, contemporaneous with early Mount Isa/McNamara Group deposition (1680–?1650 Ma). Hence, it is clear that the LRFT had a history — both depositional and tectonic — which extended from 1800 to about 1650 Ma.

Nature of the western margin of the LRFT

I agree with Sweet that the western margin of the LRFT is not satisfactorily defined. It will remain so for as long as the cover of Georgina Basin sediments remains in place. The western limit to basalt, as defined by geophysics, should be considered as a broad zone rather than a line, and it is located at depths of several hundred metres. All relevant diagrams in Derrick (1982) indicate schematic uncertainty on this matter, as do earlier papers on the topic (Plumb & others, 1980). Sweet's suggestion of a large half-graben has merit, but also remains conjectural. Analogies can be drawn with the Batten Trough, which appears to have formed as both a graben and half-graben structure at various times in its development (Plumb & others, 1980, fig. 6).

Extent of the Mount Gordon Arch

Sweet points out the difficulty in tracing the Mount Gordon Arch northwards from Gunpowder. This task is complicated by 20 kms of right lateral displacement on the Mount Gordon Fault north of gunpowder. When this displacement is allowed for, the trace of the Mount Gordon Arch is tentatively located just east of the trachybasalt flows in the Quilalar Formation — hence my suggestion that the projected arch areas may have controlled distribution of the flows.

These observations apply only to Quilalar Formation time; no such claim is made for younger units (Surprise Creek Formation, McNamara Group) in the far northern areas. It is clear from thickness variations in the Surprise Creek Formation that the northern areas of the LRFT were submergent relative to southern areas; even in areas near Gunpowder, it is clear that the influence of the Mount Gordon Arch had waned by Oxide Chert time, and the arch was increasingly submergent to the north (Derrick, 1982, p.89). In this respect Sweet and myself appear to be in broad agreement that existence of the Mount Gordon Arch north of Gunpowder is conjectural, especially in depositional periods younger than Quilalar time.

References

Derrick, G.M., 1982 — A Proterozoic rift zone at Mount Isa, Queensland, and implications for mineralisation. *BMR Journal of Australian Geology & Geophysics*, 7, 81–92.

Glikson, A.Y., Derrick, G.M., Wilson, I.H. & Hill, R.M., 1976 — Tectonic evolution and crustal setting of the middle Proterozoic Leichhardt River fault trough, Mount Isa region, northwestern Queensland. *BMR Journal of Australian Geology & Geophysics*, 1, 350–352.

Plumb, K.A., Derrick, G.M. & Wilson, I.H., 1980 — Precambrian geology of the McArthur River–Mount Isa region, northern Australia. *In* Henderson, R.A. & Stephenson, P.J. (editors), The geology and geophysics of northeastern Australia. *Geological Society of Australia (Queensland Division), Brisbane*, 71–88.

BMR Journal of Australian Geology & Geophysics, 8, 167-174

ABSTRACTS: TWELFTH BMR SYMPOSIUM, 17–18 MAY 1983, CANBERRA

Introduction to marine geoscience in BMR

D.A. Falvey

The Division of Marine Geosciences & Petroleum Geology came into existence on 1 July 1982. It has drawn staff from the previous specialist areas of marine geology, marine geophysics, and marine micropalaeontology. The Division conducts multidisciplinary research in three major programs.

Fossil fuels — the investigation of shelf and continental-margin sedimentary basins (stratigraphy, evolution, and crustal framework) as a basis for understanding the geological processes controlling passive-margin formation. This will help develop an understanding of the genesis and distribution of petroleum offshore and provide a basis for exploration and assessment. In addition to these explicitly resource-related projects, a major sub-program is concerned with study of modern marine processes, particularly the evolution of the Great Barrier Reef. This will provide an understanding of reef evolution as a basis for environmental management and pollution and hazard monitoring.

Minerals — the investigation of offshore mineral resources, in the context of margin and spreading-ridge evolution, as a basis for exploration and assessment. Work under this program is currently restricted to studying metalliferous sediments and deep-sea processes.

Overseas programs — these are conducted in two major sub-programs: (i) the study of the island arcs of the Australia-Pacific active plate margin, with particular reference to the evolution and resource potential of fore-arc and intra-arc sedimentary basis (this is conducted by BMR, in conjunction with ADAB, primarily in response to specific development aid requests from Pacific island nations); (ii) the study of the continental margin offshore Antarctica and the Heard–Kerguelen Plateau as a basis for resource assessment.

In addition to these field programs, the Division is also active in research and development of advanced marine geo physical systems, covering such fields as data acquisition, data processing, and database management.

Stratigraphic and structural framework studies of the Bass Basin: preliminary results

J.C. Branson, K.L. Lockwood, M.A. Etheridge, & A.S. Scherl

The Bass Strait Study aims to (1) describe the geological history of the Bass Basin; (2) provide regional correlation between the Otway, Bass, and Gippsland Basins, and (3) present a regional interpretation of the development of the continental margins that flank Bass Strait. A geophysical survey conducted under contract to BMR in March–May, 1982, recorded 3209 km of multichannel seismic data, together with gravity and magnetics. The results of the research into recording and processing techniques, together with preliminary results from the continental margins, have been discussed elsewhere (Lockwood & others, 1982; Branson, 1982). Public release of the data will be made later in 1983.

The Bass and Gippsland Basins have much in common, but display significant differences that may have important consequences for hydrocarbon reservoir formation. The Bass Basin contains much the same sedimentary sequence and early structures as the Gippsland Basin, and Nicholas & others (1981) have argued that hydrocarbon generation should have taken place from various parts of the Bass sequence. The Gippsland Basin reservoirs are primarily associated with middle to late Eocene structures that were apparently formed during a dextral wrench phase related to the Rosedale and parallel fault systems. This deformational phase was, at best, only weakly developed in the Bass Basin, but a number of other potentially suitable structural traps have been drilled, and favourable reservoir characteristics are present. The shortage of hydrocarbon discoveries in the Bass Basin is therefore considered to be at least partly a function of plumbing history. In this respect, a major difference between the basins is that the Gippsland Basin was facing open ocean during Tasman Sea rifting, whereas the Bass Basin was isolated by basement ridges around its whole perimeter. Detailed studies of the Bass Basin sedimentological and structural history are, therefore, aimed at elucidating its hydrological history as well as providing the basis for fresh exploration guidelines.

Studies of the seismic stratigraphy in the Bass Basin recognise alluvial, fluvial, upper-delta plain, lower-delta plain, marine, and volcanic environments throughout the Cretaceous and Tertiary, even below the extensive Eocene coal measures. Analysis of the movements of fault-blocks early in the Bass Basin history has also commenced, and a regional synthesis of this information will be the basis of a comprehensive basin formation model.

Two possible models of early basin development are being investigated: (1) extensional basins, and (2) wrench-fault basins. Extensional basins contain recognisable features such as normal faults and half-grabens parallel to the basin margins, wrench faults perpendicular to basin margins, tilted wedges of pre-rift and syn-rift fault sediments, and late 'thermal' broad-basin subsidence. Wrench-fault basins contain features such as corners to the basin with complex intersections of faults and unconformities, irregular basin margins, braided wrench zones, small thrusts, talus breccia, and rapid facies changes at the margins, and volcanic floor with remnant marginal blocks.

For the extension model, fault-block geometry and the age range of sediment wedges allow computation of the amount and history of extension of the basin floor. An example of this type of modelling is described from the southeastern Bass Basin, where a 50-km wide zone has undergone approximately 30–40 per cent extension over about 20 Ma in the Late Cretaceous. These calculations are based upon planar, rotational faults, which produce the maximum extension with a minimum of internal block deformation. This pattern also avoids space problems encountered with substantially curved (listric) faults.

The wrench-fault basin requires parallel offset faults that may reach the surface and terminate within the region. Models for these basins can produce elevation of the basin flanks. Models with flanking fault movements of 10 km can induce a tectonic subsidence of 1500 m at the depocentre. This tectonic subsidence is of the same magnitude as the extensional model.

Overall, this study will lead to a significant improvement in our knowledge of the tectonic and environmental history of the sedimentary basins of the region. This, in turn, will permit the more sophisticated thermal and hydrological modelling so important to the development of rational exploration.

References

Lockwood, K.L., Scherl, A.S., & Brazier, P., 1982 — Seismic exploration problems in the Bass Basin — recent results. *In* Petroleum geophysics — its role in Australia's energy future. *ASEG/PESA Petroleum Geophysics Symposium, 14–15 February 1982, Melbourne* (Abstracts).

Branson, J.C., 1982 — New seismic data from the Gippsland and Otway continental margins. *In* Lithosphere dynamics and evolution of the continental crust. *Sixth Australian Geological Convention, 20–25 February 1982, Canberra* (Abstracts).

Nicholas, E., Lockwood, K.L., Martin, A.R., & Jackson, K.S., 1981 — Petroleum potential of the Bass Basin. *BMR Journal of Australian Geology & Geophysics*, 6, 199–212.

Evolution of the Great Barrier Reef province

P.J. Davies & P. Symonds

The evolution of the Great Barrier Reef province has been determined from modern process studies in conjunction with shallow- and intermediate-focus seismic reflection profiling. Throughout much of its history, the province was dominated by terrigenous sedimentation: the reefs are Pleistocene features, the development of which drastically changed slope sedimentation patterns.

The principal control on sedimentation has been the relative position of sea level. During periods of low sea level, fluviatile processes affected the shelf, while wave- and tide-dominated deltaic progradation affected the upper slope. Three periods of low sea level in the late Oligocene, the late Miocene, and Pleistocene produced massive progradation. During periods of high sea level, sedimentation was confined to coastal deltaic progradation and transgressive onlap of the continental slope concomitant with extensive upper-slope erosion.

The reef facies appeared first as a fringing reef, probably in the Eocene, but was established as an extensive shelf-dominating facies during Pleistocene high sea-level periods. Reef establishment had a profound effect on slope sedimentation processes and products: during low sea level, the passages between the reefs channelled fluvial sediments onto the slope as point-source inputs, producing canyons in the upper slope and depositional fans on the middle and lower slope; during high sea-level periods, reef-derived, fine-grained carbonates and organic material formed organic-rich drapes on the upper and mid slope.

Low sea-level, shelf-edge deltaic sands and prodelta muds prograded 8 km (0.38 km thick) in the late Oligocene, 6 km (0.7 km thick) in the late Miocene, and 4–20 km (0.6 km thick) in the Pleistocene. In contrast, modern coastal deltaic progradation has occurred and is occurring at a rate of 1–2 km. 10^{-3} yrs, owing to a point-source annual fluviatile input of 3.5 million tonnes by the Burdekin River. High sea-level reef accretion has occurred at rates of 1–10 m.10^{-3} yrs vertically; massive leeward progradation of 40–120 m.10^{-3} yrs contrasts with slight windward growth of 1–2 m.10^{-3} yrs. Total sediment shed from the reefs is of the order of 0.3 tonnes per metre of reef edge per year; nearly 60 per cent of this load is organic carbon and much of it settles on the upper and middle slope. The Plio-Pleistocene witnessed an explosion in sediment production during both high and low sea levels.

Much of the Great Barrier Reef appears to be only 150–200 m thick, yet it grew during periods of high sea level, when there was rapid production of calcium carbonate; however, the growth periods were short in comparison to the intervening periods of low sea level, when subaerial erosion of the order of 7–14 cm.10^{-3} yrs could decimate a reef that had accreted 20 m of carbonate during the preceding high sea level. The Great Barrier Reefs are, therefore, composite features — remnant reefs laid upon remnant reefs and separated by angular unconformities. Each unconformity is equivalent to a period of shelf-edge, low sea-level progradation.

Regional sedimentary basin framework of the Prydz Bay area, offshore Antarctica

H.M.J. Stagg

A BMR marine geophysical survey in early 1982 indicated that much of Prydz Bay is underlain by a sedimentary basin that is an extension of the onshore Lambert Graben. Severe seismic multiples preclude an accurate estimate of the total sediment thickness, but interpretation of the seismic and magnetic data suggest it could be of the order of 5 km. Overall, the basin has a north- northeast trend, roughly orthogonal to the continental margin.

In the south of Prydz Bay, two seismic series are evident, separated by a mild erosional unconformity. The lower series ranges from poorly to well stratified, has minor folding and faulting, and is probably the expression of continental and, perhaps, shallow-marine breakup sediments. The upper series is generally well stratified, becoming prograded near the shelf edge, and probably represents shallow-marine post-breakup sediments. The sea bed is a distinct unconformity, and it would appear that both upper and lower series sediments have been bulldozed off by advances of the Amery Ice Shelf during glacial maxima, and that present sedimentation rates are very low. The glacial advances deposited a thin sequence of tillites in the northeast part of the bay.

Indo-Antarctic breakup has been tentatively dated as early Neocomian (130 Ma); the east-west orientation of breakup labels the Lambert Graben–Prydz Bay structure as a possible failed rift arm. There is no direct information on the age and nature of the sediments under Prydz Bay, but Permian conglomerate, sandstone, and coal that crop out at Beaver Lake, to the south, may correspond to the breakup series. Analogies may also be drawn with fault-bounded intracratonic basins in India, which may have been juxtaposed prior to breakup and which contain Permian to Triassic continental strata. The upper series probably consists of Late Cretaceous and Cainozoic sands and shales, with tillites near the top of the section.

Sedimentary basins in active island volcanic arcs: Tonga, Vanuatu, and Solomon Islands

N.F. Exon & D.A. Falvey

Thick offshore sedimentary basins lie either between linear oceanic trenches and island arcs (fore-arc basins) or within island arcs (intra-arc basins). East of Tonga, the Pacific Plate is subducted beneath the Australian Plate, and the Tonga Platform, just west of the Tonga Trench, is a fore-arc basin nearly 1500 km long and 200 km wide. Off Vanuatu, the Australian Plate is being subducted beneath the Pacific Plate at the New Hebrides Trench, and a series of intra-arc basins, 1300 km long and 150 km wide, has developed between the twin island chains to the east of the trench. Off the Solomon Islands, the situation is similar: the Australian Plate is being subducted, and there is a series of intra-arc basins, 1000 km long and 150 km wide, lying to the northeast of the trench, between twin island chains.

In 1982, three cruises of the USGS vessel R.V. *Lee* investigated these basin areas under the auspices of a Tripartite Agreement between Australia, New Zealand, and the United States. On each cruise, more than 2500 km of multichannel seismic data, other under-way geophysical data, and bottom samples were gathered. The cruise results, in conjunction with earlier work, have led to a considerable increase in our understanding of the basins and their petroleum potential. On the Tonga Platform, a westward-dipping Cainozoic sequence, 3 km thick, rests on basement rocks, probably Eocene island-arc volcanics. The Cainozoic sequence consists of limestone, marl, and volcaniclastic sediments: most were laid down in deep water. A major unconformity corresponds to the early Pliocene opening of the Lau Basin, which separated the Tonga Platform from the Lau Ridge. The volcanic arc formed the eastern Tonga Platform in the Palaeogene, but moved westward in the Pliocene. The best petroleum prospects appear to be buried mounds that may be Miocene reefs.

In Vanuatu, where the arc basement may be as old as late Eocene, and the Solomon Islands, where basement is Late Cretaceous or early Tertiary, subduction was initially to the west, and thick Oligocene and Miocene volcaniclastics and limestones accumulated in the fore-arc basins. In the late Miocene a structural ridge formed in the fore-arc region and the direction of subduction reversed. Volcaniclastics and limestones continued to accumulate in the new intra-arc basins. There is now 5 km of normally faulted Cainozoic section between the island chains, and a major unconformity may represent the period where subduction reversed.

Possible carbonate build-ups of probable Miocene age are present in the Solomons, but have not been found in Vanuatu, downgrading Vanuatu's petroleum potential. However, in Vanuatu, there are shallow-water perched basins east of Santo and Malekula, which could have entrapped hydrocarbons generated in the deep Central Basin to the east.

Subduction of a spreading axis beneath an island arc: magmatic, tectonic, and economic consequences in the western Solomon Islands

R.W. Johnson

A tectonically unique area, where an active ridge–transform sequence is being subducted almost orthogonally beneath a presumed oceanic island arc, is represented in the Woodlark Basin/New Georgia Group area of the western Solomon Islands. The Woodlark Basin spreading axis began opening about 3.5–4 million years ago, and has since been developing at an average total spreading rate of about 6–7 cm per year. New sea floor in the basin abuts the fore-arc slope of the New Georgia Group, beneath which it is consumed northeastwards at about 10 cm per year. Presumably, therefore, the New Georgia Group, and possibly the sedimentary succession in New Georgia Sound (The Slot) behind the arc, are underlain by a subducting thermal anomaly. This unusual tectonic configuration is of considerable interest in addressing questions of arc-magma genesis. In particular, do the underthrust youthful crust and thermal anomaly contribute to magma compositions that are significantly different from those in 'normal' island arcs? What implications does this have for 'porphyry' Cu-Au mineralisation? Further, does subduction of the thermal anomaly significantly raise the depth of petroleum–hydrocarbon conversion from organic material in the sediments of New Georgia Sound? A suite of volcanic rocks from the New Georgia Group has been studied, both petrologically and geochemically, in conjunction with the Solomon Islands Geological Division, and these data have been supplemented by results from sea-floor samples dredged by the *Kana Keoki* (Tripartite cruise 820316, Leg 4) in May–June 1982. The most striking types of volcanic rock in the New Georgia Group are picrite and picritic basalt, which are found together with less-magnesian basalt, two-pyroxene andesites, hornblende andesites, and biotite tonalite. Some of these rock types were also recovered in the *Kana Keoki* dredges, but other rocks, not yet located in the islands, include unusual types, such as orthopyroxene-rich magnesian andesite ('boninite'), basalt high in Na_2O/K_2O (about 65:1) and TiO_2 (2.3 wt %), and dacite from a newly discovered volcano on the floor of the Woodlark Basin. The emplacement of such a variety of rock types, including some with island-arc characteristics, so close to the presumed line of subduction is a puzzling aspect of the triple-junction geology, and apparently relates to subduction of the spreading axis. However, heat-flow values are not high in New Georgia Sound, and the picrites appear to be olivine-accumulative rocks rather than high-Mg magmas produced by large degrees of mantle partial melting. A pronounced shift of the main volcanic axis towards the presumed line of subduction is the only obvious indication that ridge subduction has strongly influenced magma genesis beneath the island arc.

The Division of Geophysics and its research programs

M.W. McElhinny

Research in the Division of Geophysics is directed towards the study of the structure and characteristics of the crust and upper mantle. Use is made of the most sophisticated modern techniques of seismology, magnetics, gravity, and electrical geophysics to probe the structure of the Australian continent and to detect present and past movements of the crust. Emphasis is placed on multidisciplinary studies of large geological structures, especially major sedimentary basins and metallogenic provinces. The focus of such studies is the Australian Continental Reflection Profiling Program (ACORP), involving deep seismic profiles of the Australian continent.

The functions of the Division include the operation of an Australia-wide network of seismic and magnetic observatories. These form part of a worldwide network aimed at locating earthquakes and monitoring changes in the Earth's magnetic field. The Division undertakes airborne radiometric and magnetic surveys as a basis for mineral and petroleum exploration and carries out research into geophysical exploration techniques and applications.

Australia-wide airborne geophysical mapping — future program

G.A. Young

Reconnaissance magnetic and radiometric mapping of the Australian continent is vital to BMR in fulfilling its role to 'develop a comprehensive understanding of the geology of the Australian continent', and to industry for mineral and petroleum exploration. Since 1951, BMR has used its own aircraft to survey the Australian continent geophysically and thus create the necessary regional magnetic and radiometric database to support the search for minerals, including petroleum, to delineate the extent and depth of sedimentary basins, and to provide assistance to mapping in 'hard-rock' mineral provinces.

Primary strategic objectives are: to complete basic survey coverage of the Australian continent by 1989; to complete production of full suites of maps at scales between 1:250 000 and 1:1 000 000 by 1990; and to undertake a comprehensive program of research into the regional geology and mineral potential of sedimentary basins and mineral provinces, involving the interpretation of airborne magnetic and radiometric data in conjunction with other geophysical data.

Secondary objectives are: to use the BMR aircraft to carry out more detailed and specialised surveys, to solve specific geological problems and assist in resource-related research projects; and to test, and, where appropriate, further develop new technologies in surveying, data processing, and interpretation.

With reference to the first two primary objectives, the aeromagnetic coverage of Australia as at December 1981 will be presented as the basis of surveys programmed for completion by December 1983, and that being considered for progressive completion by December 1985 and by December 1987. Most of the work so programmed falls into three major regions: northeast Queensland, to be flown by the end of 1984; Pilbara Block, and Hamersley and Bangemall Basins, WA, likely to be flown by end of 1986; and the Clarence-Moreton and Maryborough Basins, NSW/Qld, also likely to be flown by end of 1986. Maps showing survey results at 1:250 000 and 1:1 000 000 scales will, in general, be released within one year of a survey being flown.

Consideration is being given to the production of a final series of magnetic maps at scales of 1:2 500 000 and 1:1 000 000, the first of which would cover the region south of latitude 24°S and be published in the mid to late 1980s. Both map series would be colour contour maps containing sufficient detail to depict the major magnetic lineations and other regional features. A by-product would be a computer database containing gridded magnetic data, levelled to a common datum, and incorporating all available data at the highest possible data density. The benefit of having such a digital database (as compared to analogue data only) will be demonstrated with reference to the reprocessing of some early BMR data.

Earthquake risk in Australia

D. Denham

Although the earthquake hazard in Australia is smaller than that in countries such as Japan, which are situated near active plate-margins, it is significant. During the last 30 years, earthquake damage in Australia has amounted to more than $15 million, and every year it is usual for at least one earthquake to cause some damage.

Most Australian earthquakes are caused by compressive forces acting in the upper crust. Because they are all shallow (less than 30 km), those of moderate size (4.5 to 5.5 on the Richter Scale) are likely to cause damage if they occur near areas of habitation. To properly assess risk from earthquakes we need to know where and how often they are likely to occur. At present, the coverage of seismograph stations is adequate for this purpose in most of the four southeastern States, but, in Queensland and Western Australia, there are deficiencies in the network.

In addition to knowing the frequency of occurrence of earthquakes, we need to

know the ground response, so that the risk can be quantified for engineering purposes. Until recently, we have had to rely on results from overseas for these estimates, but we now have enough Australian data to make significantly better estimates than those obtained in 1976, when the first attempt was made to provide a continent-wide assessment of the earthquake risk.

An omnidirectional downhole EM probe

R. Cobcroft

Recognising the importance of borehole geophysics in the future of metalliferous exploration, BMR has developed and tested a three-axis (omnidirectional) downhole EM probe capable of operating to a depth of 500 m in holes as small as BQ (60-mm diam.) and having superior sensitivity and target characterisation compared with existing single-axis probes. The primary field is set up by a sinusoidal audio-frequency current flowing in a large loop on the surface. The downhole omnidirectional probe permits the measurement of the axes and the orientation of the polarisation ellipse resulting from the interaction of primary and secondary fields. These measurements are invariant with probe orientation, are simple to interpret, provide a good guide to the location of subsurface conductors, and permit the use of complex transmit loops to enhance target detection. The results of a program of field tests in eastern NSW, Tasmania, and near Broken Hill are discussed and demonstrate the superiority of the omnidirectional probe over the traditional single-axis probe in detecting and defining subsurface conductors.

Gravity, magnetic, and radiometric characteristics of the Davenport Geosyncline, Northern Territory

I.G. Hone

The Davenport Geosyncline consists of a strongly folded sequence of sedimentary and volcanic rocks, the Hatches Creek Group, which is between 1810 and 1660 Ma old and located between Tennant Creek and Alice Springs. The geophysical characteristics of the geosyncline are being studied in conjunction with a joint BMR–NTGS investigation of the detailed stratigraphy, structure, geological history, tectonic setting, and mineral potential.

The Hatches Creek Group, which has been divided into three divisions on the basis of lateral facies changes, volcanic content, and depositional environment, lies unconformably on the Warramunga Group to the north and the Arunta Block to the south, and is unconformably overlain by the Georgina and Wiso Basins to the east and west. It is intruded by many gabbro, dolerite, and granophyre sill-like bodies, especially in the lower parts, and by granite. The sedimentary rocks of the group, quartz-rich sandstone and subordinate conglomerate, siltstone, shale, and carbonate, are interlayered with mafic (basaltic) and felsic (dacitic and rhyolitic) lavas and pyroclastics.

Gravity and magnetic expressions of the Hatches Creek Group resemble those of the Tomkinson Creek Beds, which lie north of Tennant Creek, suggesting the two are correlatives. The two occur as flanks of an anticlinal structure, having the Tennant Creek Block as its core. Residual gravity patterns over the Hatches Creek Group broadly correlate with the distribution of the Lower, Middle, and Upper divisions of the Group, highest values occurring over the lower parts, which contain the greatest proportion of mafic volcanics and intrusives Strong lows occur over granites. The broad station spacing of the reconnaissance gravity survey of Australia was infilled to define gravity features for interpretation. Gravity anomalies indicate that the granites intruding the Hatches Creek Group are small steep-sided plutons extending to considerable depth, whereas granites intruding the Warramunga Group to the north are broader.

Newly acquired aeromagnetic data outline magnetic layers within volcanic units and sills. Granites do not have magnetic contact aureoles. Detailed aeromagnetic surveys are very effective mapping tools, and units can be traced for considerable distances and structures outlined under cover, and the thickness of cover rocks determined. Results of aeromagnetic surveys show that the Hatches Creek Group extends well beyond its exposed limits.

The granites, granophyres, and felsic volcanics are relatively radioactive. Occasional radiometric anomalies occur over the sandstones, possibly from leaching of radioactive minerals from acid volcanics.

Wolframite deposits near Hatches Creek may have as a source the granite a few kilometres to the south. This granite has only a small area of exposure, but is shown by gravity to be the upper extremity of a pluton at shallow depth. The Devil's Marbles Granite, which is close to the wolframite deposits of the Wauchope Mineral Field, is also seen to be the upper extremity of a larger pluton at shallow depth.

The 1982 BMR seismic survey — Adavale Basin

M.J. Sexton

BMR conducted a seismic survey in the Central Eromanga Basin in Queensland from July to late November 1982. The survey was a continuation of the work undertaken in 1980 and 1981 to investigate the structure, stratigraphy, geological and tectonic evolution, and petroleum potential of the area. The survey obtained 485 km of 6-fold CDP seismic reflection data in the Adavale Basin, Cooladdi Trough, and Pleasant Creek Arch area. Gravity observations were made at 667-metre intervals along all traverses. Data quality is generally fair to good; and although processing is still incomplete, several interesting features are apparent. Suspected pre-Eromanga sediments east of the Pleasant Creek Arch have been confirmed. Confident lithologic correlations can be made for the Cooladdi Trough and the structure of the Gilmore gasfield is clearly defined. Interpretations are proceeding, using, where possible, modern company seismic data, well-log information, and an extensive network of seismic data reprocessed at BMR. This will allow structure-contour and isopach maps to be made for the study area and enable a reappraisal of the petroleum potential of the area.

Note: Copies of the sections at a scale of 10 cm/s will be available from the Copy Service, Government Printer (Production), PO Box E84, Queen Victoria Terrace, ACT, 2600, after July 1983.

Magnetotelluric soundings over a Precambrian boundary in Australia

J.P. Cull

The Early Proterozoic Willyama Complex crops out over a substantial area near Broken Hill. However, Adelaidean cover is widespread and the eastern limits of the complex are obscured by the Phanerozoic strata of the Murray- Darling Basin. Consequently, geophysical techniques must be used as an aid to regional mapping. Vertical contacts are readily located in terms of a lateral variation in apparent resistivity. Adequate data can be obtained by magnetotelluric surveys, which give structural details at a fraction of the cost of seismic surveys. Consequently, an MT traverse was established across the eastern margin of the Willyama Block to investigate the nature of the contact between the complex and the younger, unmetamorphosed strata. Data were obtained at 14 sites, from Broken Hill to Ivanhoe. Apparent resistivities presented as pseudosections reflect the major structural units identified from surface geology. Continuity between sites can be demonstrated from similarity in apparent resistivities between successive sites. Lateral changes are generally gradational, but a major discontinuity is evident between Broken Hill and Menindee. A characteristic divergence is generated in orthogonal components of apparent resistivity. A corresponding response has been obtained using 2D models. The foliated Willyama Complex can be represented using a succession of steeply dipping beds generating the required anisotropy at depths of 15–35 km. On this assumption, the Early Proterozoic basement appears to extend at least as far east as Menindee. However, resistivities assigned to surface layers are not sufficiently constrained to allow accurate estimates of depth.

Research in the Division of Continental Geology

P.J. Cook

Research in the Division of Continental Geology is directed towards understanding the nature and origin of onshore sedimentary basins and systems which may host fossil fuels, mineral deposits, or groundwater resources; determining the characteristics and origin of fossil fuels; establishing the effects of surface processes on the bedrock of Australia; studying the application of remote-sensing techniques to regional geological studies; and understanding the geological factors governing the quality and quantity of groundwater resources.

The BMR program on fossil fuels is addressed through Divisional projects concerned with the palaeogeographic distribution of resources, the characterisation and controls on the distribution of fossil fuels, and the biochronological framework of resources. A second group of projects concerned with onshore sedimentary basins analysis includes projects on the Proterozoic McArthur Basin, the Late Proterozoic/Palaeozoic Amadeus Basin, Late Palaeozoic/Mesozoic Basins (Clarence-Moreton and Eromanga), and Cainozoic Basins (Lake Eyre and Lake George).

A series of Divisional projects is concerned with minerals. These are directed towards determining the characteristics and controls on the distribution of sedimentary mineral resources, and understanding the weathered zone and its related resources by the use of remote sensing and other techniques.

The third program is concerned with groundwater. Because of limited staff, this is a relatively small Divisional program at the present time directed mainly towards the hydrogeology of the Murray and Eromanga Basins in SE Australia.

Sea-level changes and Cainozoic sedimentation in the Murray Basin

C.M. Brown

Recent work by BMR, in cooperation with State Geological Surveys, has resulted in a revised interpretation of stratigraphic relationships in the Murray Basin, and leads to the conclusion that fluctuations in supply, preservation, and erosion of sediment in the basin can readily be accommodated by eustatic models. These involve global changes in relative sea level and related intrabasinal isostatic adjustments associated with sediment loading. The Murray Basin sedimentary record may be subdivided into three and possibly four depositional sequences, each consisting of a package of genetically related formations, separated by surfaces of erosion or non-deposition. The Cainozoic history of the basin has been characterised by slow relative subsidence rates, low rates of sediment supply, and minimal compaction rates. Depositional sequences show an apparently close correlation with the 'second-order cycles' (supercycles) of relative rise and fall in global sea level as recorded by Vail & others (1977), and Vail & Hardenbol (1979). Framework tectonics provide the primary control on development of the basin; however, within this context, sediment accumulation appears to have been sensitive to secondary eustatic and palaeoclimatic influences, and to consequent fluctuations in erosional and depositional potential of the fluvial systems that drain the basin. Laterally extensive intercalations of fluviodeltaic, paralic, and shallow-marine sediments appear to have been deposited during periods of high global sea level, whereas non-preservation, because of erosion or non-deposition, appears to have occurred during major periods of lowered sea level. Jones & Veevers (1982) have proposed an alternative model of tectonic cycles. They interpreted depositional cycles in the Murray Basin to be the erosional products of cycles of tectonic uplift and Cainozoic volcanism in the SE Highlands of Australia, and correlated periods of non-depositional hiatus in the basin with proposed periods of 'tectonic settling' and diminished erosion in the highlands. Interpretation of the new Murray Basin data in terms of eustatic influences is believed to provide a more acceptable model.

References

Jones, J.G., & Veevers, J.J., 1982 — A Cainozoic history of Australia's Southeast Highlands. *Journal of the Geological Society of Australia*, 29, 1–12.

Vail, P.R., Mitchum, R.M., & Thompson S. (III), 1977 — Global cycles of relative changes of sea level. *In* Seismic stratigraphy — applications to hydrocarbon exploration. *American Association of Petroleum Geologists, Memoir* 26, 83–97.

Vail, P.R., & Hardenbol, J., 1979 — Sea level change during the Tertiary. *Oceanus*, 22, 71–79.

Interpretation of conodont colour alteration and thermal maturation in the Amadeus Basin

J.D. Gorter[1] & R.S. Nicoll

The Amadeus Basin contains 11 500 m of Late Proterozoic to Late Devonian sediment, generally thickening northward across the basin towards the MacDonnell Ranges. A complex series of anticlinal structures, some of them fault-bounded, in the north-central part of the basin contains accumulations of hydrocarbons in sediments of Early Ordovician, Cambrian, and Late Proterozoic ages. Hydrocarbons have been produced from the Ordovician in two fields — the Palm Valley gas field and the Mereenie gas and oil field.

Study of conodont colour alteration to define organic maturation levels and trends is based principally on samples collected from the Early Ordovician (Arenig) Horn Valley Siltstone from both outcrop and subsurface localities. Additional faunas have been recovered from the overlying Early-Middle Ordovician Stairway Sandstone and Stokes Formation. The conodont colour alteration isograds in the Amadeus Basin appear to be primarily related to events of the Alice Springs orogeny, when the thick mass of molasse sediments (Pertnjara Group), resulting from erosion of the uplifted Arunta Block, was deposited. Anomalies in the conodont colour isograds appear to be related to erosion associated with the Rodingan orogeny and also, possibly, to the effect of salt structures.

[1] Pancontinental Petroleum Ltd

Morphotectonics, palaeodrainage, and regolith studies

C.D. Ollier

The deep weathering of rocks is developed to an exceptional extent in Australia, and is of considerable economic importance to mining and mineral exploration companies. Some weathered material is itself of economic value; more often the weathered zone is a barrier between explorers and their target. The weathered zone and its cover together constitute the regolith; regolith is a general term for the mantle of unconsolidated rock material, whether residual or transported, that covers the bedrock. We are concerned with its description, regional distribution, and age.

Because of the great age of landscapes in Australia, regolith can also be very old, and hence there are many deep-weathering profiles in the continent. Many Australian landscapes are etchplains in varying degrees of stripping, that is, erosion of the weathering profile down to the level of fresh bedrock. Weathering is still taking place, but present-day weathering is not the cause of the deep-weathering profiles, which were formed under different climates and a long time ago.

Regolith can be dated by several methods. Associated sediments can give a stratigraphic age if dates can be obtained from the youngest sediments that are weathered, and from the oldest unweathered sediments overlying an earlier weathered surface. In eastern Australia, volcanic rocks can provide an age, using the K-Ar method. Some old basalts are very deeply weahered, and may be overlain by relatively fresh younger basalt. Palaeomagnetism may be applied to suitable materials in a weathering profile, and possibly reveal the age of weathering. Where these straightforward geological and physical methods cannot be applied, more devious geomorphic techniques may be used.

Some weathering profiles have been related to erosion surfaces. There is much controversy over the origin, number, and spatial and temporal relationships of erosion surfaces, and a major task is to

map and understand the major features of erosion surfaces in relation to regolith. Elsewhere, regolith may be related to drainage patterns. An understanding of the palaeodrainage may then help to place the associated regolith in a time-scale. Australian palaeodrainage can be traced in places back to Permian times, and there have been many changes of drainage pattern and style since then, so there is a good chance of establishing a reasonably full drainage pattern history, helping to establish a regolith history. Many major features of Australian drainage-patterns result from changes brought about by tectonic movement. Some rivers apparently existed before uplift of features, such as the Flinders Ranges horst or the Eastern Highlands; some may even be older than the break-up of Gondwanaland and the formation of the continental edges of Australia. Tectonic movements also created Cainozoic sedimentary basins. The sedimentary history of these basins reflects not only the local tectonics, but that of the surrounding region, so the sedimentary record should be matched by an erosion history in the catchment, including stripping of old regolith.

Regolith formation is on the same time-scale as sedimentary basin formation, mountain building, and continental drift, and its study bears on many other aspects of geology and geomorphology.

Morphotectonics of Australia and remote sensing

R.F. Moore & C.J. Simpson

Morphotectonics (the study of the interrelationships of major landforms and tectonic processes) is undergoing a resurgence of interest with the application of digital image-processing techniques. The detection and verification of major structures on a continental scale is an important preliminary phase in morphotectonic studies. It is demonstrated that digital image-processing techniques applied to topographic spot-height or digital terrain data over continental Australia help in the detection and study of those geomorphological features that apparently relate to the tectonic framework of the continent, and reveal features previously unknown. Manipulation of pseudocolour, gradient, synthetic-reflectance, and bit-plane images can provide specific information unobtainable from conventional topographic maps. Information derived from such images is of value in regional geomorphic studies, and in the analysis of linear, curvilinear, and circular features. The method also provides an excellent medium for merging other digital data sets of direct relevance to morphotectonics. The technique can be used at different scales, in areas of any size. Digital image processing allows the integration and analysis of remotely sensed imagery and photographic, topographic, and geophysical data to help discover and confirm the existence of morphotectonic features.

Regional groundwater movement and hydrocarbon migration in the Eromanga Basin

M.A. Habermehl

In the Eromanga Basin, which is a constituent sedimentary basin of the hydrogeological Great Artesian Basin, confined aquifers occur in continental quartzose sandstones of Jurassic and Cretaceous age. A thick argillaceous sequence of sediments of marine origin and Cretaceous age forms the main confining unit.

Large-scale groundwater movement, interpreted from potentiometric maps based on data from flowing artesian water wells in the basin, is generally directed to the west, southwest, and south in the main part of the basin. In the western part, regional groundwater movement is towards the southeast and south; in the most northern part a northerly flow direction exists. Epeirogenic uplift of the eastern recharge areas and lowering of the southwestern area during Late Cretaceous and Tertiary times established the present flow regime. The hydraulic gradient steepened slightly in the late Quaternary, as the spring levels in the southwestern margin were lowered. Groundwater development by flowing artesian water wells since about 1880 has caused significant changes to the potentiometric surface. The artesian groundwater, which is of meteoric origin, as shown by environmental isotope analysis, moves only slowly. Residence times of the water are large, but groundwater salinities are low, generally between 500 and 1500 mg/l total dissolved solids, and increase only slightly along the flow paths. Hydrochemical differences characterise different aquifers and regional groundwater flow patterns, particularly in the southwestern part, where groundwater derived from the eastern recharge area is characterised by Na–HCO_3–Cl and water from the western recharge area by Na–Cl–O_4. Waters in the central part of the basin are mainly of the Na–HCO_3–Cl and Na–HCO_3–Cl–SO_4 type.

Hydrocarbons have been generated in the marginally mature to mature fine-grained Jurassic and Cretaceous sediments since Late Cretaceous time. Most Jurassic–Lower Cretaceous sandstones are reservoir rocks, and some commercial and subcommercial oil and gas discoveries have been made in them. Migration of the hydrocarbons has probably been influenced by the artesian groundwater flow. Gas samples were taken at the surface from about 60 long-established (several decades) flowing artesian water wells (which were 'randomly' drilled, in contrast to petroleum exploration wells) in the central part of the Eromanga Basin in 1980. Methane concentrations from the upper, main Lower Cretaceous–Jurassic aquifer (Cadna-owie Formation/Hooray Sandstone) range up to about 510 000 microlitres per litre, and the sum of the hydrocarbons ethane to heptane ranges up to about 14 000 microlitres per litre. The relatively high values for the hydrocarbons methane to heptane suggest that hydrocarbons derived from the adjoining source rocks or from existing accumulations are migrating in the artesian groundwater.

The Division of Petrology & Geochemistry and its research programs

J. Ferguson

Research in this Division is designed to undertake basic geochemical, petrological, and mineralogical studies of major sedimentary and igneous rock suites, the environments of metalliferous deposits, and the deposits themselves. It has the main carriage of multidisciplinary studies of metallogenic provinces.

The functions of the Division include the development of the understanding of the origin, abundance, age, and distribution of Australia's metalliferous mineral resources in the context of the structure and geological history of the continent and its various geological provinces, as a basis for exploration and assessment.

Diamond province studies: contrasts in the South Australian and West Kimberley fields

A.L. Jaques & J. Ferguson

Diamondiferous kimberlitic rocks occur in the north, east (Argyle) and west Kimberley (Ellendale) and Carnarvon Basin areas of Western Australia, and in the Orroroo area of South Australia. Diamond grades range from economic (Argyle) to subeconomic (Ellendale) to trace only. That many of the kimberlitic rocks of Western Australia differ significantly from the 'classical' kimberlites of southern Africa is shown by the contrasts between the West Kimberley and South Australian provinces.

The South Australian kimberlites are of Jurassic age (164–174 Ma) and occur as dykes, blows, sills, and pipes intruding the Adelaidean of the Adelaide Fold Belt and Stuart Shelf. Petrographically they are hypabyssal calcite-phlogopite kimberlites and resemble the kimberlites from the Kimberley region of South Africa. No mantle nodules have been found, but typical kimberlite indicator minerals (pyrope, Cr-diopside, picro-ilmenite, spinel) are common. The South Australian rocks also closely resemble the kimberlites of southern Africa in terms of their bulk chemistry.

The diamondiferous rocks of the West Kimberley, in contrast, are of Miocene age (20 Ma) and occur intimately associated with leucite lamproite (Fitzroy Lamproites), forming a broad belt of more than 100 separate pipes, plugs, sills, and rare dykes. Crater sediments occur in a number of pipes, indicating little erosion since their emplacement. A feature of the pipes is the common late-stage emplacement of massive, magmatic rock in the form of a

lava blister. The West Kimberley rocks show a petrographic gradation from phlogopite peridotite resembling kimberlite, through olivine-rich leucite-poor lamproite, to leucite lamproite. Major mineralogical differences between the West Kimberley and South Australian provinces include the gradation to leucite-bearing rocks, the presence of amphibole and glass, the absence of primary carbonate, and the rarity of garnet and the absence of picro-ilmenite from the indicator suite. Compared to the South Australian and South African kimberlites, the kimberlitic rocks of the West Kimberley are richer in SiO_2, TiO_2, K_2O, and 'incompatible' elements, and poorer in CaO and CO_2. In common with the associated leucite lamproites, the kimberlitic rocks have $K_2O > Al_2O_3$, and similarly high $^{87}Sr/^{86}Sr$ and low $^{143}Nd/^{144}Nd$ ratios, indicating that they form a consanguineous ultrapotassic suite.

Hydrothermal alteration in the Mount Gunson area of the Stuart Shelf and its possible relevance to copper mineralisation

J. Knutson[1], T.H. Donnelly[1], P. Eadington[2], & D.G. Tonkin[3].

The aim of this project is to determine the depositional and post-depositional processes operative in the pre-Adelaidean rocks in the Mount Gunson area, SA, and to assess the possible significance of these to base-metal mineralisation throughout the sequence. Geochemical, petrological, stable isotope, and fluid inclusion studies are being carried out in order to indentify the types and extent of secondary alteration in these pre-Adelaidean rocks and the major processes responsible for the alteration.

The core material being studied comes from a drill hole approximately 10 km north of Mount Gunson. The hole penetrated to a depth of 1000 m and intersected, in turn, the Pandurra Formation (500 m thick), a sequence of tuffs, siltstones, basic, intermediate, and felsic volcanics and volcanic breccias (300 m), metasediments (200 m), and finally granitic breccia (10 m — bottom of drillhole).

All units below the Pandurra Formation are strongly hematitised and K-feldspar metasomatism is ubiquitous. Textural relationships indicate that there were a number of different and×or overlapping veining episodes, including at least two episodes of calcite introduction: one early in the alteration sequence and one late. The early carbonate is fine-grained and dusted with hematite, and is associated with K-feldspar and secondary quartz. Coarse crystalline calcite formed very late in the metasomatic episodes and commonly replaces feldspar, quartz, and, to a lesser extent, tourmaline and fluorite. Specular hematite and minor chalcopyrite were probably introduced at the same time as this late calcite. Fine brittle fracturing of the feldspathic rocks postdates K-metasomatism as well as the main tourmaline and fluorite mineralisation, and could be associated with the later calcite mineralisation. The extreme secondary alteration makes precise identification of the original igneous rock types difficult. Overall, the volcanic and volcaniclastic rocks are basic to intermediate in composition. Most rocks analysed are depleted in Na_2O and Sr and enriched in K_2O. Iron values vary greatly, ranging from 3.5% in a tuff to 50% in a hematite-rich rock.

Carbon isotope results indicate that calcite in vugs and veins of the feldspathic rocks overlying the calc-silicate unit is of magmatic origin. Generally, there is a tendency for $\delta^{13}C$ values to become less negative away from these rocks. Preliminary sulphur isotope results also indicate that sulphides with isotopic values consistent with an origin from magmatic-hydrothermal fluids occur at the same stratigraphic levels as the magmatic $\delta^{13}C$ values.

Fluid-inclusion results suggest the presence of magmatic, mixed magmatic and connate, connate, and meteoric fluids. It may be significant that the magmatic-hydrothermal fluids occur in the same rock types in which the $\delta^{13}C$ values indicate a substantial magmatic component. Estimated salinities of these hydrothermal fluids range up to 30–35 wt % NaCl and temperatures range up to 380°C. Some of the fluid inclusions of magmatic origin are vapor-rich, suggesting that boiling has taken place.

[1] Baas Becking Laboratory
[2] CSIRO, North Ryde
[3] CSR Ltd, Adelaide

Proterozoic and Palaeozoic extensional tectonics and mineralisation in the western Georgetown Inlier

D.E. Mackenzie & B.S. Oversby

The Proterozoic (about 1430 Ma) dominantly ignimbritic Croydon Volcanic Group and a locally superimposed Permian acid-to-basic igneous suite, which includes the Bullseye Rhyolite, reflect broadly analogous tectonic regimes. Accumulation of the Croydon Volcanic Group and emplacement of related granitoids appear to have been influenced by roughly E–W-oriented extension, which followed similarly oriented compression during the 'Jana Orogeny' (about 1470 Ma); the Permian rocks probably formed under the influence of NE-SW-oriented extension.

The northwestern part of the Croydon volcanics is interpreted as a second-order synvolcanic subsidence structure. Gold-bearing quartz reefs and veins, commonly associated with graphite concentrations, and stanniferous greisens are spatially, and probably genetically, related to altered rhyolite dykes, extensive zones of alteration, and/or shear zones in the volcanics and associated granitoids. Some of the quartz reefs, greisens, and rhyolite dykes are in NW-trending swarms, and may have formed under the influence of the Permian extensional regime. However, the bulk of the available evidence indicates a Proterozoic age: the quartz reefs and veins were probably emplaced into fractures formed during late-stage 'settling-in' of the volcanic-granitoid pile. Extensions of known mineralisation might be stratigraphic discontinuities in the volcanic sequence, in zones at or near the granite-volcanics contact, and in vent-facies rocks in the northwest 'structure'.

The Permian Bullseye Rhyolite, along with possibly Permian andesite, is preserved in a group of closely-spaced, NNW-trending horsts and grabens that lie at the northwestern end of a major NW-trending composite fault zone, which includes the Robertson Fault, and on which also lie the Permian Agate Creek Volcanics. Similar rhyolitic ignimbrite crops out 15 km to the west, where it is associated with Permian andesite, and dacite, granodiorite (Awring Granodiorite), and dolerite of probable Permian age; most of these rocks are preserved in a small northwest-trending graben. The Awring Granodiorite and small roof pendants of altered Permian(?) rhyolitic ignimbrite contain late-stage hydrothermal Ag-Cu-W mineralisation. Areas along the 'Agate Creek–Bullseye' trend where small-scale block faulting and Permian igneous rocks occur, such as the Bullseye Rhyolite itself, may also be prospective for metals such as Cu, W, Sn, Ag, and Au, and this has clear implications for exploration in other areas of Permian magmatism and tensional tectonics in northeastern Queensland.

Volcanic-hosted massive sulphide deposits — the state of the art

M. Solomon

Among the diversity of form and composition, three prominent styles can be recognised — Cyprus-type, Kuroko-type, and Rosebery-type, the latter being particularly important in eastern Australia and eastern Canada. The quantification of potential for new finds and the efficiency of subsequent discovery and development are linked to our understanding of the genesis of these deposits and the reasons for their diversity.

Genetic problems fall under three headings: (a) growth on the sea floor; (b) the formation of subsurface stockwork zones; and (c) the generation of the ore solutions.

(a) for Cyprus and Kuroko types, based on field and laboratory studies and the discovery of chalcopyrite chimneys on the East Pacific Rise, involves the growth of a sulphide mound at temperatures < 400°C by fall-out from escape plumes and the incorporation of collapsed chimneys. In contrast, Rosebery-type orebodies grow by precipitation from saline solutions that reverse buoyancy and collect in basins. Major-element and $\delta^{18}O$ values around some deposits indicate that hydrothermal

flow continues long after accumulation of the hanging wall.

(b) involves partial sealing of the subsurface flow channel as a result of thermal and chemical disequilibrium between rising ore fluid and country rock. Re-equilibration of the convective circulation in response to the decreased permeability results in fluid pressures that commonly exceed the tensile strength of the rock, forming stockwork pipes in which quartz precipitation follows the attendant pressure fluctuation.

The current model for (c) involves convective circulation of sea water (magmatic water) driven by magmatic heating. For the Cyprus-type deposits, the heater is a wedge-like basaltic magma chamber beneath a spreading ridge; for Kuroko deposits it is a small plug-like felsic pluton; and for Rosebery it is a shallow, extensive felsic sill. Suspected heater-deposit relationships have only been observed in two localities — Tasmania (in the Murchison Gorge) and Canada. Theoretical and experimental modelling of idealised fluid flow patterns allows prediction of the mineralogy throughout the circulation cells, and preliminary field studies in Tasmania indicate potential for (and the difficulties involved in) mapping flow paths.

East Australian stratabound sulphides: comparative studies

F.M. Vokes[1]

Studies are in progress aimed at comparing the base-metal-bearing stratabound sulphide deposits of two of the world's major Early Palaeozoic mobile belts, the Caledonides of the North Atlantic Region and the Australian Tasmanides. As a result of the IGCP Project No 60, 'Correlation of Caledonian Stratabound Sulphides', considerable advances have been made in Scandinavia in recent years in understanding the palaeotectonic/geographical and stratigraphic/lithological environments of formation of these deposits, as well as their chemical characteristics, their morphology and structure, and their response to metamorphism and deformation.

Geological age, host-rock lithology, and stratigraphic/tectonic position permit a number of types or groups of generally stratabound (sometimes stratiform) sulphide ores to be distinguished within the Late Precambrian and Early Palaeozoic sequences of the Norwegian Caledonides, the two main classes being: A — Mainly disseminated deposits of galena with minor sphalerite (fluorite and barite) in Late Precambrian and Early Cambrian sandstones. These deposits belong to the class of 'lead-in-arenite' ores which occur in a belt extending from southwest Norway along the Caledonian Front Zone through central and northern Sweden to the northernmost country of Norway. Such ores are only economically important in Sweden, where the Laisvall mine is one of Europe's major lead producers. Equivalents of this type of stratabound ore do not seem to have been recognised so far in the Tasmanides. B — Massive, semi-massive, and disseminated, polymetallic (Cu + Zn + Fe ± Pb) sulphide deposits in volcanic and mixed sedimentary-volcanic sequences of dominantly Early-Middle Ordovician age in the allochthonous metamorphic sequences of the central Caledonides. Economically these have been the most important sulphide deposits of Norway and currently account for the country's total production of Cu, Zn, and Pb concentrates. Among these classical 'volcanogenic' deposits the following distinct types have been recognised: (a) Cu-Zn deposits associated with metabasaltic volcanites of ocean floor affinities ('Cyprus type'); (b) Zn-Cu deposits associated with mixed mafic and felsic volcanites related to island-arc formation.

In addition, a rather distinctive, if numerically minor, group of Zn-Pb-Cu ores occurs in a high-metamorphic nappe in the northern Caledonides. Their lithological associations indicate that their environment of deposition was dominantly sedimentary, perhaps with some felsic volcanic intercalations. Metabasic rocks (with a relatively high TiO_2 content) are quantitatively minor and occur well into the foot-wall country of the ores. These, and the metasedimentary lithology, indicate an intracratonic environment.

Comparisons between this last group and geochemically similar Australian deposits (Rosebery, Woodlawn, Captains Flat) are being made with a view to arriving at a better understanding of the highly metamorphosed and deformed Norwegian examples. On a global scale, similarities may be recognised to the Canadian New Brunswick deposits and to the Tertiary Japanese Kuroko-type ores.

[1] Consultant to BMR: University of Trondheim, Norway

CONTENTS

Front cover: Precambrian high-grade metamorphic rocks of the Vestfold Hills-Prydz Bay area, Princess Elizabeth Land, East Antarctica. The geology of these rocks is described in this issue in a paper by Sheraton & Collerson.

R81/103(6) Cat. No. 83 0273 2